Electronic Theses and Dissertations   Student Works

8-2019

The Distinct Expressions of Integrins **α**D**β**2 and **α**M**β**2 Differently Regulate Macrophage Migration in 3D Matrix in vitro and in Tissue during Inflammation

Kui Cui
East Tennessee State University

Follow this and additional works at: https://dc.etsu.edu/etd

Part of the Biochemistry Commons, Cell Biology Commons, Immunity Commons, Immunopathology Commons, and the Molecular Biology Commons

Recommended Citation

The Distinct Expressions of Integrins $\alpha_D\beta_2$ and $\alpha_M\beta_2$ Differently Regulate Macrophage Migration

in 3D Matrix in vitro and in Tissue during Inflammation

_____

A dissertation

presented to

the faculty of the Department of Biomedical Sciences

East Tennessee State University

In partial fulfillment

of the requirements for the degree

Doctor of Philosophy in Biomedical Sciences

_____

by

Kui Cui

August 2019

_____

Dr. Valentin Yakubenko, Ph.D., Chair

Dr. Donald B. Hoover, Ph.D.

Dr. Meng-yang Zhu, M.D., Ph.D.

Dr. Diego J. Rodriguez Gil, Ph.D.

Dr. Chuanfu Li, M.D.

Keywords: β2 integrins, macrophage, migration, inflammatory diseases

ABSTRACT

The Distinct Expressions of Integrins $\alpha_D\beta_2$ and $\alpha_M\beta_2$ Differently Regulate Macrophage Migration in 3D Matrix in vitro and in Tissue during Inflammation

by

Kui Cui

Chronic inflammation is an essential mechanism during the development of cardiovascular and metabolic diseases. The outcome of diseases depends on the balance between the migration and accumulation of macrophages in damaged tissues. Macrophage motility is highly regulated by adhesive receptors, integrins. Namely, intermediate expression of integrin supports macrophage migration, while a high integrin density inhibits it. Our studies are focused on evaluation of the contribution of related integrins $\alpha_D\beta_2$ and $\alpha_M\beta_2$ to macrophage migration and development of chronic inflammation.

We found that integrin $\alpha_D\beta_2$ is upregulated on M1-macrophages in vitro and pro-inflammatory macrophages in atherosclerotic lesions. Interestingly, the expression of ligand-sharing integrin $\alpha_M\beta_2$ remains unaltered. Using in vitro three-dimensional migration and in vivo tracking of adoptively-transferred fluorescently-labeled macrophages during the resolution of inflammation, we found that robust adhesion of M1-activated macrophages translates to weak 3D migration, which depends on the high expression of $\alpha_D\beta_2$, since α_D-deficiency decreases M1-macrophage adhesion and improves macrophage migration. In contrast, α_D- and α_M-knockouts decrease M2-macrophages migration, demonstrating that moderate integrin expression supports cell motility. In model of high fat diet-induced diabetes, α_D-deficiency prevents the retention of inflammatory macrophages in adipose tissue and improves metabolic parameters, while α_M-deficiency does not affect macrophage accumulation.

We detected a new ligand for integrins $\alpha_M\beta_2$ and $\alpha_D\beta_2$, 2-(ω-carboxyethyl)pyrrole (CEP). CEP is preferentially generated during inflammation-mediated oxidation and forms adduct with ECM proteins generating novel substrate for $\alpha_M\beta_2$ and $\alpha_D\beta_2$. Targeting CEP-dependent macrophage adhesion can be a useful approach to control $\alpha_D\beta_2$-mediated chronic inflammation.

Using specially designed peptide library, protein-protein interaction and adhesion assay, we identified a peptide, called P5, which significantly inhibited α_D-CEP binding. P5 peptide regulates macrophage migration in three-dimensional matrix in vitro and reduced macrophage

2

accumulation during thioglycollate-induced peritoneal inflammation. Effect of P5 is completely eliminated in α_D-deficient macrophages. Tracking of adoptively-transferred fluorescently-labeled WT and $\alpha_D^{-/-}$ monocytes in diabetic mice confirmed that α_D-dependent inhibition of macrophage accumulation in adipose tissue is mediated by P5 peptide.

Taken together, these results demonstrate the importance of $\alpha_D\beta_2$ and $\alpha_D\beta_2$-CEP interaction for the accumulation of infiltrating macrophages during inflammation and propose P5 peptide as a potential inhibitor of atherogenesis and diabetes.

DEDICATION

I dedicated this dissertation to my family members, my father Binghe, my mother Yuhua, my little brother Yuantang and elder sister Duanduan. They have been my main source of support and encouragement, and I am forever grateful for their love, sacrifice, and patience through my graduate studies.

ACKNOWLEDGEMENTS

TABLE OF CONTENTS

LIST OF FIGURES

13

ABBREVIATIONS

ApoE$^{-/-}$- apolipoprotein E knockout

BME- commercial basement membrane extract

BAT- brown adipose tissue

BSA- bovine serum albumin

CDM- cell-derived matrix

CEP- 2-(ω-carboxyethyl)pyrrole

CEP-KLH- CEP-modified keyhole limpet hemocyanin

CNS- central nervous system

DHA- docosahexaenoate

DOHA- γ-dicarbonyl compounds

ECM - Extracellular matrix

EDTA - Ethylenediaminetetraacetic acid

EP- ethylpyrrole

FACS - Fluorescence-activated cell sorting

Fg-fibrinogen

FMLP - N-Formylmethionine-leucyl-phenylalanine

Fn- fibronectin

HAS- human serum albumin

HHE- 4-hydroxyhexenal

HOHA- 4-hydroxy-7-oxo-hept-5-eonate

HUVEC- human umbilical vein endothelial cells

ICAM-1- intercellular cell adhesion molecule-1

IFNγ - interferon-γ

IL-4 - interleukin 4

iNOS- inducible nitric oxide synthase

LDL- low-density lipoprotein

LFA-1- Lymphocyte function-associated antigen 1

LPS- lipopolysaccharides

MCP-1 - Monocyte chemoattractant protein-1

MIDAS-metal-ion-dependent adhesion site.

MPO Myeloperoxidase

ROCK - Rho-associated protein kinase

oxLDL- oxidized LDL

PMA- phorbol 12-myristate 13-acetate

PGC-1β- PPARγ-coactivator-1β

PUFA- Oxidation of polyunsaturated phospholipids

STAT6- signal transducer and activator of transcription 6

T1D- Type 1 diabetes

T2D- Type 2 diabetes

TG - thioglycollate

Th- T helper

VCAM-1- vascular cell adhesion molecule

WAT- white adipose tissue

2D - 2 dimensional

3D - 3 dimensional

CHAPTER 1

INTRODUCTION

<u>Leukocyte Migration</u>

Cell migration is a basic and essential process in cell growth and development. It is also a ubiquitous form of movement in living cells. Leukocyte migration is one of the most essential types of cell migration in immune response and pathological conditions. Embryonic development (Reig et al. 2014), angiogenesis (Graupera et al. 2008; Kurosaka and Kashina 2008), wound healing (Qin et al. 2019), immune response(Luster et al. 2005), inflammation (Chavakis 2012), atherosclerosis (Koelwyn et al. 2018; Wang et al. 2018), and cancer metastasis (Yamaguchi et al. 2005) all require the orchestrated leukocyte migration (including monocytes, neutrophils and lymphocytes) to the injury, infected and stressful sites in a proper time with a proper direction. Aurora and co-authors found macrophage are requisite for neonatal heart regeneration (Aurora et al. 2014). The failure of leukocyte migration to appropriate locations or removal of retained cells in specific regions can result in serious consequences, such as chronic inflammation, atherosclerotic diseases (Zernecke et al. 2008) and tumor invasion (Jacquemet et al. 2015). Generally, eukaryotic cell movements consist of different migration modes, such as mesenchymal, amoeboid or collective migration, which are much more complicated than that of prokaryotic organisms (Verollet et al. 2011). To decipher the mechanism of leukocyte migration through various tissues and leukocyte retention within the inflamed sites may lead to potentially therapeutic strategies for preventing immune diseases and invasive signals.

<u>Cell Migration in 2D and 3D Matrix</u>

The ability of leukocytes to infiltrate through tissues in response to chemoattractant stimuli is of considerable importance to fulfill their various functions such as immune cell development, immune surveillance and effector function. Appropriate in vitro models are one of the prerequisite steps to reveal the mechanisms of cell migration. Diverse models of cell migration have been performed in 2D and 3D environments during the last three decades (Even-

Ram and Yamada 2005; Jacquemet et al. 2015; Zhong et al. 2012). Typically, on 2D surfaces, cells migrate based on lamellipodia. This circular process mainly consists of the formation of large protrusions at the leading edge, attachment to the matrix context, forward flow of cytosol, and retraction of the rear of the cell (Meyer et al. 2012; Wiesner et al. 2014) (Fig.1-1A). However, in vivo, cell migration primarily requires complex interactions among extracellular matrix (ECM), integrins and intracellular signaling molecules. Cells display dramatically different migration strategies in 3D matrices (Fig.1-1B). For instance, macrophages, dendritic cells and neurons employ quite different ways during migration through 3D matrix. Even the same cell will use a variety of migration strategies in different environments. For example, during vascularization, both the attachment of macrophages to the endothelial wall of blood vessels and the movement of macrophages along the lumen of organs are 2D situations in vivo. Whereas, depending on the extracellular circumstances, macrophages employ different modes (amoeboid and mesenchymal) for infiltrating through interstitial space (Wiesner et al. 2014). However, each kind of models has its disadvantages and advantages. On the one hand, 2D migration assays defined as cell movement on flat plates without any cross-link network have been extensively utilized for studying cell migration. Their simplicity helps the investigators better understand individual cellular behaviors. Nevertheless, not only the morphology during migration in 2D substrates but also adhesion and cell signaling are reported other than the in vivo scenario (3D) (Baker and Chen 2012; Petrie et al. 2009). On the other hand, 3D matrices supply valuable biological responses and structures which might not be observed or vary from that in 2D matrices (Huebsch et al. 2010). But it is usually difficult for 3D modes to mimic natural physical parameters of ECM such as gel density, pH value, gel crosslinking and pore size (Doyle et al. 2015; Even-Ram and Yamada 2005; Lanir et al. 1988). The development of imaging analysis and computational methods largely facilitate 3D matrices visual inspection and interpretation (Driscoll and Danuser 2015; Zaman et al. 2005). It is therefore necessary to consider both advantage and weaknesses based on the real physical properties before performing a specific process for cell migration.

There are several protein sources for the generation 3D matrix in vitro such as: 1) Collagen gel, which comprised of collagen type I (Hesse et al. 2010); 2) fibrin gel, which is formed after the cleavage of fibrinogen (Fg) by thrombin (Ciano et al. 1986; Ye et al. 2000); 3) cell-derived matrix (CDM) produced from fibroblasts, consisting of fibronectin fibrils (Kutys et

al. 2013) and 4) commercial basement membrane extract (BME) (Kleinman and Martin 2005) (e.g. Matrigel), which is mixed of collagen IV and laminin. Hakkinen and colleagues have demonstrated that fibroblasts have more spindles shaped with fewer lateral protrusions and substantially reduced actin stress fibers in 3D than on 2D matrices, and cells failed to spread in 3D BME (Hakkinen et al. 2011). A number of studies use different assays to investigate macrophage migration on 2D matrices (including random migration, directional migration, scratch wound assay, insert removal assay and 2D cell tracking assay) (Justus et al. 2014; Moutasim et al. 2011). However, migration on 2D rigid substrates such as plastic plates always lacks fiber networks which will affect the cell motility. Controlling cell spreading by using 2D ECM-coated plates can influence cell proliferation, apoptosis and differentiation (Mendes 2013; Sun et al. 2006). Methods to perform cell migration and adhesion assay in 3D matrices are in their infancy. Trans-well/Boyden chamber migration assay (Cui et al. 2018; Van Goethem et al. 2011), circular invasion assay (Yu and Machesky 2012) and μ-slide chemotaxis migration assay (Zengel et al. 2011) are three of the commonly used macrophage migration assays in 3D matrix. These methods can be valuable models to mimic cell trans-barrier of interstitial tissues, and further allow the investigators to measure the distance of cell migration and quantify the number of transmigrated cells within a 3D environment (Soman et al. 2012). However, in trans-well migration assay, a considerable number of cells still remain on the chamber membranes (2D) embedded in 3D systems. Compared to former stated 3D assays, spheroid invasion assay, vertical gel invasion assay, 3D cell tracking assay and spheroid gel invasion are considered as genuine 3D models (Wiesner et al. 2014). In these situations, cells are pre-seeded in the gels at the gel making process. The preponderances of these models are that the addition of chemokines or inhibitors can be operated at the step of gel polymerization and there is no need to transfer 2D matrix to 3D models. Furthermore, these modes are useful to study co-culture cells (Guiet et al. 2011) and cell-cell interactions during cell migration.
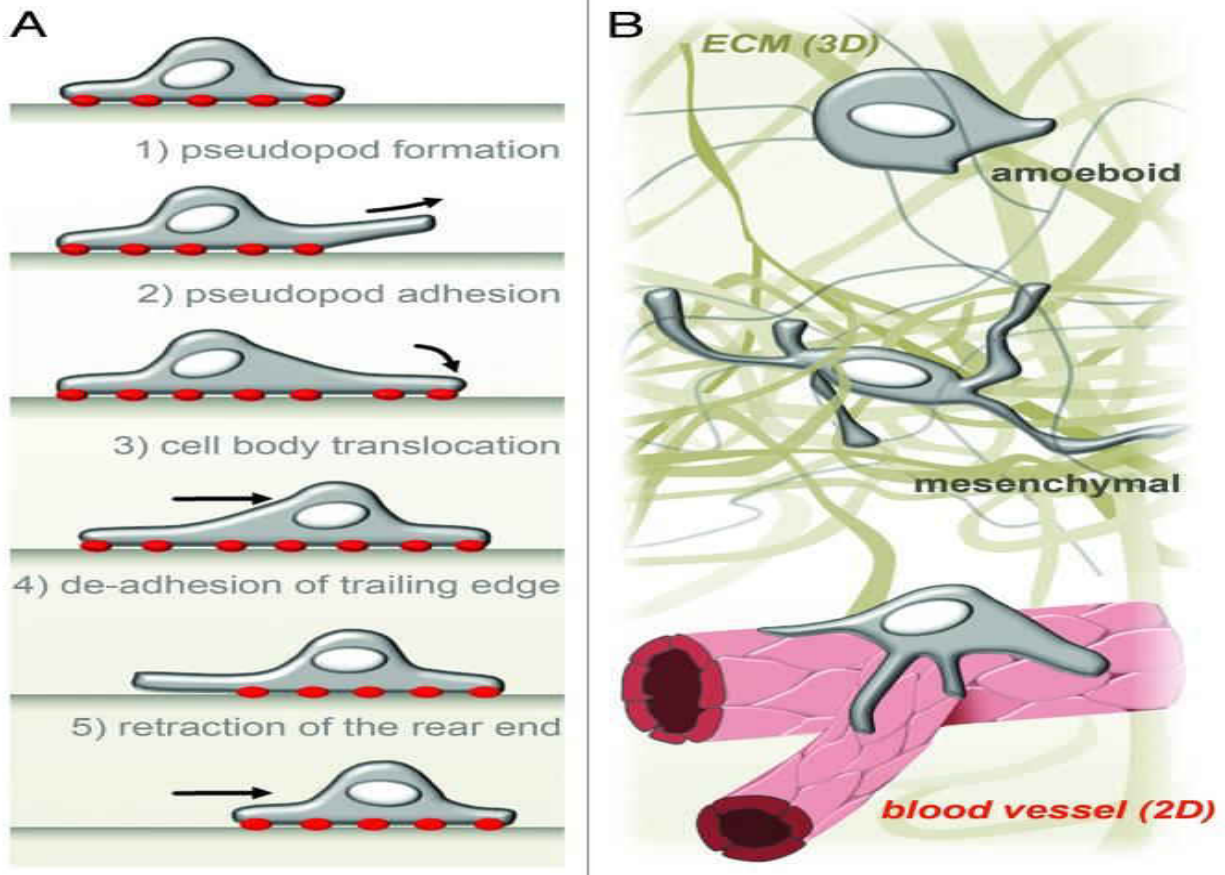
Fig. 1-1. The migration of macrophage in 2D and 3D environments (used with the permission from Dr. Stefan Linder (Wiesner et al. 2014)). (A) In vitro, macrophages exhibit a rounded morphology and migrate through a classical 5-step model on 2D surfaces. The red dots represent the adhesion receptors on cell surface. (B) In vivo, macrophages may encounter both 2D (B, bottom) and 3D (B, middle and top) environments.

Migration of Different Subsets of Leukocytes

Leukocytes migration is such a critical, complicated process that multiple mechanisms are involved simultaneously. Mesenchymal migration is characterized by integrin-dependent and proteinase-dependent slow migration. This migration consists of actin protrusions, attachment with extracellular matrix, and retraction to achieve moving forward (Pals et al. 2007). Fibroblasts in both 2D and 3D modes as well as some tumor cells (Liu et al. 2015) display mesenchymal movement to fulfill their migration. In contrast, amoeboid migration, rapid and non-proteolytic fashion, is the basic movement mode for leukocytes including neutrophils, monocytes, lymphocytes, dendritic cells, eosinophils and basophils (Friedl et al. 2001; Friedl and Weigelin

2008; Pals et al. 2007; Wolf et al. 2003). Depending on different extracellular contexts in vivo, leukocyte subsets employ different strategies to move along or infiltrate most tissues. Lymphocytes and neutrophils primarily utilize the amoeboid mode to migrate to the infection or injury sites in an integrin-independent manner (Friedl et al. 2001). In other studies, neutrophils migrate across ECM accompanied with pericellular proteolysis and adhere to endothelial cells mediated by tightly binding to β2 integrins (Hanlon et al. 2014; Luo et al. 2015). Dendritic cells flow and squeeze through 3D matrix do not require the engagement of functional β1and β2 integrins (Lammermann et al. 2008). However, macrophages can migrate in both 2D substrates such as vessel walls or peritoneum, and 3D matrix such as fibrillar extracellular matrix with either the amoeboid or mesenchymal manner respectively (Wiesner et al. 2014). Furthermore, there are basically three dynamic states in leukocyte migration and adhesion to tissues, thus composing of rapid movement (3 to 30 μm/min), restricted condition (1 to 3 μm/min) and migration arrest (less than 1 μm/min) (Friedl and Weigelin 2008). These dynamic states are orchestrated by balancing migration and attachment through the interaction between adhesion receptors and ECM. For example, Lymphocyte function-associated antigen 1 (LFA-1), a member of the integrin family, bind to its counterpart ligand intercellular cell adhesion molecule-1 (ICAM-1) to induce the migration of T-lymphocyte at a speed of around 15 μm/min (Smith et al. 2007). These adhesion receptors and ECM together associate leukocyte subsets–specific recruitment to infected sites.

Integrins on Leukocytes

Cell-cell interactions and cell–ECM interactions are critical for assembling cells into tissues, controlling cell shape and function and determining the development fate of cells. To defense infection and remove injured tissues, leukocyte subsets (neutrophil, lymphocyte or macrophage) must move rapidly to reach the sites of infection or inflammation (Chavakis 2012; Nourshargh and Alon 2014). The recruitment of leukocyte through bloodstream to the sites of inflammation is termed extravasation, which requires accurate association of adhesive molecules and constant establishment and breaking of cell-cell interactions (Fig.1-2). The sequential steps: activation, binding, rolling, adhesion and extravasation are defined as the leukocyte-adhesion cascade (Ley et al. 2007). Various adhesion molecules and receptors facilitate these processes and

they are essential for efficacious leukocyte recruitment. Among these complex steps, integrins are the primary adhesion receptor families.
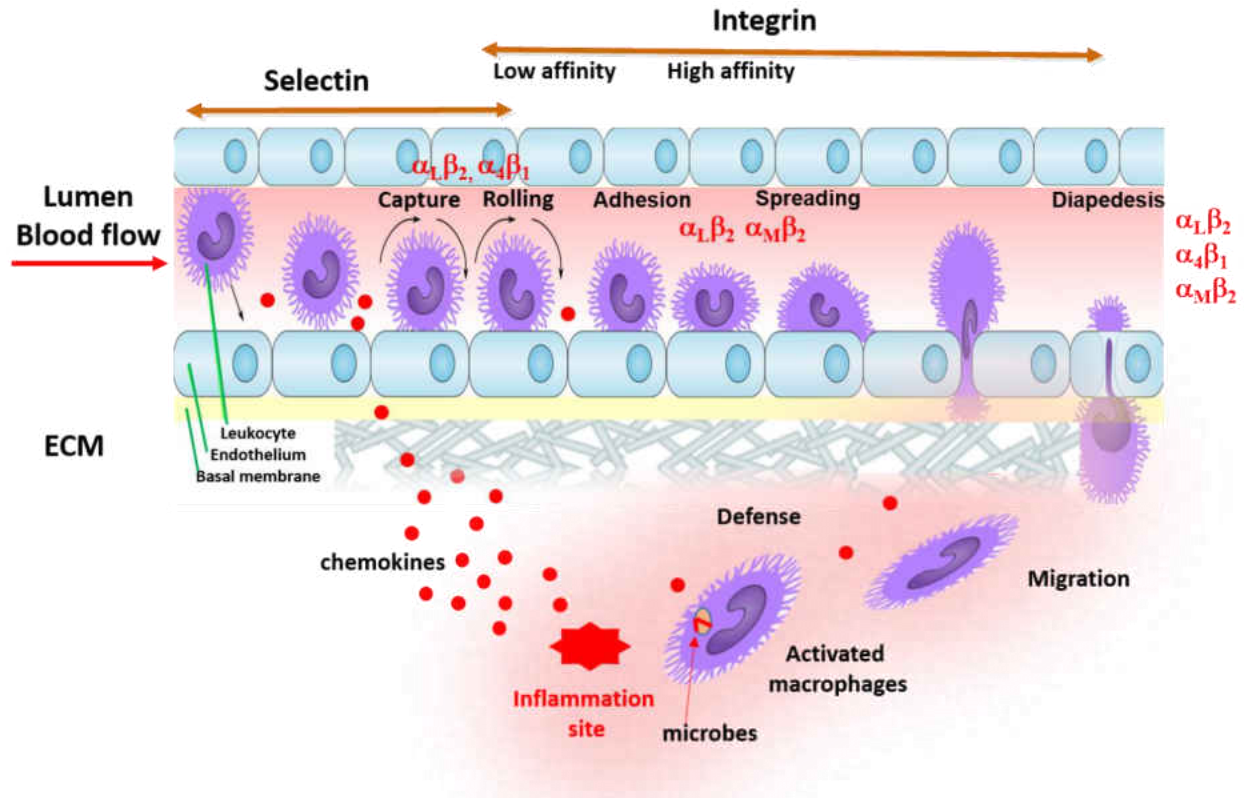
Fig. 1-2 The Recruitment of Leukocyte. The recruitment of leukocyte through blood stream to the sites the inflammation involved multiple steps including capture, rolling, adhesion and spreading, trans-endothelial migration and migration through extracellular matrix. Fig.1-2 is adapted from https://commons.wikimedia.org/wiki/File:Esquema_diapedesis.png, and (Ley et al. 2007).

Integrins are widely distributed type I transmembrane receptors that mediate a series of crucial functions such as cell signaling, adhesion, migration, dynamic interactions between actin cytoskeleton and ECM (Evans et al. 2009). Each integrin is composed of a non-covalently linked α/β heterodimers. To date, 18 α-subunits and 8 β-subunits form at least 24 different integrins in vertebrates have been identified (Barczyk et al. 2010). Depending on specific integrin-ligand binding or heterodimer compositions, integrins can be paired and divided into four categories: RGD receptors, collagen receptors, laminin receptors and leukocyte-specific receptors (Fig.1-3). Generally, each β subunit can associate with several α subunits to compose an integrin subfamily,

22

but α_V and α_4 are the two exceptions. The α-subunit determines integrin ligand specificity and β subunit connects to cell cytoskeleton to affect various signaling pathways (Barczyk et al. 2010). The α-I-domain is an inserted domain composed of about 180 amino acids (Luo et al. 2007; Qu and Leahy 1995). Integrin β_2 subfamily presents highly homogenous among α I-domain containing integrins $\alpha_L\beta_2$ (CD11a/CD18), $\alpha_M\beta_2$ (CD11b/CD18), $\alpha_X\beta_2$ (CD11c/CD18) and $\alpha_D\beta_2$ (CD11d/CD18). Particularly, we are focused on β_2 leukocyte specific integrins. They are all leukocyte-specific receptors associating with multiple ligands and receptors during leukocyte recruitment.

The expression of integrins presents in a leukocyte-specific manner. Integrin $\alpha_L\beta_2$ is present primarily on neutrophils, monocytes and lymphocytes (Smith et al. 2007; Weber et al. 1999), Integrin $\alpha_L\beta_2$ (LFA-1), binding to Ig superfamily ligands (e.g. ICAMs), mediates the arrest of leukocytes rolling on vascular endothelial cells. Ser/thr-rich domain of thrombomodulin acts as a new ligand for Integrin $\alpha_L\beta_2$ and $\alpha_M\beta_2$ (Kawamoto et al. 2016). Integrin $\alpha_L\beta_2$ can modulate the recruitment of regulatory T-lymphocytes and facilitate Tregs migration into the CNS during CNS autoimmunity (Glatigny et al. 2015).

While $\alpha_M\beta_2$ (Mac-1, CD11b/CD18) is primarily expressed on neutrophils and monocytes/ macrophages (Li 1999; Lim and Hotchin 2012; Pluskota et al. 2008). Integrin $\alpha_X\beta_2$ (CD11c/CD18, CR4) is expressed on macrophages and dendritic cells (Bilsland et al. 1994). Integrin $\alpha_M\beta_2$ and $\alpha_X\beta_2$ have been extensively studied for its functions in facilitating leukocytes firm adhesion to vessel walls, promoting the succeeding diapedesis, and mediating neutrophil infiltration (Cao et al. 2005; Dunne et al. 2003; Van der Vieren et al. 1999). Numerous of neutrophil responses such as phagocytosis, homotypic aggregation, degranulation, and adherence to microorganisms, also depend on Mac-1 (Ding et al. 1999; Pluskota et al. 2008; van Spriel et al. 2001). Over 30 proteins or non-proteins have been reported serving as $\alpha_M\beta_2$ ligands including fibronectin, laminin, and collagens (Dunne et al. 2003; Kawamoto et al. 2016; Lishko et al. 2004). Because of its broad ligand binding properties, the role of Mac-1 is in leukocyte migration has still not found a consensus relative to mechanism. Peptides P2 and P1, two Fg γC domains, are efficient binding sites of integrin $\alpha_M\beta_2$ (Lishko et al. 2004). By employing surface plasmon resonance, D fragment of Fg was proved to be able to interact with multiple α_M I-domain molecules. Mutations of βD-α5 can significantly diminish the binding affinity $\alpha_M\beta_2$ to P2-C peptide of Fg. Insertion of residues

Lys^{245} - Arg^{261} from the α_M I-domain of $\alpha_M\beta_2$ to α_L I-domain converted $\alpha_L\beta_2$ into a Fg-binding integrin (Yakubenko et al. 2002).

Interestingly, in contrast to the other three $\beta2$ subfamily members, integrin $\alpha D\beta2$ is significantly upregulated on macrophages in atherosclerotic lesions, but rarely on peripheral blood leukocytes (el-Gabalawy et al. 1996; Noti 2002; Noti et al. 2000). In addition, most of the papers (there are less than 80 papers about integrin $\alpha_D\beta_2$ on PubMed search results) just simply record its presence rather than its functions on cells. Although the functions of integrin $\alpha_D\beta_2$ during the inflammatory response are still not well known, its unique expression pattern suggests that it may play a role in the process of atherosclerosis (Noti 2002).

Integrin $\alpha_D\beta_2$ is a novel but largely undefined member of integrin family (Takada et al. 2007). Unlike its other two homologous integrins $\alpha_X\beta_2$ and $\alpha_M\beta_2$, it is preferentially expressed on macrophages foam cells in atherosclerotic lesions or rheumatoid arthritis but seldom found on peripheral circulating leukocytes. However, whether and how integrin $\alpha_D\beta_2$ is involved in leukocytes recruitment to infectious or inflammatory sites is not yet clear. The α_D I-domain of integrin $\alpha_D\beta_2$ has a high homology (70%) to α_M I-domain of $\alpha_M\beta_2$. Previous findings indicate that, similar to integrin $\alpha_M\beta_2$, integrin $\alpha_D\beta_2$ is also a multi-ligands receptor (Yakubenko et al. 2006). Intercellular adhesion molecule 3 (ICAM-3) and vascular cell adhesion molecule (VCAM-1) are capable to bind to α_D I- domain of integrin $\alpha_D\beta_2$ (Grayson et al. 1998; Van der Vieren et al. 1995). By using α_D-specific antibody, the interaction between VCAM-1 and $\alpha_D\beta_2$ can be blocked. This blocking reduced the inflammatory response of leukocytes migration to the injured spinal cord, which will largely attenuate inflammation caused secondary damage to neurons and glia (Mabon et al. 2000).
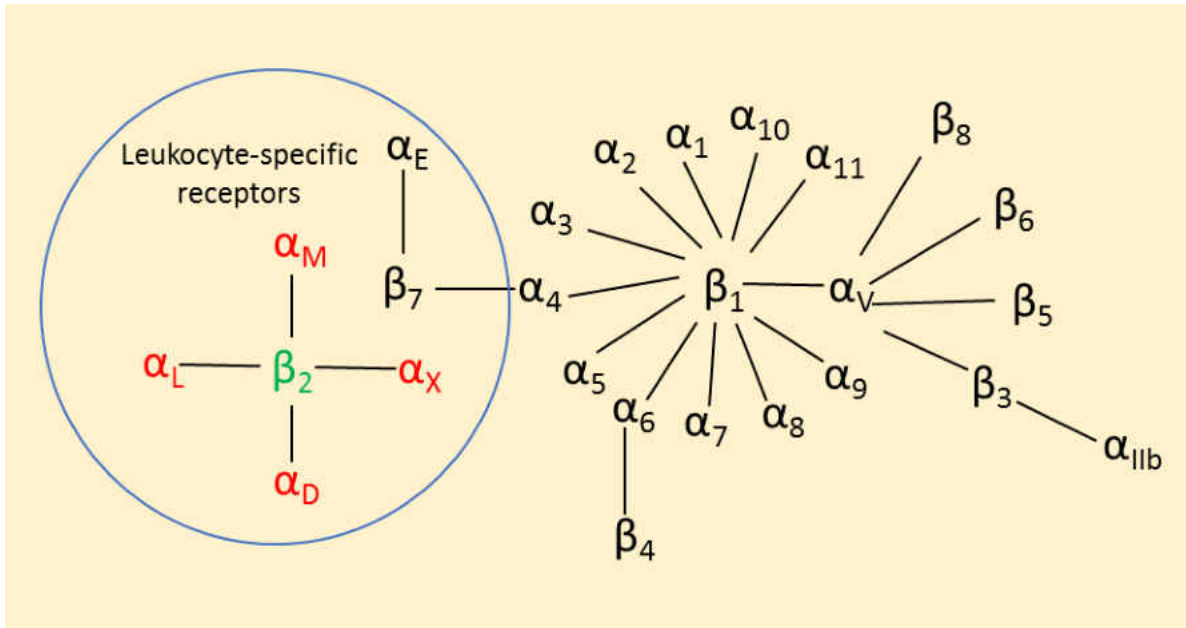
Fig. 1-3 The Superfamily of Integrins (adapted from reference (Niu and Chen 2011)). 24 different integrins have been identified in human consisting of 18 α subunits and 8 β subunits. Leukocyte-specific integrins have distinct ligand-binding specificity and tissue and cell distribution. Integrin β_2 subfamily presents highly homogenous among α I-domain containing integrins $\alpha_L\beta_2$, $\alpha_M\beta_2$, $\alpha_X\beta_2$ and $\alpha_D\beta_2$.

Inflammatory Diseases

Inflammation is a crucial part of the body's response to injury and infection. The purpose of inflammation is to eliminate the damaged tissues, irritant and pathogens (Eming et al. 2017). Inflammation can be classified as either acute or chronic. Acute inflammation occurs after the affection of harmful bacteria or injured tissue, which starts rapidly and have a short-term process (Kumar et al. 2004). Unlike acute inflammation, chronic inflammation can have long-term and whole-body effects. It is also called persistent, low-grade inflammation because it produces a steady, low-level of inflammation throughout the body (Lowe and Storkus 2011). There are many diseases associated with inflammation, such as atherosclerosis (Frostegard 2013; Woollard and Geissmann 2010), obesity (Johnson et al. 2012), diabetes (Lontchi-Yimagou et al. 2013), arthritis

(Young et al. 2013), Alzheimer's disease (Apostolova 2016; Watson and Craft 2006) and others. The development of chronic inflammation is characterized by excessive accumulation of macrophages at inflammatory sites (Parisi et al. 2018).

In this thesis, we study the role of macrophage integrins during inflammation and its associated diseases.

Atherosclerosis

Atherosclerosis, a leading cause of morbidity and mortality in western society, is a multifactorial and chronic inflammatory disease (Falk 2006; Lusis 2000). It is characterized by low-density lipoprotein (LDL) cholesterol deposition and macrophage accumulation in the arterial intima (Bobryshev et al. 2016; Charo and Taubman 2004; Hilgendorf et al. 2015). The massive uptake of oxidized LDL (oxLDL) and excessive cholesterol esterification result in the formation of foam cells and subsequently create plaques (Chistiakov et al. 2016; Moore et al. 2013; Yu et al. 2013). These plaques may eventually ruptures and causes hemorrhages, which leads to severe conditions such as stroke, heart attack and other cardiovascular diseases (Swirski and Nahrendorf 2013). Recent studies suggest that macrophages play an important role in the development of atherosclerotic lesions because they participate in all stages of plaque formation and progression (Bories and Leitinger 2017; Groh et al. 2018). In the early stage, circulating monocytes migrate from the blood stream to the intimal layer, locally polarized into macrophage subsets, engulf the accumulated oxidized lipids and become foam cells, which is a key step of the formation of atherosclerosis (Shapiro and Fazio 2017). Foam cells accumulate at the lesions and eventually cause the failure of the resolution. During immune responses, T helper (Th) cells are capable to influence macrophage phenotypes which contribute to the process of atherosclerotic lesions. Th1 cytokines, including IFN-γ and TNF-α, mediate a pro-inflammatory activation of macrophage in the lesion sites. While Th2 cytokines, IL-4 and IL-10, may suppress various of cytokines including IL-2 and IFN-γ in Th cells and macrophages, which attenuates macrophage-mediated inflammation and facilities the tissue remodeling (Jenkins et al. 2011; Verreck et al. 2004).

The phenotype of accumulated macrophages in the lesions regulates the fate of atherosclerosis. In our previous study, we found that integrin $\alpha_D\beta_2$, significantly up-regulated in atherosclerotic lesions (Aziz et al. 2017), suggesting an important function of integrin $\alpha_D\beta_2$ within

the sites of the lesions. To understand the role of the highly-expressed integrin $\alpha_D\beta_2$ on macrophage during the migration and retention of inflammation may facilitate the therapeutic intervention against atherosclerosis.

Obesity and Diabetes

Diabetes is characterized by metabolic disorders with high blood sugar levels over the prolonged period (Shirin et al. 2019). It is an increasing global epidemic and remains the 7th leading cause of death in the United States in 2015 with enormous social and healthcare costs according to World Health Organization database. There are mainly three types of diabetes: Type 1 diabetes (T1D) is referred as a failure to produce enough insulin due to the defective function of pancreas (de Ferranti et al. 2014). Type 2 diabetes (Baxter et al. 2016) (T2D) is an obesity-associated chronic metabolic inflammation and characterized by insulin resistance and relative lack of insulin. Gestational diabetes (Coustan 2013) occurs when a woman without diabetes develops high blood sugar levels during pregnancy and usually resolves after the baby is born. Here, we will focus on obesity-associated T2D making up about 90% of cases of diabetes among these three types.

Diabetes is associated with serious health complications, such as atherosclerosis, heart disease ischemia, diabetic retinopathy and impaired wound healing (Haberka et al. 2019; Jenkins et al. 2015; Jin et al. 2016; Lejay et al. 2016; Tellechea et al. 2016). During obesity, immune cells such as macrophages accumulate in visceral adipose tissue which is a major mechanism leading to the low-grade inflammation (Engin 2017; Jing et al. 2018). Adipose tissue is composed of the white adipose tissue (WAT) and brown adipose tissue (BAT). Compared to BAT, WAT appears to be a major site for production of inflammatory cytokines, including TNF-α, IL-1, IL-6, IL-10 and many other biomarkers involved in the inflammatory pathways (Shoelson et al. 2006). Inflammatory cytokines and chemokines can be markedly increased during hyperglycemia through the activation of nuclear factor-κB, which can further result in an increasing expression of various adhesion molecules (Antonov et al. 2011; Sheikh et al. 2005). The upregulated expression of adhesion molecules and chemokines can not only aggravate the pathological state of diabetes (Devaraj et al. 2010), but also affects the infiltration, recruitment and retention of immune cells in different organs (Lammermann et al. 2008; Yakubenko et al. 2008). In particular, macrophages as

a critical subset of immune cells are attracted to an inflamed site by chemoattractant, act as effector immune cells in pathogens killing, tissue remodeling, initiation of inflammation and insulin resistance (Parisi et al. 2018; Thomas and Apovian 2017). The recruitment and accumulation of monocytes/macrophages at the inflammatory sites depends on macrophage adhesive receptors (Shi and Pamer 2011). The mechanism of macrophage retention is an important subject that has a strong therapeutic potential.

Macrophages and Inflammatory Diseases

Macrophages are cells of the innate immune system that populate every organ. They display great functional plasticity and are required for maintenance of tissue homeostasis, immunity against invading pathogens, and tissue repair (Kierdorf et al. 2015; Lavin et al. 2015; Wynn and Vannella 2016). In response to different microenvironmental stimulus, macrophage may polarize into several phenotypes (pro-inflammatory M1 or anti-inflammatory M2 subsets) at the sites of inflammation and exhibit different morphology and functional properties after activation (Chinetti-Gbaguidi et al. 2015). Classically activated-M1 macrophages can be induced by interferon (IFN)-γ and lipopolysaccharides (LPS). It has pro-inflammatory, microbicidal, phagocytic and tissue damage functions and releases a broad proinflammatory cytokines, such as interleukin (IL)-6, IL-12, tumor necrosis factor (TNF)-α and inducible nitric oxide synthase (iNOS). Unlike M1 macrophages, the alternative activated-M2 macrophages are induced by IL-4 and IL-13 expresses high levels of IL-10, IL-1β and low levels of IL-12 (McNelis and Olefsky 2014). From a functional view, M2-activated macrophages can scavenge debris and promote tissue repair and healing during resolution of inflammation (Roszer 2015). Moreover, recent studies indicate that anti-inflammatory M2 macrophages induced by IL-4 are associated with the activation of signal transducer and activator of transcription 6 (STAT6) and PPARγ-coactivator-1β (PGC-1β), and involved in lipid oxidative metabolism to the anti-inflammatory program of macrophage activation (Vats et al. 2006).

In addition, macrophages are plastic and can adapt their phenotypes based on the microenvironment they encountered. Evidence of phenotype switching in neuroinflammatory disease like multiple sclerosis suggests that monocytes enter the central nervous system (CNS) and polarize into M1 macrophages. Over the course of the disease, the conversion from M1 phenotype

to M2 macrophage were observed in the lesion. Also, macrophage phenotypes are reversible under the stimulating by inflammatory cytokines (Locatelli et al. 2018). Carey's study demonstrated that diet-induced obesity can result in a M1 proinflammatory state contributing to insulin resistance. Upon high-fat feeding, a switch from M2 polarized macrophage to an M1-activated state lead to the loss of protective potential under lean conditions (Lumeng and Saltiel 2011).

The apolipoprotein E knockout (ApoE$^{-/-}$) mouse lacks the glycoprotein apolipoprotein E, which is essential for lipid transport and metabolism (Getz and Reardon 2016). These mice have a poor ability to clear lipoprotein, making it a useful mouse model to study human atherosclerosis when placed on a high-fat diet. Macrophage from the blood circulation to the inflammatory sites is an important part of the innate immune response. According to the physical conditions, macrophages are able to migrate in different modes. They may encounter 2D surfaces, such as the endothelial monolayers of blood vessels or basement members using classical five-step migration model (Wiesner et al. 2014). However, in vivo, 3D environments, macrophages can migrate through most tissues or ECM using at least two distinct migration modes (Sridharan et al. 2019). The amoeboid migration mode which is characterized by a movement of spherical or ellipsoid cells that squeeze along the porous ECM, such as fibrillar collagen I, and with a relatively high speed (Liu et al. 2015; Pals et al. 2007). Another migration mode, mesenchymal migration, displays an elongated morphology with multiple long protrusions and a low migration speed to infiltrate high dense matrices, such as matrigel or fibrin gel (Doyle et al. 2015; Driscoll and Danuser 2015). In heterogeneous environments, macrophage combines the two migration modes to get to the destination. Importantly, mesenchymal migration strongly depends on the involvement of integrins.

Our published results and others indicate that cell migration has a bell-shape pattern based on the cell adhesiveness (Lishko et al. 2004; Palecek et al. 1997; Yakubenko et al. 2008). The low adherent property is insufficient for macrophage migration, the intermediate level of adhesiveness generates good cell migration, but very high adhesiveness will prevent cells releasing from the extracellular matrix, which inhibit cell motility.

However, the mechanism of the retention of macrophage at the site of inflammation is still under debate. Our work demonstrated that the expression of integrin $\alpha_D\beta_2$ on classically activated

macrophage is significantly upregulated and the high expression of integrin $\alpha_D\beta_2$ increases cell-substratum adhesiveness, which causes macrophage retention at the inflammatory sites of the lesions.

Questions to be Answered in These Studies

The migration, accumulation and retention of macrophages in the inflammatory sites are critical steps during the process of many devastating diseases including arthritis, diabetes, obesity and atherosclerosis (Libby 2002; Mallat 2014; Moore and Tabas 2011; Tabas and Bornfeldt 2016; Weber et al. 2008). Adhesion molecules such as β_2 integrins are extensively involved in the recruitment of leukocytes from the bloodstream to the damaged peripheral tissues and the retention of macrophage within the lesions (Herter and Zarbock 2013; Mitroulis et al. 2015). However, a typical ECM has a limited availability of ligands for β_2 integrins. One of the possible mechanisms of directing macrophage migration is the modification of existing ECM during inflammation.

2-(ω-Carboxyethyl)pyrrole (CEP) is formed through adduction of the end products of DHA oxidation with the ϵ-amino groups of protein lysyl residues. CEP generation was reported to contribute to a number of inflammation-associated diseases, including macular degeneration, hyperlipidemia, atherosclerosis, thrombosis, and tumor progression (Kim et al. 2015; Panigrahi et al. 2013). However, the pro-inflammatory mechanism of CEP function is not clear. So far, the accumulation of CEP in the damaged tissue and induction of pro-inflammatory cytokines from macrophages in response to CEP represents the data that may explain the contribution of CEP to the augmentation of inflammatory responses (Cruz-Guilloty et al. 2014; Kettle et al. 1995; Schneider and Issekutz 1996; Stelmaszynska et al. 1992; Zerouga et al. 1996). The first section of my studies is to seek a possible link between CEP and β_2 integrins-mediated macrophage migration/accumulation at the site of inflammation. This section of my work is partial of our published paper in *Blood* and is highlighted in Chapter 2, demonstrating a novel mechanism of macrophage migration during inflammation mediated by integrins $\alpha_D\beta_2$ and $\alpha_M\beta_2$.

In the first section, we found that both integrins ($\alpha_D\beta_2$ and $\alpha_M\beta_2$) are involved in the migration of macrophages during inflammation. However, the expression levels of integrin $\alpha_D\beta_2$ and $\alpha_M\beta_2$ are significant different on macrophages within the atherosclerotic lesions. Integrin $\alpha_M\beta_2$

is a major β_2 integrin on macrophages, while integrin $\alpha_D\beta_2$ (CD11d/CD18) is the most recently discovered, but largely undefined, member of β_2 integrins. Unlike the other three members of β_2 integrins ($\alpha_M\beta_2$, $\alpha_L\beta_2$ and $\alpha_X\beta_2$), it is poorly expressed on peripheral blood leukocytes but significantly up-regulated in the atherosclerotic lesions (Noti 2002; Van der Vieren et al. 1995). Moreover, our publication in *Journal of Immunology* indicates that α_D-deficiency on an ApoE$^{-/-}$ background reduces the development of atherosclerosis (Aziz et al. 2017). This specific expression pattern of integrin $\alpha_D\beta_2$ indicates that it is likely to have important functions within the sites of inflammation. <u>The goal of the second section</u> is to determine the role of β_2 integrins, particularly $\alpha_D\beta_2$ and $\alpha_M\beta_2$, in regulating the migration of macrophage to the inflammatory sites and the retention of macrophage within the lesions (Cui et al. 2018). This part of work is published in *Frontiers in Immunology* and is highlighted in Chapter 3, entitled "Distinct migratory properties of M1, M2 and resident macrophages are regulated by $\alpha_D\beta_2$ and $\alpha_M\beta_2$ integrin-mediated adhesion."

Based on our publications and current studies, we suggest that 1) integrin $\alpha_D\beta_2$ is a multi-ligand receptor, which is strongly expressed on macrophages in atherosclerotic lesions (Yakubenko et al. 2006), and α_D-deficiency on an ApoE$^{-/-}$ background reduces the development of atherosclerosis. 2) Low expression of integrin $\alpha_D\beta_2$ facilitates macrophage migration whereas a high density of $\alpha_D\beta_2$ integrin promotes macrophage retention within the site of inflammation (Aziz et al. 2017; Yakubenko et al. 2008). Our studies suggest that integrin $\alpha_D\beta_2$ is not only involved in macrophage migration, but also may play a critical role in regulating macrophage retention at inflammatory sites. Therefore, targeting integrin $\alpha_D\beta_2$ could potentially reduce the retention of macrophages in the inflamed lesions and may provide a new therapeutic approach for the treatment of macrophage mediated-chronic inflammatory diseases.

In Chapter 4, we propose a new strategy for the treatment of chronic inflammation by targeting macrophage retention in the inflamed tissue by focusing on the development of the inhibitor, which is exclusively specific for $\alpha_D\beta_2$-CEP interaction. The advantage of CEP as a new therapeutic target resides in its unique formation in inflamed tissue.

CHAPTER 2

NEW MECHANISM OF MACROPHAGE MIGRATION DURING INFLAMMATION MEDIATED BY INTEGRINS $\alpha_D\beta_2$ AND $\alpha_M\beta_2$

Valentin P. Yakubenko PhD*[¥][®], Kui Cui*, Christopher L. Ardell*, Moammir H. Aziz PhD*, Kathleen E. Brown[¥], Xiaoxia Z. West[¥], Robert G. Salomon PhD[#], Eugene A. Podrez PhD[¥], Tatiana V. Byzova PhD[¥].

[¥]*Department of Molecular Cardiology, Lerner Research Institute, Cleveland Clinic; *Department of Biomedical Sciences, Quillen College of Medicine, East Tennessee State University; [#]Department of Chemistry, Case Western Reserve University.*

Short title: CEP induces integrin-mediated macrophage migration

[®] Correspondence to Dr. Valentin Yakubenko, Department of Biomedical Sciences,

 Quillen College of Medicine, East Tennessee State University, PO Box 70582, Johnson City, Email: yakubenko@etsu.edu, Phone: (423) -439-8511.

Abstract

Early stages of inflammation are characterized by extensive oxidative insult by recruited and activated neutrophils. Secretion of peroxidases, including the main enzyme, myeloperoxidase, leads to the generation of reactive oxygen species. We show that this oxidative insult leads to polyunsaturated fatty acid (eg, docosahexaenoate), oxidation, and accumulation of its product 2-(ω-carboxyethyl)pyrrole (CEP), which, in turn, is capable of protein modifications. In vivo CEP is generated predominantly at the inflammatory sites in macrophage-rich areas. During thioglycollate-induced inflammation, neutralization of CEP adducts dramatically reduced macrophage accumulation in the inflamed peritoneal cavity while exhibiting no effect on the early recruitment of neutrophils, suggesting a role in the second wave of inflammation. On macrophages, CEP adducts were recognized by cell adhesion receptors, integrin $\alpha_M\beta_2$ and $\alpha_D\beta_2$. Macrophage migration through CEP-fibrin gel was dramatically augmented when compared with fibrin alone, and was reduced by β_2-integrin deficiency. Thus, neutrophil-mediated oxidation of abundant polyunsaturated fatty acids leads to the transformation of existing proteins into stronger adhesive ligands for $\alpha_M\beta_2$- and $\alpha_D\beta_2$-dependent macrophage migration. The presence of a carboxyl group rather than a pyrrole moiety on these adducts, resembling characteristics of bacterial and/or immobilized ligands, is critical for recognition by macrophages. Therefore, specific oxidation-dependent modification of extracellular matrix, aided by neutrophils, promotes subsequent $\alpha_M\beta_2$- and $\alpha_D\beta_2$-mediated migration/retention of macrophages during inflammation.

Introduction

Understanding the mechanism of leukocyte migration is essential for the treatment of chronic inflammation, which is a major factor contributing to many devastating diseases including arthritis, diabetes, obesity and atherosclerosis[1-3]. Neutrophil recruitment is the first wave of immune response directed to fight inflammation[4] primarily by secreting peroxidases, which, in turn, generate an excess of reactive oxygen and nitrogen species to facilitate a speedy inactivation of pathogens while releasing chemotactic signals to promote a second wave of immune response, monocyte/macrophage migration[5, 6]. Arrived macrophages play a central role in the resolution of acute inflammation, essentially by removing the debris and promoting tissue healing. However, excessive or uncontrolled macrophage accumulation contributes to chronic inflammation and a number of pathologies[7].

To date, the mechanisms controlling the transition between first and second wave of inflammation are not fully understood. While chemokine gradients seem to be critical for macrophage migration, the importance of adhesive receptors and their respective ligands remains questionable. Macrophage receptors, integrins, are the major players in adhesion-mediated migration. Prominent among the leukocyte adhesion receptors are the four members of the integrin β_2 subfamily: $\alpha_L\beta_2$ (CD11a/CD18, LFA-1), $\alpha_M\beta_2$ (CD11b/CD18, Mac-1), $\alpha_X\beta_2$ (CD11c/CD18, p150, 95) and $\alpha_D\beta_2$ (CD11d/CD18)[8]. Although α_X is an important marker of pro-inflammatory macrophage activation, its expression on monocytes/macrophages is low, which reduces the contribution of α_X to macrophage migration[9]. In contrast, $\alpha_M\beta_2$ is a major β_2 integrin on macrophages and $\alpha_D\beta_2$ is upregulated during pro-inflammatory macrophage activation[10]. In our previous studies, we found that $\alpha_M\beta2$ and $\alpha_D\beta_2$ are highly homological multiligand receptors that share common ligands[11, 12] and participate in macrophage migration and retention at the site of inflammation[10]. However, a typical extracellular matrix (ECM) has a limited availability of ligands for β_2 integrins. What types of adhesive ligands are able to mediate inflammation-specific and directed macrophage migration that remains to be determined.

One of the possible mechanisms of directed macrophage migration is the modification of existing ECM during inflammation. Oxidation of polyunsaturated phospholipids (PUFA) by reactive oxygen species produced in inflamed tissues, might generate protein modifications, which, in turn, might provide macrophages with inflammation-specific ligands. As oxidation substrates, PUFAs are readily available as a part of cellular membranes as well as from dietary sources, and their products were shown to exhibit a wide spectrum of biological activities[13; 14; 15]. Despite widely advertised opinion regarding the beneficial role of 3-PUFA (particularly docosahexaenoate (DHA)) for overall health, current results of clinical trials are questioning its protective role for the cardiovascular system[16; 17; 18; 19]. Apparently, DHA derived products generated in vivo may have effects distinct from DHA itself.

2-(ω-Carboxyethyl)pyrrole (CEP) is formed through adduction of the end products of DHA oxidation with the ε-amino groups of protein lysyl residues[20, 21] (Fig.2-1). To develop tools for testing CEP function, ω-carboxyethylpyrrole-modified proteins were synthetized using Paal-Knorr reactions of γ-dicarbonyl compounds (DOHA) with the ϵ-amino group of lysyl residues of proteins[22]. DOHA was used to prepare CEP-modified keyhole limpet hemocyanin (CEP-KLH), bovine serum albumin (CEP-BSA) and human serum albumin (CEP-HSA). Using these proteins,

highly specific monoclonal and polyclonal antibodies against CEP were generated and tested for specificity[20]. Notably, a structurally similar protein modification, ethylpyrrole (EP), is generated through the alternative oxidative cleavage of DHA (Fig. 2-1). Compared to CEP, this modification lacks a carboxyl group, which makes it an excellent control for CEP functional studies[23].

CEP generation was reported to contribute to a number of inflammation-associated diseases, including macular degeneration, hyperlipidemia, atherosclerosis, thrombosis, and tumor progression[24,25,23, 26]. However, the pro-inflammatory mechanism of CEP function is not clear. So far, the accumulation of CEP in the damaged tissue and induction of pro-inflammatory cytokines from macrophages in response to CEP represents the data that may explain the contribution of CEP to the augmentation of inflammatory responses[27; 28; 23; 29; 30]. The goal of our investigation was to seek a possible link between CEP and macrophage migration/accumulation at the site of inflammation.

Materials and Methods

Materials

Reagents were purchased from Sigma-Aldrich (St. Louis, MO). Human fibrinogen and thrombin were obtained from Enzyme Research Laboratories (South Bend, IN). Fibronectin and plasmin were purchased from Millipore. Myeloperoxidase (MPO) was from Sigma-Aldrich (St. Louis, MO). Anti-CD68 mAb was from eBioscience. Anti-Fg antibody was from LifeSpan Biosciences (Seattle, WA). The mAb IB4 directed against the β_2 integrin subunit and mAb 44a directed against the human α_M integrin (CD11b) subunit was purified from the conditioned media of the hybridoma cell line obtained from American Type Culture Collection (ATCC, Manassas,VA) using protein A agarose (GE Healthcare, Piscataway, NJ). Anti-human integrin α_D mAb (clone 240I) was generously provided by Eli Lilly Corporation (Indianapolis, IN). Purified rabbit, mouse and rat IgG were purchased from Sigma-Aldrich (St. Louis, MO). Polyclonal antibody against CEP and monoclonal IgM anti-CEP antibody were obtained as described previously[31, 32]. Blocking IgG anti-CEP antibody (Clone 3C9) was generated in Dr. Tatiana Byzova's laboratory[33]. Rabbit polyclonal antibody against α_D I-domain was generated in Dr. Tatiana Ugarova's laboratory and produced as described previously[34].

Mice

Wild type (C57BL/6J) mice, β_2-deficient mice (B6.129S7-*Itgb2^{tm2Bay}*/J) and MPO-deficient mice (B6.129X1-*Mpo^{tm1Lus}*/J) were bought from Jackson laboratory (Bar Harbor, ME). All procedures were performed according to animal protocols approved by the Cleveland Clinic and East Tennessee State University IACUC.

To generate macrophage-depleted mice, a Clodrosome macrophage depletion kit was used according to the manual. In brief, mice were injected with 0.15 ml of control or Coldronate-liposome intravenously (1st day) and intraperitoneally (2nd and 3rd days) for 3 consecutive days. For neutrophil depletion, mice were injected intraperitoneally with anti-Ly-6G antibody (100 µg/ml) following 24 hours of incubation. The depletion was evaluated by a marked reduction of neutrophils or macrophages in the peritoneal cavity after thioglycollate injection.

Peritoneal model of inflammation and macrophage isolation

Peritonitis was induced by intraperitoneal injection of 1 ml 3% Brewer thioglycollate medium (Sigma-Aldrich, St. Louis, MO) in C57BL/6 mice (Jackson Laboratories, Bar Harbor, ME). It has been shown that sterile inflammation, mediated by thioglycollate, leads to the accumulation of leukocytes in the peritoneal cavity with neutrophils peaking at 6-18 hours and macrophages at 72-96 hours after thioglycollate injection. After 18 or 72 hours, the mice were euthanized by isoflurane inhalation and the peritoneal cavities were lavaged with 5 ml PBS. In experiments with antibodies, 5 µg of purified anti-CEP monoclonal IgM antibody per gram of body weight or the same concentration of normal mouse IgM diluted in PBS were injected intraperitoneally 30 min before thioglycollate injection. Peritoneal cells were counted in a hemocytometer followed by FACS with anti-macrophage antibody (F4/80).

For macrophage isolation, peritoneal cells at 72 hours after thioglycollate injection were isolated from the cavity and plated on a 10 cm petri dish for 2 hours at 37 °C in humidified air containing a 5% CO_2 atmosphere. After incubation, petri dishes were washed with PBS to remove non-adherent cells. Adherent cells were collected with 5 mM EDTA in PBS, then centrifuged to change the media to Hank's balanced salt solution supplemented with 1 mM $MgCl_2$ and 1 mM $CaCl_2$. These cells were then used for adhesion or migration assays.

Immunostaining

Cryosections (10 µm) of peritoneal tissue were warmed to room temperature for 30 minutes prior to immunofluorescence staining. Tissue sections were fixed in ice-cold acetone for 10 minutes, followed by permeabilization with 0.2% Tween-20 for 10 minutes to increase the signal of intracellular binding sites. Tissue sections were washed in PBS and incubated with SuperBlock (PBS) Blocking buffer (Thermo Scientific, Rockford, IL, USA) for 45 min to block nonspecific binding. Tissues were then incubated at 4 °C overnight with the primary antibodies (rabbit polyclonal anti-CEP and rat anti-mouse CD68 (macrophage marker)). After washing several times with PBS, the sections were incubated with Alexa Fluor 488-conjugated donkey anti-rabbit IgG and Alexa Fluor 568-conjugated donkey anti-rat for 1 hour at room temperature. The sections were subsequently washed and sealed. The tissue sections were examined with a fluorescence microscope (EVOS, Thermo Fisher Scientific, Waltham, MA USA). Control sections without primary antibody were also generated at the same time.

Immunoprecipitation and Western blot

Mouse peritoneal exudate at 72 hours after injection of thioglycollate was incubated with anti-CEP or anti-fibrinogen antibodies (10 µg) for 4 hours at 4 °C. The mAb-specific complex was captured by incubating with 50 µl of Protein G Sepharose (Amersham Biosciences, Inc., Piscataway, NJ) for 12 h at 4°C. The immunoprecipitated proteins were eluted with SDS-PAGE loading buffer and analyzed by (4-15%) SDS-PAGE electrophoresis or Western blotting. The Immobilon-P membranes (Millipore) were incubated with rabbit polyclonal anti-CEP antibody, followed by incubation with goat anti-rabbit secondary antibody conjugated to horseradish peroxidase and developed using enhanced SuperSignal Chemiluminescent Substrate (Pierce).

Isolation of human neutrophils and CEP formation assay

The protocol for isolation of human neutrophils complied with all relevant federal guidelines and institutional policies regarding the use of human subjects. Neutrophils were isolated by centrifugation as described before [35]. Eosinophils were removed by sorting [36].

Neutrophils were isolated and incubated in phenol-free RPMI 1640 medium. 10^6 neutrophils were activated with IL1β (200 ng/ml) and LPS (100ng/ml) from Difco (Voigt Global Distribution Inc, Lawrence, KS), and incubated for 2 hours in media supplemented with 5% FCS and L-arginine (100 μM) as described before [37]. MPO inhibitor 4-ABH (BioVision, Milpitas, CA) was used at 1 μM. Resorcinol (Sigma-Aldrich) was used at 10 μM (at this concentration it was shown to affect Eosinophil peroxidase but to a lower extent MPO [38]). Supernatant samples were collected, and 100 μM (final concentration) of butylated hydroxytoluene (Sigma) was added. CEP and EP production was measured by competitive ELISA as described previously [31].

Generation of CEP-modified fibrinogen by recombinant MPO

Human fibrinogen was coated on a 96-well plate at a concentration of 50 μg/ml for overnight incubation at 4^0C. Wells were post-coated with 0.5% polyvinyl alcohol for 1 h at 37^0C. 2 μM DHA and 0.5mU/ml MPO in 20mM Hepes, 150 mM NaCl, 0.01% H_2O_2, and 1mM $CaCl_2$ were added to the wells and incubated in an oxygen-free environment (under argon atmosphere) for 18 hours at 37^0C. After incubation, the plate was washed out with PBS supplemented with 0.05% Tween 20 and incubated with anti-CEP polyclonal antibody (0.9 μg/ml) for 2 hours at 37^0C. After washing, wells were incubated with goat anti-rabbit HRP conjugated antibody for 1 h at 37^0C and the binding was developed using TMB-ELISA substrate solution (Pierce). The result was detected by a plate reader using a wavelength of 450 nm.

In a parallel experiment, 100 μg/ml fibrinogen was incubated with 2 μM DHA and 0.5 mU/ml MPO in 20 mM Hepes, 150 mM NaCl, 0.01% H_2O_2, a 1mM $CaCl_2$ buffer in a microtube in an oxygen-free environment (under argon atmosphere) for 18 hours at 37^0C. After incubation, the samples were analyzed by Western Blot with anti-CEP polyclonal antibody as described above.

Neutrophil and macrophage 3-D migration in fibrin gel

Neutrophils or macrophages were labeled with PKH26 red fluorescent dye or PKH67 green fluorescent dye. Cell migration assay was performed for 24h (neutrophils) or 48h

(macrophages) at 37 °C in 5% CO_2 under sterile conditions. Labeled leukocytes were plated on the membranes of transwell inserts of a Boyden chamber with a pore size of 8 μm and 6.5 mm in diameter (Costar, Corning, NY), precoated with fibrinogen (Fg). Fibrin gel in the transwell (100 μl/sample) was made using 0.75 mg/ml Fg containing 1% FBS and 1% P/S and activated by 0.5 U/ml thrombin. Before the experiment, the gel was analyzed for the presence of autofluorescence /non-specific signal using a Leica Confocal microscope (Leica-TCS SP8). 100 nM FMLP or 30 nM MCP-1 were added on the top of the gel to initiate the migration. Migrating cells were detected by Leica Confocal microscope (Leica-TCS SP8) using a 3x3 area (9 fields of view per sample) with magnification 100x; up to a depth of 1000 μm with a step size of 5 μm. The results were analyzed by IMARIS 8.0 software.

FACS analysis

FACS analyses were performed to assess the expression of receptors on the surface of the cells transfected with $\alpha_D\beta_2$, $\alpha_M\beta_2$, and $\alpha_L\beta_2$ integrins. The cells were incubated with anti-α_D (Clone 1566) [8], anti-α_M (clone M1/70), anti-α_L (clone 38) and anti-β_2 (clone IB4) antibodies and analyzed using a FACScan™ (Beckton Dickinson) or Fortessa X-20 (Beckton Dickinson) as described previously.[10]

For the binding assay, $1x10^6$ $\alpha_M\beta_2$- and $\alpha_D\beta_2$-HEK293 cells were incubated with 400 nM CEP-BSA or 400 nM EP-BSA for 30 min at 37^0C followed by incubation with 10 μg/ml blocking anti-α_M (clone 44a) and anti-α_D (clone 240I) antibody. After incubation, cells were analyzed with a Fortessa X-20 (Beckton Dickinson).

Cell adhesion and 2D migration

The adhesion assay was performed as described previously[39], with some modifications. Briefly, 96-well plates (Immulon 2HB, Cambridge, MA) were coated with different concentrations of CEP-BSA, EP-BSA, fibrinogen or other ligands for 3 h at 37 °C. The wells were post-coated with 0.5% polyvinyl alcohol for 1 h at 37 °C. Mouse peritoneal macrophages or HEK 293 cells transfected with $\alpha_L\beta_2$, $\alpha_M\beta_2$, or $\alpha_D\beta_2$ integrins were labeled with 10 μM Calcein AM (Molecular Probes, Eugene, OR) for 30 min at 37 °C and washed with DMEM and resuspended in the same

medium at a concentration of 1×10^6 cells/mL. Aliquots (50 µL) of the labeled cells were added to each well. For inhibition experiments, cells were mixed with antibodies and incubated for 15 minutes at 22 °C before they were added to the coated wells. After 30 minutes of incubation at 37 °C in a 10% CO_2 humidified atmosphere, the nonadherent cells were removed by washing with HBSS. The fluorescence was measured in a Synergy H1 fluorescence plate reader (BioTek, Winooski, VT), and the number of adherent cells was determined from a labeled control.

2D cell migration assays with calcein-labeled cells were performed under sterile conditions using uncoated Transwell® inserts with a pore size of 8 µM and that were 6.5 mm in diameter (Costar, Corning, NY). Briefly, the lower chambers contained 600 µl of CEP or EP. Cells (150 µl) in DMEM/F-12 at a concentration of 2.5 x 10^6/ml were placed in the upper chamber and allowed to migrate for 18 h at 37 °C in 5% CO_2. 2 hours prior to the completion of the migration assay, calcein AM was added to the lower chamber in order to label cells. Assays were stopped by removing cells from the upper surface of the polycarbonate membrane. Cells migrating to the bottom of the filter were detected using a Synergy H1 fluorescence plate reader Synergy H1 fluorescence plate reader (BioTek, Winooski, VT).

Isolation of recombinant α_D, α_M and α_L I domains in the active and non-active conformation

The construct for α_D I domains, α_M I domains and α_L I domain were generated and recombinant proteins were isolated as described in our previous paper [34]. Briefly, α_D in non-active conformation (Pro^{128}-Ala^{323}), α_M in active conformation (E^{123}-K^{315}), α_M in non-active conformation (Q^{119}-E^{333}) and α_L in active conformation (Gly^{128}-Tyr^{307}) were inserted into a PGEX4T-1 vector. In α_L I domains, two lysines, Lys^{287} and Lys^{294}, were substituted to cysteins to create a disulfide bond and thus lock the protein in the active conformation as described before [40]. In "active" α_M I domains, the unpaired Cys^{128} was substituted to Ser to prevent I domain dimerization [41]. Proteins were expressed in E. Coli and purified using affinity chromatography on glutathione agarose and its fusion part removed by thrombin. α_D in active conformation (Pro^{128}-Lys^{314}) was inserted into a pET15b vector, expressed in E. Coli as a His-tag fusion protein and purified using affinity chromatography on Ni-chelating agarose (Qiagen Inc., Valencia, CA).

Statistical analyses were performed using Student's *t*-test or Student's paired *t*-tests, as indicated in the text, using SigmaPlot 13. A value of p<0.05 was considered significant.

Results

CEP is involved in macrophage accumulation in the peritoneal cavity.

Numerous data demonstrate the involvement of CEP in the inflammatory process [27; 28; 23; 29; 30]. We tested CEP and EP accumulation during acute inflammation in the peritoneal tissue after thioglycollate-induced peritoneal inflammation. Normal tissue is characterized by strong deposition of EP, but was devoid of CEP completely. However, induction of inflammation led to the marked accumulation of CEP in the peritoneal wall (Fig. 2-2 A, B). Interestingly, CEP staining often overlaps with macrophage staining, which suggests a link between CEP and macrophage accumulation during peritoneal inflammation. It has been shown that sterile inflammation mediated by thioglycollate leads to the accumulation of leukocytes in the peritoneal cavity with neutrophils peaking at 6-18 hours and macrophages at 72-96 hours after thioglycollate injection [42]. Anti-CEP monoclonal antibody was injected into the peritoneal cavity of mice one hour before and 24 hours after injection of thioglycollate. We found that thioglycollate-induced accumulation of macrophages in the peritoneal cavity after 72 hours was dramatically reduced in the presence of anti-CEP antibody, while neutrophil accumulation after 18 hours was not affected (Fig. 2-2C).
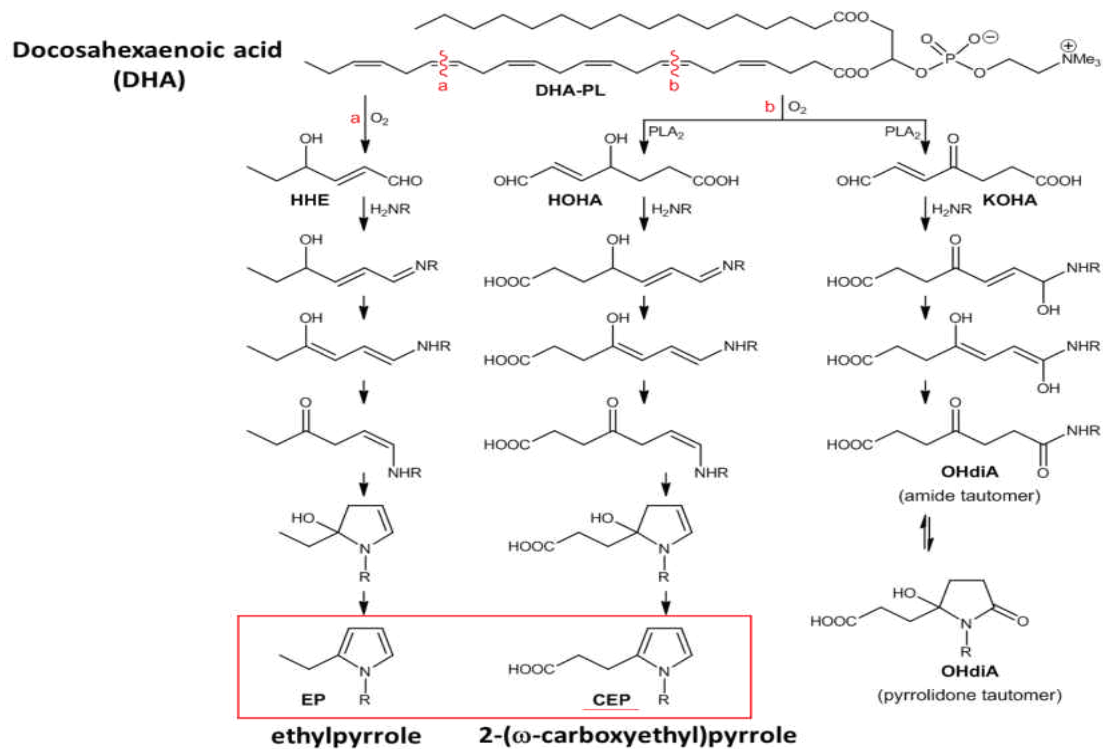
Figure 2-1. Schematic representation CEP and EP formation. PLA2-catalyzed hydrolysis of DHA generates HOHA, which, in turn, produces CEP–protein derivatives through condensation with the primary amino groups of protein lysyl residues, as was described previously.[18] A structurally similar protein modification, EP, is generated through the alternative oxidative cleavage of DHA to give 4-hydroxyhex-2-enal followed by condensation of 4-hydroxyhex-2-enal with the e-amino group of lysyl residues. Compared with CEP, this modification lacks a carboxyl group. HHE, 4-hydroxyhexenal; HOHA, 4-hydroxy-7-oxo-hept-5-eonate.
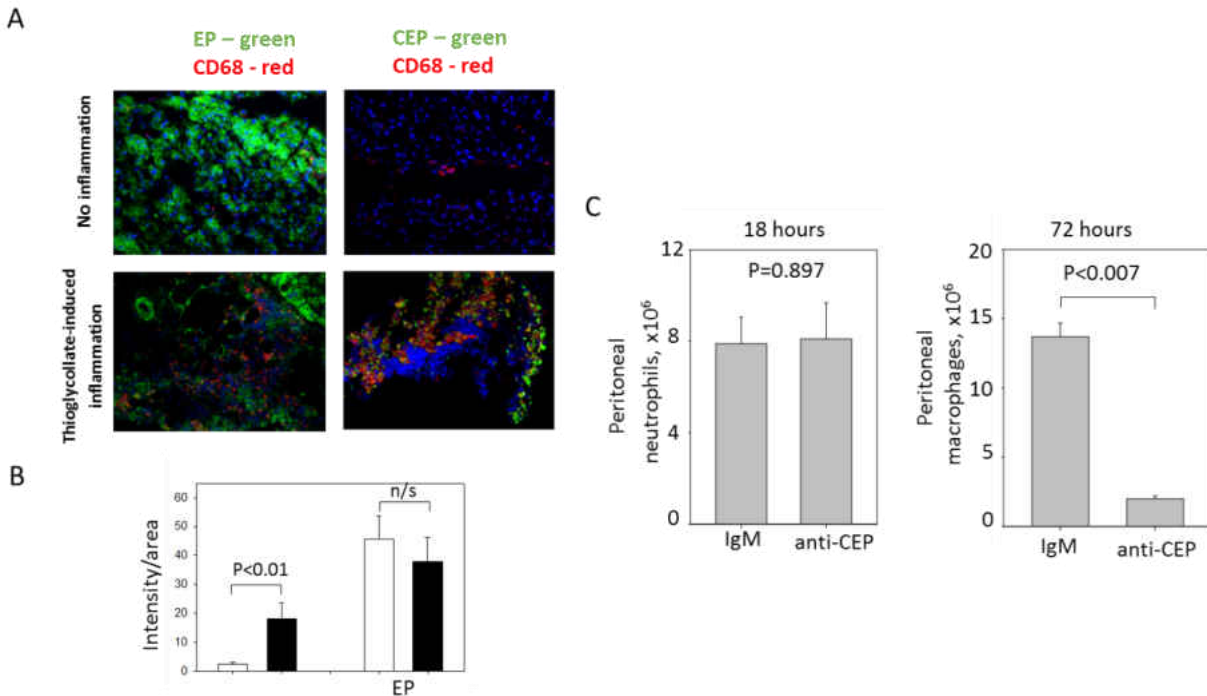
Fig. 2-2. A, B. Deposition of EP (A, left panels) and CEP (A, right panels) in the normal and inflamed peritoneal tissues. Peritoneal tissues were isolated from mice at 72 hours after thioglycollate-induced inflammation (A, lower panels) or from non-treated mice as a control (A, upper panels). Immunofluorescent staining demonstrates EP or CEP (green fluorescence) and CD68 (red fluorescence). Magnifications 200x. **B**. CEP and EP staining was analyzed using Fiji software. **C. Neutrophil and macrophage accumulation in the peritoneal cavity during thioglycollate-induced peritoneal inflammation after anti-CEP mAb treatment.** Mice were injected twice with anti-CEP mAb or IgM control (30 min before and 24 after the injection of 1 ml of 3% thioglycollate). Neutrophils were isolated at 18 hours and macrophages were isolated at 72 hours after thioglycollate injection. Statistical analysis was performed using Student's t-test (n=5 per group for neutrophils and n=9 per group for macrophages).

$\alpha_M\beta_2$ and $\alpha_D\beta_2$, but not $\alpha_L\beta_2$-transfected cells, adhere to CEP.

The subfamily of b2 integrins consists of 4 members, $\alpha_M\beta_2$, $\alpha_D\beta_2$, $\alpha_L\beta_2$, and $\alpha_X\beta_2$. Although $\alpha_M\beta_2$, $\alpha_D\beta_2$, and $\alpha_L\beta_2$ demonstrate strong expression on macrophages, the level of integrin $\alpha_X\beta_2$ is low, which reduces its potential role in integrin-mediated adhesion and migration. To further

confirm the role of β_2 integrins, we used $\alpha_M\beta_2$-, $\alpha_D\beta_2$-, and $\alpha_L\beta_2$-transfected HEK293 cells previously generated in our laboratory (Figure 2-3C).[11,12] We tested their ability to bind CEP-BSA and found that $\alpha_D\beta_2$- and $\alpha_M\beta_2$-transfected, but not $\alpha_L\beta_2$-transfected or control mock-transfected cells, strongly adhered to CEP (Figure 2-3B). In contrast, adhesion to BSA or EP was not detected for $\alpha_D\beta_2$- and $\alpha_M\beta_2$-transfected cells (Figure 2-3B-D). HEK 293 cells express endogenous β_1 integrins including $\alpha_1\beta_1$, $\alpha_2\beta_1$, $\alpha_4\beta_1$, and $\alpha_5\beta_1$; therefore, the lack of adhesion of mocktransfected HEK293 cells to CEP confirmed integrin β_2 specificity for CEP. The adhesion of $\alpha_D\beta_2$- and $\alpha_M\beta_2$-transfected cells was significantly inhibited by anti-CEP, anti-β_2, and anti- α_D (or anti- α_M) antibodies, but not by anti-β_1 antibody (Figure 2-3C-D). In addition, we demonstrated that preincubation of $\alpha_M\beta_2$ and $\alpha_D\beta_2$ cells with CEP in solution decreased the binding of blocking anti-α_M and anti-α_D antibodies more than twofold (Figure 2-4). These data prove the hypothesis that integrin $\alpha_M\beta_2$ and $\alpha_D\beta_2$ are receptors for CEP-modified proteins.
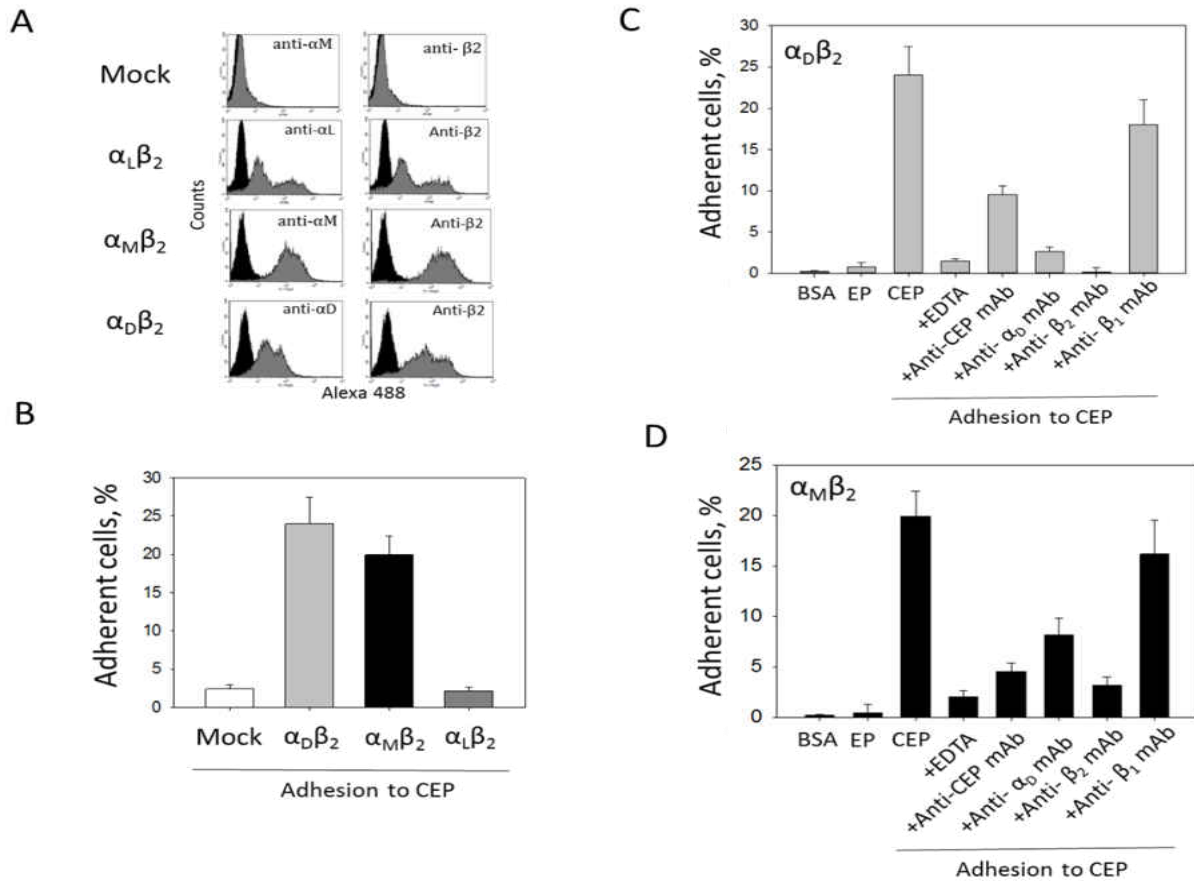
Fig. 2-3. Adhesion of HEK 293–transfected cells to CEP. A-D. (A) $\alpha_M\beta_2$, $\alpha_D\beta_2$, and $\alpha_L\beta_2$-HEK 293-transfected cells were generated as described in the "Materials and methods" section and

tested by flow cytometry analysis. The mock-transfected cells are shown only with anti-α_M mAb. A similar result was obtained with anti- α_L and anti- α_D antibodies. Ninety-six-well plates were coated with CEP (B) or different ligands (C-D) for 3 hours at 37°C. $\alpha_M\beta_2$, $\alpha_D\beta_2$, $\alpha_L\beta_2$, or mock-transfected cells were labeled with 10 mM Calcein AM. (C-D) For some experiments, cells were preincubated with anti-integrin blocking antibodies. In separate wells, immobilized CEP-BSA was preincubated with anti-CEP mAb. After incubation, cells were added to the wells and cell adhesion was determined after 30 minutes in a fluorescence plate reader. Statistical analyses were performed using Student t test. Fn, fibronectin.
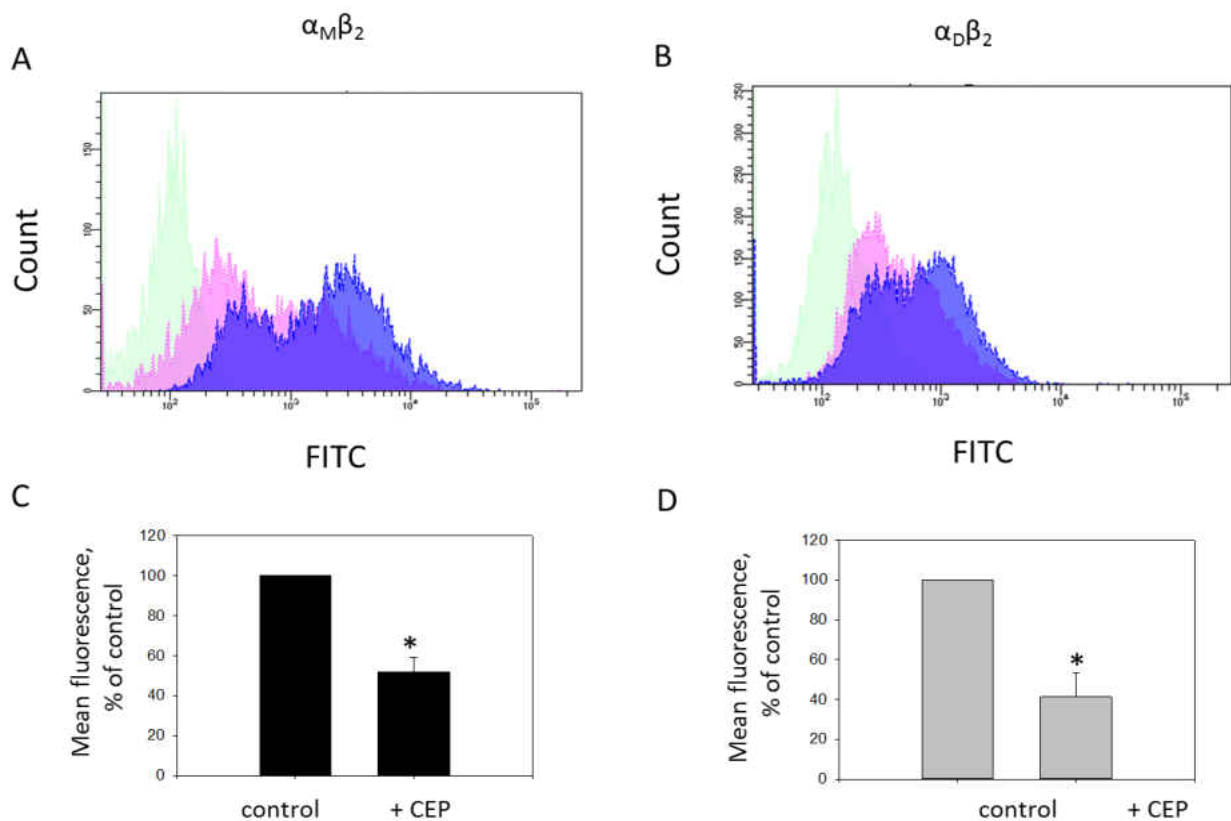
Fig. 2-4. **The effect of CEP on the binding of blocking anti-α_M (A, C) and anti-α_D (B, D) antibodies to $\alpha_M\beta_2$-and $\alpha_D\beta_2$-HEK293 transfected cells.** Cells were preincubated with 400 nM CEP-BSA for 30 min at 37^0C followed by incubation with blocking anti- α_M (or anti- α_D) antibody for 30 min. Bound antibody was detected with FITC conjugated donkey-anti-mouse antibody and analyzed by FACS using a BD FortessaX-20. The results are shown as representative experiments(A,B)from four executed. Statistical analyses were performed using Student's pairedt-tests.(C,D). *, P<0.05.

CEP stimulates migration of macrophages via β₂ integrin.

To characterize CEP as a migratory substrate for $\alpha_M\beta_2$ and $\alpha_D\beta_2$ integrins, we first demonstrated that β_2 deficiency significantly reduced macrophage adhesion to CEP (Figure 2-5A). Then, we compared the migration of WT and β_2-deficient macrophages within 3D CEP-enriched fibrin matrix. WT cells and β_2-deficient cells were labeled with green fluorescent dye PKH67 and red fluorescent dye PKH26, respectively. Macrophages were mixed at a ratio of 1:1 (Figure 2-5B), placed on the bottom of a fibrin gel in a Boyden chamber, and then migration against gravity was initiated by MCP-1 added to the top surface of the gel. The migration was evaluated after 48 hours (Figure 2-5C-D) and revealed that β_2 deficiency dramatically reduced the 3D migration of macrophages into the CEP-enriched matrix (Figure 2-5E). To exclude the contribution of a particular dye, the experiment was repeated with the opposite labeling conditions and revealed a similar result (Figure 2-6). To demonstrate that the difference between WT control and β_2-deficient macrophages was due to mesenchymal rather than amoeboid migration, this experiment was performed in the presence of ROCK inhibitor (Y-27632), known to block the amoeboid (adhesion-independent) component of cell migration. The presence of ROCK inhibitor did not alter the pattern of migration and the difference between WT control and β_2-deficient macrophages remained. This confirms that macrophage migration in 3D CEP-enriched matrix was integrin-dependent, or mesenchymal type (Figure2-7). The quality of ROCK inhibitor was verified using M2-activated macrophages that strongly depend on amoeboid motility (data not shown).

To rule out the potential interplay between WT and $\beta_2^{-/-}$ cells in 3D gel, we tested the migration of individual subsets of macrophages in CEP- and EP-enriched fibrin matrices (Figure 2-8A-B). The migration of WT macrophages involving CEP was substantially stronger in comparison with EP. In contrast, the migration of β_2-deficient macrophages was similar between CEP and EP (Figure 2-8B), which clearly indicates the critical role of β_2 integrins, primarily $\alpha_M\beta_2$ and $\alpha_D\beta_2$ (Figures 2-3), in CEP-mediated migration. Because neutrophils also express $\alpha_M\beta_2$ and $\alpha_D\beta_2$ integrins, neutrophil migration might also depend on the presence of CEP within the matrix. We evaluated the migration of human neutrophils within CEP-enriched fibrin gel; however, no additional effects of CEP on neutrophil migration were detected (Figure 2-8C). These results correspond to the published data showing that, in contrast to macrophages, neutrophil 3D migration is exclusively mediated by the amoeboid mode.[43]
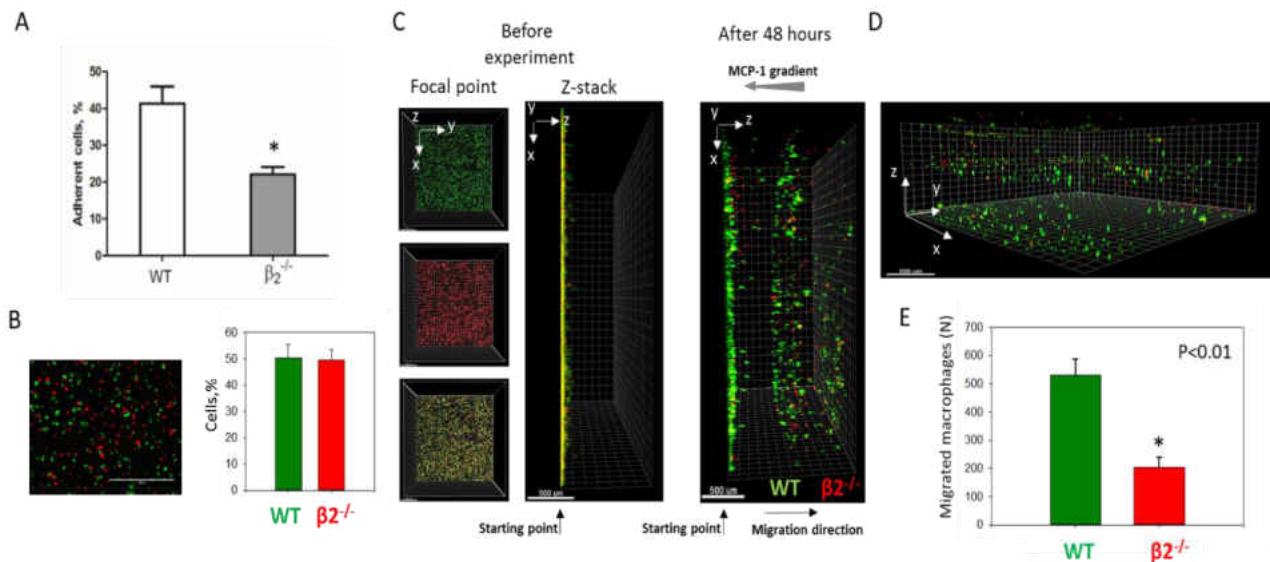
Fig. 2-5. CEP-dependent macrophage migration in a 3D matrix. (A) Thioglycollate-induced peritoneal macrophages were isolated from WT or $\beta_2^{-/-}$ mice and their adhesion to CEP was evaluated as described for Figure 4. (Bi) Isolated WT and $\beta_2^{-/-}$ macrophages were labeled with green (WT) or red ($\beta_2^{-/-}$) fluorescent dyes. Cells were mixed in equal number and the similar amounts of cells were verified by cytospin of mixed cells. Bar represents 400 mm. (Bii) The cell number was calculated by Image Analysis Software (EVOS, Thermo Fisher) using 5 random fields. (C-E) Thrombin-treated fibrinogen forms a 3D polymerized gel in a Boyden chamber. (Ci) Labeled cells were plated on 3D polymerized fibrin in transwell inserts. Migration of macrophages was stimulated by 30 nM MCP-1 added to the top of the gel. (Cii and D) After 48 hours, migrating cells were detected by a Leica Confocal microscope. The first 30 mm of the gel from the starting point (where many nonmigrated cells reside) is not shown to reduce a gradient of brightness intensity for the sample. (E) The results were analyzed by IMARIS 8.0 software and plotted. Statistical analyses were performed using Student paired t tests (n=4 samples per group). Bar represents 500 mm.
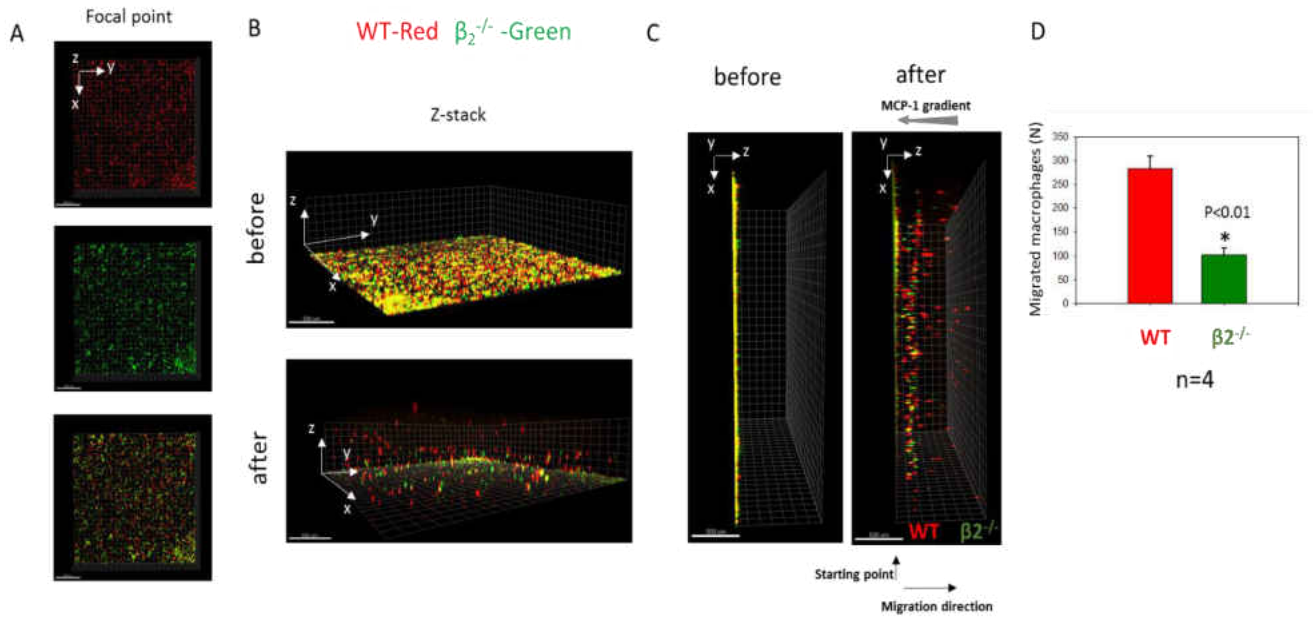
Fig. 2-6. Setup for the macrophage 3-D migration in Fibrin matrix supplemented with CEP. Cells were labeled with the opposite dyes to compare with Fig.2-5. WT and integrin $\beta2^{-/-}$ macrophages were labeled with red PKH26 and green PKH67 fluorescent dyes, respectively. Cells were mixed in equal amounts before the experiment. The similar number of cells were verified by the cytospin of mixed cells (not shown) and by analysis of macrophage starting points before migration (A). The background fluorescence of fibrin gel was verified by scanning samples with a confocal microscope before the initiation of migration (B, upper panel) and (C, left panel). Migration of macrophages was stimulated by 30 nM MCP-1 that was added to the top of the gel. After 48 hours, migrating cells were detected by a Leica Confocal microscope (Leica-TCS SP8) (B, lower panel) and (C, right panel). The results were analyzed and calculated by IMARIS 8.0 software (D). First 30 μm of the gel from the starting point (where many non-migrated cells reside) is not shown to reduce a gradient of brightness intensity for the sample. Statistical analyses were performed using Student's paired t-tests (n=4).
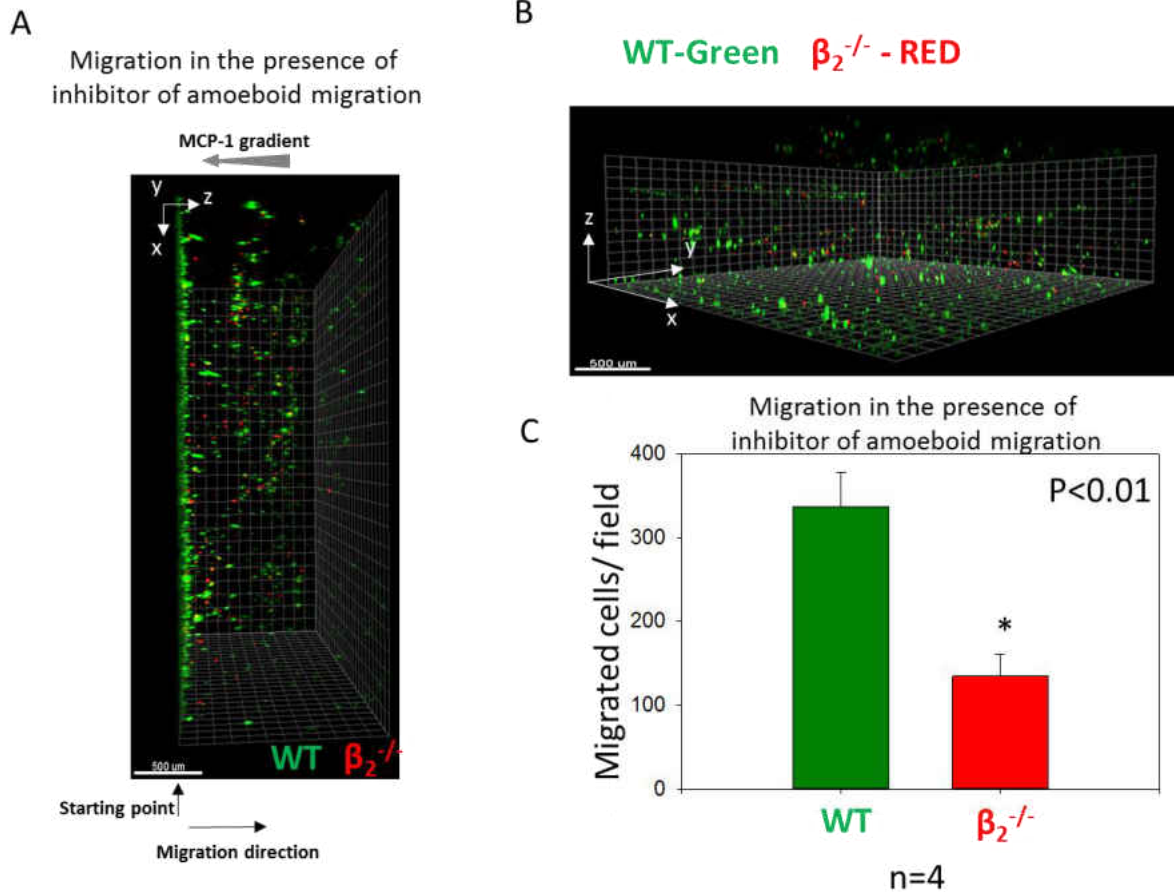
Fig. 2-7. Migration of macrophages in the presence of ROCK inhibitor (Y-27632) in 3-D Fibrin matrix supplemented with CEP. WT and integrin $\beta_2^{-/-}$ macrophages were labeled with green PKH67 and red PKH26 fluorescent dyes, respectively. Cells were mixed in equal amounts before the experiment and preincubated with ROCK inhibitor, Y-27632 (20µM). The ROCK inhibitor was also added to the matrix. Migration of macrophages was stimulated by 30 nM MCP-1 that was added to the top of the gel. After 48 hours, migrating cells were detected by a Leica Confocal microscope (Leica-TCS SP8) (A, B). The results were analyzed by IMARIS 8.0 software (C). First 30 µm of the gel from the starting point (where many non-migrated cells reside) is not shown to reduce a gradient of brightness intensity for the sample. Statistical analyses were performed using Student's paired t-tests (n=4).
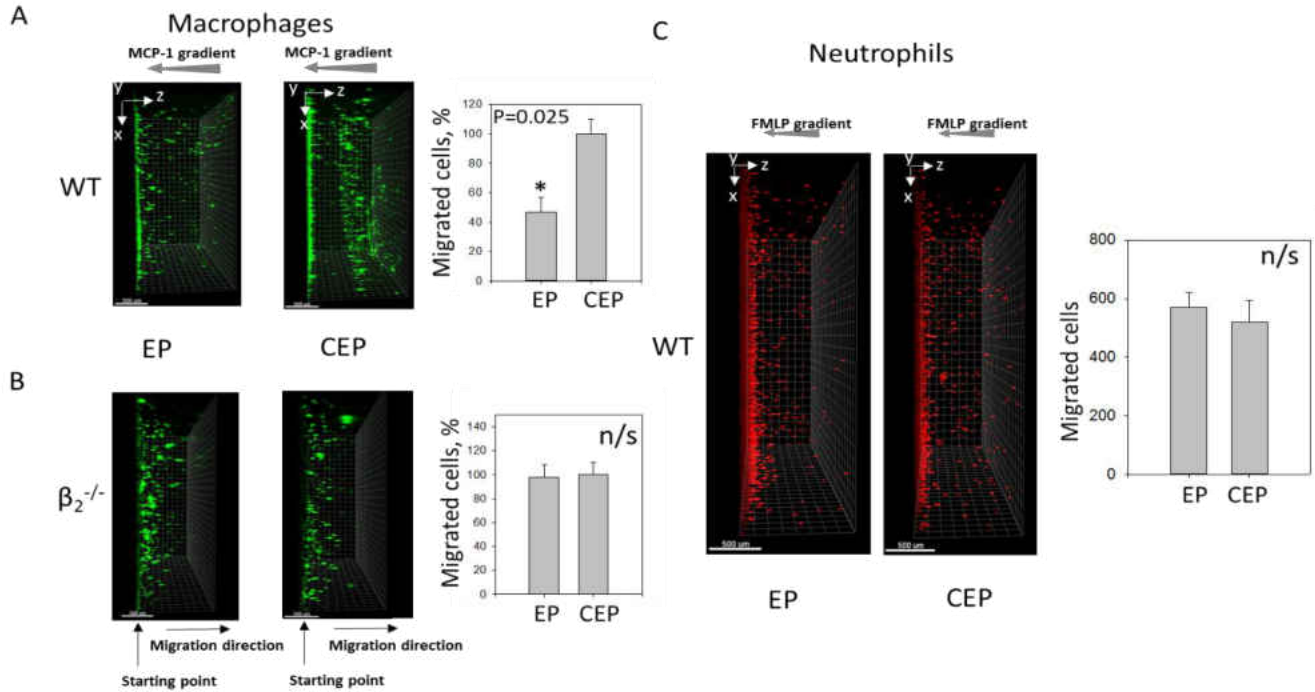
Fig. 2-8. CEP supplemented in 3D fibrin matrix increases macrophage migration, but not neutrophil migration. Thrombin-treated fibrinogen forms a 3D polymerized gel in a Boyden chamber. Thioglycollate-induced WT (A) or $\beta_2^{-/-}$ (B) peritoneal macrophages were labeled with PKH67 green fluorescent dye and plated on the gel. Macrophage migration was stimulated with 30 nM MCP-1. A total of 9 mMEP (left) or CEP (right) was incorporated in the gel during polymerization. Results were evaluated in 4 to 6 samples per group (9 field of view per sample), analyzed by IMARIS 8.0 software, and plotted. (C) Neutrophils were labeled with PKH26 red fluorescent dye and plated on fibrin matrix with incorporated CEP or EP. The migration was detected after 24 hours as described for macrophages. The first 30 mm of the gel from the starting point (where many nonmigrated cells reside) is not shown to reduce a gradient of brightness intensity for the sample. Statistical analyses were performed using Student paired t tests (n=4 per group). Bar represents 500 mm.

To assess whether MPO is able to directly contribute to CEP–protein adduct formation, human fibrinogen was incubated with active recombinant MPO and DHA.[44] Resulting CEP formation was quantified by enzyme-linked immunosorbent assay (Figure 2-9A). As anticipated,[45] the formation of CEP–protein adducts required the presence of all 3 main components: DHA (as a lipid substrate), MPO (as a source of oxidation), and a protein (eg, fibrinogen, as a source of

lysines). Incubation of fibrinogen with MPO or DHA alone was not sufficient for CEP generation. The presence of CEP adducts on fibrinogen was confirmed by western blot with monoclonal anti-CEP antibody (Figure 2-9B). These results clearly demonstrate that MPO-mediated DHA oxidation is one of the main mechanisms for CEP generation. Based on the results with MPO-deficient mice, MPO seems to be a clear source of CEP generation in vivo; however, it appears that other oxidative enzymes might participate in this process.
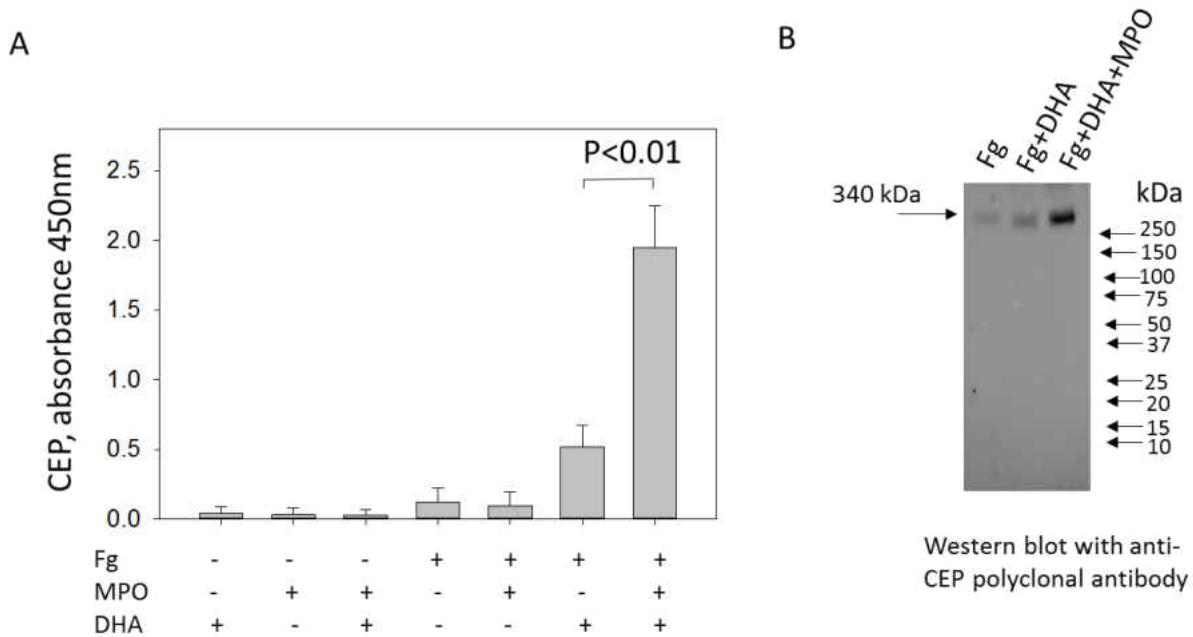
Figure2-9. Generation of CEP-modified fibrinogen by recombinant MPO. **A**. Human fibrinogen was coated on 96-well plate at concentration 50 μg/ml for overnight at 4^0C. Wells were post-coated with 0.5% polyvinyl alcohol for 1 h at 37^0C. 2 μM DHA , 0.5mU/ml MPO, alone or together, were added to the wells coated with Fg or only with polyvinyl alcohol in 20 mM Hepes, 150 mM NaCl, 0.01% H_2O_2, 1mM $CaCl_2$ and incubated in oxygen-free environment (under argon atmosphere) for 18 hours at 37^0C. After incubation the plate was washed out with PBS supplemented with 0.05% Tween 20 for 3 times and incubated with anti-CEP polyclonal antibody (0.9 μg/ml) for 2 hours at 37^0C. After washing, wells were incubated with goat-anti-rabbit HRP conjugated antibody for 1 h at 37^0C and the binding was developed using TMB-ELISA substrate solution (Pierce). The result was detected by plate reader using wavelength 450 nm. Statistical analyses were performed using Student's paired *t*-tests from 3 independent experiments. **B**. In

parallel experiment the 100 μg/ml fibrinogen was incubated with 2 μM DHA and 0.5mU/ml MPO in 20 mM Hepes, 150 mM NaCl, 0.01% H_2O_2, 1mM $CaCl_2$ buffer in the microtube in oxygen-free environment (under argon atmosphere) for 18 hours at 37^0C. After incubation the samples (in non-reduced conditions) were analyzed by Western Blot (4-20% gradient PAAG) with anti-CEP polyclonal antibody. The molecular weight of fibrinogen is 340 kDa.

Discussion

In the present study, we demonstrated that recruited neutrophils by the means of MPO are able to modify existing components of ECM by CEP adducts, which, in turn serve as adhesive ligands for macrophage integrins. The following conclusions are drawn from this study: 1) While CEP is not present in healthy tissues, its levels are dramatically increased at the sites of inflammation. 2) Inhibition of CEP does not affect the response of neutrophils to inflammation, but prevents the consequent macrophage recruitment. 3) Neutrophil activation and migration through ECM results in the generation of CEP-modified proteins. 4) CEP-modified proteins promote macrophage adhesion and migration. 5) Integrins $\alpha_M\beta_2$ and $\alpha_D\beta_2$ are specific macrophage receptors for CEP-mediated adhesion and migration. Thus, CEP is a natural inflammatory product generated during the first phase of inflammation by recruited neutrophils to facilitate the second wave of inflammation, namely, the recruitment of macrophages. By the means of oxidation, neutrophils seem to "pave the road" for future macrophage invasion by modifying ECM with CEP.

CEP was initially described in the retina of patients with age-related macular degeneration [20]. However, later the link between inflammation and CEP was demonstrated in several pathologies associated with chronic inflammation including atherosclerosis, tumor progression, aging and others [46; 47; 26; 48; 24]. Several groups reported the secretion of pro-inflammatory mediators from macrophages after its engagement with CEP-modified proteins. Particularly, the increased expression of TNFα, IL-6, IL-1β and IL-12 was reported [28; 23; 29; 30]. In agreement with this, CEP induced M1 macrophage polarization[27]. Therefore, CEP function is closely related to the development of inflammation.

Previously, several receptors were detected for the CEP on the surface of macrophages including TLR2, CD36, TLR1 and TLR6 [23; 46]. While these receptors contribute to macrophage activation and reprogramming by CEP, they do not directly mediate macrophage migration. Our

52

data demonstrated that CEP is not able to serve as a chemoattractant for macrophages or their integrin activation agonist. These results suggest that macrophages use another receptor for CEP that can mediate migration.

A subfamily of β_2 integrins are the major adhesive receptors on the surface of macrophages. Since $\alpha_L\beta_2$ interacts only with cell-counter receptors ICAMs and the expression of $\alpha_X\beta_2$ on macrophages is low [9], two other members of subfamily, $\alpha_M\beta_2$ and $\alpha_D\beta_2$ are the best candidates for the macrophage migration and retention in the extracellular matrix. $\alpha_D\beta_2$ and $\alpha_M\beta_2$ recognize a wide range of ligands, including fibronectin, thrombospondin and vitronectin [11, 12]. CEP modifications seem to generate the new inflammation-specific substrate for $\alpha_M\beta_2$ and $\alpha_D\beta_2$ macrophage migration or retention. Importantly, even known β_2 integrin ligands such as fibrinogen, can be "improved" by CEP modification. Inflammation promotes the leak of fibrinogen from blood to the inflamed tissue. Importantly, while the affinity of soluble fibrinogen for β_2 integrins is low, it increases substantially upon immobilization or partial digestion due to the exposure of carboxyl groups of glutamic and aspartic acid [49,50]. Acidic side chains of ligands are required for the binding to Mg^{2+} in MIDAS motif within the integrin I-domain, which is critical for integrin ligand recognition [51]. Likewise, the modification of fibrin with CEP (via the side-chain of lysine) reduces the positive charge on the fibrin surface and at the same time increases the number of negatively charged carboxyl groups, which are a major active element within the CEP structure (Fig.2-1). Thus, CEP adducts modify fibrinogen into the high affinity ligand for $\alpha_M\beta_2$ and $\alpha_D\beta_2$ integrins. Indeed, we show that CEP but not EP, which modifies proteins in a similar manner but lacks a carboxyl group, is able to create an adhesive β_2 ligand out of many proteins, possibly imitating bacterial ligands by exposed carboxyl groups as proposed previously. In general, the high Kd for the α_M-CEP and α_D-CEP interactions demonstrate a strong affinity that exceeds the affinity for the binding of α_M or α_D I-domains to previously identified proteins [12]. This makes CEP-modified proteins a preferential ligand for the macrophages. We found that the affinity for α_D-CEP interaction surpasses the affinity for α_M-CEP approximately 10-fold. We suggest that this effect is mediated by a difference in the electrostatic surfaces between the α_D I-domain and α_M I-domain [52]. Therefore, it is possible that integrin $\alpha_D\beta_2$ plays a more significant physiological role in the CEP-mediated macrophage adhesion and migration. Further studies are required to clarify this question.

It is well accepted that strong integrin-mediated adhesion often antagonizes or limits migration [53, 54]. Since CEP-modified proteins serve as strong ligands for β_2 on macrophages, CEP

might serve as a cell migration signal for cells with moderate integrin expression, and as a retention/arrest signal for cells with the high expression of integrins. We recently demonstrated that expression of $\alpha_D\beta_2$ is upregulated on M1 macrophages in vitro and within atherosclerotic lesions. We showed that high expression of $\alpha_D\beta_2$ mediates the retention of macrophages at the site of inflammation [10]. Thus, CEP-modified proteins are the likely ligands responsible for these phenomena.

Recent studies indicate that rapid migration of neutrophils is mediated in an integrin-independent manner by an amoeboid mode of motility [55]. Therefore, based on these observations, neutrophils do not need to use CEP as substrate for their migration. Importantly, it has been demonstrated that macrophages can use both mechanisms, amoeboid and mesenchymal migration, depending on environment and macrophage subset [56]. This, again, implies the selectivity of CEP ligands towards macrophages.

In summary, our data introduce a new mechanism for macrophage migration during inflammation. The recruitment of neutrophils and subsequent neutrophil activation generates CEP-modified proteins along the neutrophil path. CEP-modified proteins provide a track for future migration (or accumulation) of macrophages via $\alpha_M\beta_2$ and $\alpha_D\beta_2$-mediated processes.

The information obtained in our studies not only establishes the foundation for a new model of inflammation but also provides a new strategy for treatment of chronic inflammatory diseases. The advantage of CEP as a new therapeutic target resides in its unique formation in inflamed tissue. Therefore, the blocking of CEP in peripheral tissues during different inflammatory diseases can prevent macrophage accumulation and further development of chronic inflammation.

References

(1) Tobias P, Curtiss LK. Thematic review series: The immune system and atherogenesis. Paying the price for pathogen protection: toll receptors in atherogenesis. *J Lipid Res* 2005 March;46(3):404-11.

(2) Alexandraki K, Piperi C, Kalofoutis C, Singh J, Alaveras A, Kalofoutis A. Inflammatory process in type 2 diabetes: The role of cytokines. *Ann N Y Acad Sci* 2006 November;1084:89-117.

(3) Ouchi N, Kihara S, Funahashi T, Matsuzawa Y, Walsh K. Obesity, adiponectin and vascular inflammatory disease. *Curr Opin Lipidol* 2003 December;14(6):561-6.

(4) Williams MR, Azcutia V, Newton G, Alcaide P, Luscinskas FW. Emerging mechanisms of neutrophil recruitment across endothelium. *Trends Immunol* 2011 October;32(10):461-9.

(5) McLoughlin RM, Hurst SM, Nowell MA, Harris DA, Horiuchi S, Morgan LW, Wilkinson TS, Yamamoto N, Topley N, Jones SA. Differential regulation of neutrophil-activating chemokines by IL-6 and its soluble receptor isoforms. *J Immunol* 2004 May 1;172(9):5676-83.

(6) Lishko VK, Moreno B, Podolnikova NP, Ugarova TP. Identification of Human Cathelicidin Peptide LL-37 as a Ligand for Macrophage Integrin alphaMbeta2 (Mac-1, CD11b/CD18) that Promotes Phagocytosis by Opsonizing Bacteria. *Res Rep Biochem* 2016 July 7;2016(6):39-55.

(7) Subramanian S, Chait A. The effect of dietary cholesterol on macrophage accumulation in adipose tissue: implications for systemic inflammation and atherosclerosis. *Curr Opin Lipidol* 2009 February;20(1):39-44.

(8) Clemetson KJ, Clemetson JM. Integrins and cardiovascular disease. *Cell Mol Life Sci* 1998 June;54(6):502-13.

(9) Wu H, Gower RM, Wang H, Perrard XY, Ma R, Bullard DC, Burns AR, Paul A, Smith CW, Simon SI, Ballantyne CM. Functional role of CD11c+ monocytes in atherogenesis associated with hypercholesterolemia. *Circulation* 2009 May 26;119:2708-17.

(10) Aziz MH, Cui K, Das M, Brown KE, Ardell CL, Febbraio M, Pluskota E, Han J, Wu H, Ballantyne CM, Smith JD, Cathcart MK, Yakubenko VP. The Upregulation of Integrin alphaDbeta2 (CD11d/CD18) on Inflammatory Macrophages Promotes Macrophage Retention in Vascular Lesions and Development of Atherosclerosis. *J Immunol* 2017 June 15;198(12):4855-67.

(11) Yakubenko VP, Lishko VK, Lam SCT, Ugarova TP. A molecular basis for integrin a_Mb_2 in ligand binding promiscuity. *J Biol Chem* 2002;277:48635-42.

(12) Yakubenko VP, Yadav SP, Ugarova TP. Integrin alphaDbeta2, an adhesion receptor up-regulated on macrophage foam cells, exhibits multiligand-binding properties. *Blood* 2006 February 15;107:1643-50.

(13) Isobe Y, Arita M, Iwamoto R, Urabe D, Todoroki H, Masuda K, Inoue M, Arai H. Stereochemical assignment and anti-inflammatory properties of the omega-3 lipid mediator resolvin E3. *J Biochem* 2013 April;153(4):355-60.

(14) Salomon RG. Levuglandins and isolevuglandins: stealthy toxins of oxidative injury. *Antioxid Redox Signal* 2005 January;7(1-2):185-201.

(15) Subbanagounder G, Leitinger N, Schwenke DC, Wong JW, Lee H, Rizza C, Watson AD, Faull KF, Fogelman AM, Berliner JA. Determinants of bioactivity of oxidized phospholipids. Specific oxidized fatty acyl groups at the sn-2 position. *Arterioscler Thromb Vasc Biol* 2000 October;20(10):2248-54.

(16) Rizos EC, Ntzani EE, Bika E, Kostapanos MS, Elisaf MS. Association between omega-3 fatty acid supplementation and risk of major cardiovascular disease events: a systematic review and meta-analysis. *JAMA* 2012 September 12;308(10):1024-33.

(17) Ramsden CE, Zamora D, Leelarthaepin B, Majchrzak-Hong SF, Faurot KR, Suchindran CM, Ringel A, Davis JM, Hibbeln JR. Use of dietary linoleic acid for secondary prevention

of coronary heart disease and death: evaluation of recovered data from the Sydney Diet Heart Study and updated meta-analysis. *Br Med J* 2013;346:e8707.

(18) Ramsden CE, Zamora D, Majchrzak-Hong S, Faurot KR, Broste SK, Frantz RP, Davis JM, Ringel A, Suchindran CM, Hibbeln JR. Re-evaluation of the traditional diet-heart hypothesis: analysis of recovered data from Minnesota Coronary Experiment (1968-73). *Br Med J* 2016;353:i1246.

(19) Wu JH, Micha R, Imamura F, Pan A, Biggs ML, Ajaz O, Djousse L, Hu FB, Mozaffarian D. Omega-3 fatty acids and incident type 2 diabetes: a systematic review and meta-analysis. *Br J Nutr* 2012 June;107 Suppl 2:S214-S227.

(20) Gu X, Meer SG, Miyagi M, Rayborn ME, Hollyfield JG, Crabb JW, Salomon RG. Carboxyethylpyrrole protein adducts and autoantibodies, biomarkers for age-related macular degeneration. *J Biol Chem* 2003 October 24;278(43):42027-35.

(21) Wang H, Linetsky M, Guo J, Choi J, Hong L, Chamberlain AS, Howell SJ, Howes AM, Salomon RG. 4-Hydroxy-7-oxo-5-heptenoic Acid (HOHA) Lactone is a Biologically Active Precursor for the Generation of 2-(omega-Carboxyethyl)pyrrole (CEP) Derivatives of Proteins and Ethanolamine Phospholipids. *Chem Res Toxicol* 2015 May 18;28(5):967-77.

(22) Gu X, Sun M, Gugiu B, Hazen S, Crabb JW, Salomon RG. Oxidatively truncated docosahexaenoate phospholipids: total synthesis, generation, and Peptide adduction chemistry. *J Org Chem* 2003 May 16;68(10):3749-61.

(23) Kim YW, Yakubenko VP, West XZ, Gugiu GB, Renganathan K, Biswas S, Gao D, Crabb JW, Salomon RG, Podrez EA, Byzova TV. Receptor-Mediated Mechanism Controlling Tissue Levels of Bioactive Lipid Oxidation Products. *Circ Res* 2015 July 31;117(4):321-32.

(24) Kerr BA, Ma L, West XZ, Ding L, Malinin NL, Weber ME, Tischenko M, Goc A, Somanath PR, Penn MS, Podrez EA, Byzova TV. Interference with akt signaling protects

against myocardial infarction and death by limiting the consequences of oxidative stress. *Sci Signal* 2013 August 6;6(287):ra67.

(25) Hoff HF, O'Neil J, Wu Z, Hoppe G, Salomon RL. Phospholipid hydroxyalkenals: biological and chemical properties of specific oxidized lipids present in atherosclerotic lesions. *Arterioscler Thromb Vasc Biol* 2003 February 1;23(2):275-82.

(26) Panigrahi S, Ma Y, Hong L, Gao D, West XZ, Salomon RG, Byzova TV, Podrez EA. Engagement of platelet toll-like receptor 9 by novel endogenous ligands promotes platelet hyperreactivity and thrombosis. *Circ Res* 2013 January 4;112(1):103-12.

(27) Cruz-Guilloty F, Saeed AM, Echegaray JJ, Duffort S, Ballmick A, Tan Y, Betancourt M, Viteri E, Ramkhellawan GC, Ewald E, Feuer W, Huang D, Wen R, Hong L, Wang H, Laird JM, Sene A, Apte RS, Salomon RG, Hollyfield JG, Perez VL. Infiltration of proinflammatory m1 macrophages into the outer retina precedes damage in a mouse model of age-related macular degeneration. *Int J Inflam* 2013;2013:503725.

(28) Cruz-Guilloty F, Saeed AM, Duffort S, Cano M, Ebrahimi KB, Ballmick A, Tan Y, Wang H, Laird JM, Salomon RG, Handa JT, Perez VL. T cells and macrophages responding to oxidative damage cooperate in pathogenesis of a mouse model of age-related macular degeneration. *PLoS ONE* 2014;9(2):e88201.

(29) Doyle SL, Campbell M, Ozaki E, Salomon RG, Mori A, Kenna PF, Farrar GJ, Kiang AS, Humphries MM, Lavelle EC, O'Neill LA, Hollyfield JG, Humphries P. NLRP3 has a protective role in age-related macular degeneration through the induction of IL-18 by drusen components. *Nat Med* 2012 May;18(5):791-8.

(30) Saeed AM, Duffort S, Ivanov D, Wang H, Laird JM, Salomon RG, Cruz-Guilloty F, Perez VL. The oxidative stress product carboxyethylpyrrole potentiates TLR2/TLR1 inflammatory signaling in macrophages. *PLoS ONE* 2014;9(9):e106421.

(31) Gu X, Meer SG, Miyagi M, Rayborn ME, Hollyfield JG, Crabb JW, Salomon RG. Carboxyethylpyrrole protein adducts and autoantibodies, biomarkers for age-related macular degeneration. *J Biol Chem* 2003 October 24;278(43):42027-35.

(32) Crabb JW, Miyagi M, Gu X, Shadrach K, West KA, Sakaguchi H, Kamei M, Hasan A, Yan L, Rayborn ME, Salomon RG, Hollyfield JG. Drusen proteome analysis: an approach to the etiology of age-related macular degeneration. *Proc Natl Acad Sci U S A* 2002 November 12;99(23):14682-7.

(33) Kim YW, Yakubenko VP, West XZ, Gugiu GB, Renganathan K, Biswas S, Gao D, Crabb JW, Salomon RG, Podrez EA, Byzova TV. Receptor-Mediated Mechanism Controlling Tissue Levels of Bioactive Lipid Oxidation Products. *Circ Res* 2015 July 31;117(4):321-32.

(34) Yakubenko VP, Yadav SP, Ugarova TP. Integrin alphaDbeta2, an adhesion receptor up-regulated on macrophage foam cells, exhibits multiligand-binding properties. *Blood* 2006 February 15;107:1643-50.

(35) Hazen SL, Hsu FF, Heinecke JW. p-Hydroxyphenylacetaldehyde is the major product of L-tyrosine oxidation by activated human phagocytes. A chloride-dependent mechanism for the conversion of free amino acids into reactive aldehydes by myeloperoxidase. *J Biol Chem* 1996 January 26;271(4):1861-7.

(36) Thurau AM, Schylz U, Wolf V, Krug N, Schauer U. Identification of eosinophils by flow cytometry. *Cytometry* 1996 February 1;23(2):150-8.

(37) Schmitt D, Shen Z, Zhang R, Colles SM, Wu W, Salomon RG, Chen Y, Chisolm GM, Hazen SL. Leukocytes utilize myeloperoxidase-generated nitrating intermediates as physiological catalysts for the generation of biologically active oxidized lipids and sterols in serum. *Biochemistry* 1999 December 21;38(51):16904-15.

(38) Schneider T, Issekutz AC. Quantitation of eosinophil and neutrophil infiltration into rat lung by specific assays for eosinophil peroxidase and myeloperoxidase. Application in a Brown Norway rat model of allergic pulmonary inflammation. *J Immunol Methods* 1996 October 30;198(1):1-14.

(39) Yakubenko VP, Lishko VK, Lam SCT, Ugarova TP. A molecular basis for integrin a_Mb_2 in ligand binding promiscuity. *J Biol Chem* 2002;277:48635-42.

(40) Lu C, Shimaoka M, Ferzly M, Oxvig C, Takagi J, Springer TA. An isolated, surface-expressed I domain of the integrin a_Lb_2 is sufficient for strong adhesive function when locked in the open conformation with a disulfide bond. *Proc Natl Acad Sci USA* 2001;98:2387-92.

(41) Vorup-Jensen T, Carman CV, Shimaoka M, Schuck P, Svitel J, Springer TA. Exposure of acidic residues as a danger signal for recognition of fibrinogen and other macromolecules by integrin alphaXbeta2. *Proc Natl Acad Sci U S A* 2005 February 1;102(5):1614-9

(42) Ploplis VA, French EL, Carmeliet P, Collen D, Plow EF. Plasminogen deficiency differentially affects recruitment of inflammatory cell populations in mice. *Blood* 1998;91:2005-9.

(43) Yakubenko VP, Bhattacharjee A, Pluskota E, Cathcart MK. aMb2 integrin activation prevents alternative activation of human and murine macrophages and impedes foam cell formation. *Circ Res* 2011 March 4;108:544-54.

(44) Budzynski AZ, Marder VJ, Shainoff JR. Structure of plasmic degradation products of human plasmin and fibrinogen: fibrinopeptide and polypeptide chain analysis. *J Biol Chem* 1974;249:2294-302.

(45) Stelmaszynska T, Kukovetz E, Egger G, Schaur RJ. Possible involvement of myeloperoxidase in lipid peroxidation. *Int J Biochem* 1992;24(1):121-8.

(46) West XZ, Malinin NL, Merkulova AA, Tischenko M, Kerr BA, Borden EC, Podrez EA, Salomon RG, Byzova TV. Oxidative stress induces angiogenesis by activating TLR2 with novel endogenous ligands. *Nature* 2010 October 21;467(7318):972-6.

(47) *Evans*, *T.A.*, Siedlak, S.L., Lu, L., Fu, X., Wang, Z., McGinnis, W.R., Fakhoury, E., Castellani, R.J., Hazen, S.L., Walsh, W.J., Lewis, T., *Salomon*, *R.G.*, Smith, M.A,. The Autistic Phenotype Exhibits a Remarkably Localized Modification of Brain Protein by Products of Free Radical-Induced Lipid Oxidation. 4(2), 61-72. 2008. Am J Biochem Biotechnol.

(48) Biswas S, Xin L, Panigrahi S, Zimman A, Wang H, Yakubenko V, Byzova TV, Salomon RG, Podrez EA. Novel phosphatidylethanolamine derivatives accumulate in circulation in hyperlipidemic ApoE-/- mice and activate platelets via TLR2. *Blood* 2016 March 25.

(49) Lishko VK, Kudryk B, Yakubenko VP, Yee VC, Ugarova TP. Regulated unmasking of the cryptic binding site for integrin $a_M b_2$ in the gC-domain of fibrinogen. *Biochemistry* 2002;41:12942-51.

(50) Vorus-Jensen T, Ostermeier C, Shimaoka M, Hommel U, Springer TA. Structure and allosteric regulation of the aXb2 integrin I domain. *Proc Natl Acad Sci USA* 2003;100:1873-8.

(51) Li R, Rieu P, Griffith DL, Scott D, Arnaout MA. Two functional states of the CD11b A-domain: correlations with key features of two Mn^{2+} - complexed crystal structures. *J Cell Biol* 1998;143:1523-34.

(52) Vorup-Jensen T, Carman CV, Shimaoka M, Schuck P, Svitel J, Springer TA. Exposure of acidic residues as a danger signal for recognition of fibrinogen and other macromolecules by integrin alphaXbeta2. *Proc Natl Acad Sci U S A* 2005 February 1;102(5):1614-9.

(53) DiMilla PA, Barbee K, Lauffenburger DA. Mathematical model for the effects of adhesion and mechanics on cell migration speed. *Biophys J* 1991;60:15-37.

(54) Palecek SP, Loftus JC, Ginsberg MH, Lauffenburger DA, Horwitz AF. Integrin-ligand binding properties govern cell migration speed through cell-substratum adhesiveness. *Nature* 1997;385:537-40.

(55) Cougoule C, Van GE, Le C, V, Lafouresse F, Dupre L, Mehraj V, Mege JL, Lastrucci C, Maridonneau-Parini I. Blood leukocytes and macrophages of various phenotypes have distinct abilities to form podosomes and to migrate in 3D environments. *Eur J Cell Biol* 2012 November;91(11-12):938-49.

(56) Lerchenberger M, Uhl B, Stark K, Zuchtriegel G, Eckart A, Miller M, Puhr-Westerheide D, Praetner M, Rehberg M, Khandoga AG, Lauber K, Massberg S, Krombach F, Reichel

CA. Matrix metalloproteinases modulate ameboid-like migration of neutrophils through inflamed interstitial tissue. *Blood* 2013 August 1;122(5):770-80.

CHAPTER 3

DISTINCT MIGRATORY PROPERTIES OF M1, M2 AND RESIDENT MACROPHAGES
ARE REGULATED BY $\alpha_D\beta_2$ AND $\alpha_M\beta_2$ INTEGRIN-MEDIATED ADHESION

Kui Cui*, Christopher L. Ardell*, Nataly P. Podolnikova[†], Valentin P. Yakubenko*, [®]

*Department of Biomedical Sciences, Center of Excellence for Inflammation, Infectious Disease and Immunity, Quillen College of Medicine, East Tennessee State University, Johnson City, TN. [†] Center for Metabolic and Vascular Biology, School of Life Sciences, Arizona State University. Tempe, AZ

Running title: β_2 integrins regulates macrophage 3D migration

[®] Correspondence to Dr. Valentin Yakubenko, Department of Biomedical Sciences,
Quillen College of Medicine, East Tennessee State University, PO Box 70582, Johnson City,
Email: yakubenko@etsu.edu, Phone: (423) 439-8511.

Abstract

   Chronic inflammation is essential mechanism during the development of cardiovascular and metabolic diseases. The outcome of diseases depends on the balance between the migration/accumulation of pro-inflammatory (M1) and anti-inflammatory (M2) macrophages in damaged tissue. The mechanism of macrophage migration and subsequent accumulation is still not fully understood.

   Currently, the amoeboid adhesion-independent motility is considered essential for leukocyte migration in the three-dimensional environment. We challenge this hypothesis by studying the contribution of leukocyte adhesive receptors, integrins $\alpha_M\beta_2$ and $\alpha_D\beta_2$, to three-dimensional migration of M1-polarized, M2-polarized and resident macrophages. The expression of integrin $\alpha_D\beta_2$ was significantly upregulated on macrophages in atherosclerotic lesions and M1 macrophages *in vitro*. Interestingly, expression of the related ligand-sharing integrin $\alpha_M\beta_2$ was not altered. This difference defines their distinct roles in the regulation of macrophage migration. αD-deficiency reduced macrophage accumulation in atherosclerotic lesions and does not have effects on macrophage apoptosis or proliferation. Both integrins have a moderate expression on M2 macrophages and $\alpha_M\beta_2$ demonstrates high expression on resident macrophages.

   The level of integrin expression determines its contribution to macrophage migration. Namely, intermediate expression supports macrophage migration, while a high integrin density inhibits it. Using *in vitro* three-dimensional migration and *in vivo* tracking of adoptively-transferred fluorescently-labeled macrophages during the resolution of inflammation, we found that strong adhesion of M1-activated macrophages translates to weak 3D migration, while moderate adhesion of M2-activated macrophages generates dynamic motility.

   Reduced migration of M1 macrophages depends on the high expression of $\alpha_D\beta_2$, since αD-deficiency decreased M1 macrophage adhesion and improved migration in fibrin matrix and peritoneal tissue. Similarly, the high expression of $\alpha_M\beta_2$ on resident macrophages prevents their amoeboid migration, which is markedly increased in α_M-deficient macrophages. In contrast, α_D- and α_M-knockouts decrease the migration of M2 macrophages, demonstrating that moderate integrin expression supports cell motility. The results were confirmed in a diet-induced diabetes model. α_D deficiency prevents the retention of inflammatory macrophages in adipose tissue and improves metabolic parameters, while α_M deficiency does not affect macrophage accumulation.

Summarizing, β₂ integrin-mediated adhesion may inhibit amoeboid and mesenchymal macrophage migration or support mesenchymal migration in tissue, and, therefore, represents an important target to control inflammation.

Introduction

Monocyte/macrophage migration to, and accumulation within the site of inflammation are critical steps in the development of the inflammatory response. While acute inflammation is usually generated as a defensive mechanism, the development of chronic inflammation is an essential step in the initiation or progression of many devastating diseases including atherosclerosis, diabetes, obesity, arthritis and others [1-4]. Macrophage accumulation at the damaged tissue is a hallmark of inflammation [5, 6]. However, the particular subset of accumulated macrophages is critical for the further development or resolution of chronic inflammation. Classically activated (M1) macrophages produce a harsh pro-inflammatory response, while alternatively activated (M2) macrophages may have anti-inflammatory functions [7, 8]. The balance between the accumulation of pro-inflammatory and anti-inflammatory macrophages regulates the fate of inflammation. So far, the mechanism of macrophage accumulation is not fully understood.

Macrophage accumulation at the site of inflammation depends upon monocyte recruitment, macrophage retention and emigration. Monocyte recruitment includes activation, diapedesis through the endothelial monolayer (2D migration) [9, 10] and migration through the extracellular matrix to the site of inflammation (3D migration). While the role of leukocyte adhesive receptors in 2D migration is well established [9, 11], their contribution to macrophage migration through 3D extracellular matrix (ECM) is still unclear. Macrophages utilize two types of motility in a 3D environment – amoeboid and mesenchymal. Amoeboid migration is adhesion-independent movement that is based on flowing and squeezing. This migratory mode was shown to be dominant for neutrophils, dendritic cells and lymphocytes [12]. Mesenchymal migration involves the classical adhesion-mediated mechanism that includes cell protrusion and adhesion of the leading edge, followed by detachment of the trailing edge and retraction of the contractile cell rear [13]. It has been shown that cell-substratum adhesiveness regulates the fate of mesenchymal cell migration. Namely, an intermediate level of adhesiveness generates the optimal conditions for cell migration [14]. Low adhesiveness does not support cell motility, while a very high level of adhesiveness thwarts cell

locomotion because it inhibits cell detachment from the substrate [15, 16]. The density of adhesive receptors on the cell surface is one of the most critical parameters of cell-substratum adhesiveness. Therefore, a high density of cell adhesion receptors that generate a high adhesiveness may lead to the retention of cells [15, 17].

Integrins are the most important cell adhesive receptors that are involved in monocyte/macrophage migration. Of particular note is the subfamily of β_2 integrins that are exclusively expressed on leukocytes and consist of 4 members: $\alpha_L\beta_2$ (CD11a/CD18), $\alpha_M\beta_2$ (CD11b/CD18), $\alpha_X\beta_2$ (CD11c/CD18) and $\alpha_D\beta_2$ (CD11d/CD18) [18]. Integrins $\alpha_M\beta_2$ and $\alpha_D\beta_2$ are the most interesting members with regard to cell migration, since $\alpha_L\beta_2$ has no ligands in ECM [19] and $\alpha_X\beta_2$ demonstrated a very low expression on macrophages [20]. In contrast, α_M and α_D have marked macrophage expression and share many ECM ligands [21, 22].

Different subsets of macrophages have a diverse expression of integrins [23] and, most importantly, possess different migratory characteristics [24]. We hypothesize that integrin expression regulates the distinct migratory properties of M1-polarized, M2-polarized and resident macrophages. We realize that *in vitro* activated M1 and M2 macrophages do not fully represent the varieties of pro-inflammatory and anti-inflammatory macrophages *in vivo*; however, these cells are appropriate models that can help us to understand the migratory mechanisms of different macrophage subsets during inflammatory diseases.

In our previous project, we found that the pro-atherogenic role of integrin $\alpha_D\beta_2$ depends upon the upregulation of α_D on pro-inflammatory M1 macrophages *in vitro* and on macrophages in atherosclerotic lesions, which apparently mediates macrophage retention [23]. In agreement with this, α_D-deficiency reduced the development of atherosclerosis and released the migration of M1 macrophages *in vitro* [23].

In this paper we further develop this project by analyzing the role of β_2 integrins on different subsets of macrophages and attempt to depict the mechanisms that stimulate cell migration/retention based on the analysis of integrin expression, cell adhesion, secretion of proteases, and mode of cell migration. We found a strong correlation between macrophage migration and expression of $\alpha_M\beta_2$ and $\alpha_D\beta_2$. A moderate expression of $\alpha_M\beta_2$ and $\alpha_D\beta_2$ on M2 macrophages supports cell movement, while the upregulation of $\alpha_D\beta_2$ on M1 macrophages and α_M on resident macrophages prevents mesenchymal and/or amoeboid migration. These results were

verified by using α_M- and α_D-deficient macrophages in 3D *in vitro* migration and by using an *in vivo* model for the resolution of peritoneal inflammation and diet-induced diabetes.

Therefore, the regulation of β_2 integrin expression may help to shift the pro-/anti-inflammatory balance at the site of inflammation and reduced the pathophysiological outcome.

Materials and Method

Reagents and antibodies

Reagents were purchased from Sigma-Aldrich (St. Louis, MO) and Thermo Fisher Scientific (Waltham, MA). Rock inhibitor (Y27632) and aprotinin were from Sigma-Aldrich. Recombinant human and mouse IFNγ, IL-4, MCP-1 and FMLP were purchased from Invitrogen Corporation (Carlsbad, CA). Anti-human α_D mAb (clone 240I) was generously provided by Eli Lilly Corporation (Indianapolis, IN). Polyclonal antibody against the α_D I-domain was described previously (10). The antibody recognizes both human and mouse α_D I-domains and has no cross-reactivity with recombinant human and mouse α_M, α_X and α_L I-domains. The antibody was isolated from rabbit serum by affinity chromatography using α_DI-domain-Sepharose. Mouse PE-cy7 and APC- conjugated anti-α_M mAb (clone M1/70) and F4/80 mAbs were from eBioscience (San Diego, CA). The mAb 44a directed against the human α_M integrin subunit was purified from the conditioned media of the hybridoma cell line obtained from American Type Culture Collection (ATCC, Manassas,VA) using protein A agarose (GE Healthcare, Piscataway, NJ).

Animals.

Wild type (C57BL/6J, stock # 000664) and integrin α_D-deficient (B6.129S7-*Itgad*^{tm1Bll}/J, stock # 005258 and integrin α_M-deficient (B6.129S4-*Itgam*^{tm1Myd}/J, stock # 003991) mice were bought from Jackson Laboratory (Bar Harbor, ME). α_D-deficient and α_M-deficient mice have been backcrossed to C57BL/6 for at least ten generations. All procedures were performed according to animal protocols approved by East Tennessee State University IACUC.

Flow cytometry analysis.

Flow cytometry analysis was performed to assess the expression of α_D and α_M on mouse peritoneal macrophages. Cells were harvested and pre-incubated with 4% normal goat serum for 30 min at 4°C, then 2×10^6 cells were incubated with specific antibody for 30 min at 4°C. Non-

conjugated antibodies required additional incubation with Alexa 488 or PE-cy7-donkey anti-mouse IgG (at a 1:1000 dilution) for 30 min at 4°C. Finally, the cells were washed and analyzed using a Fortessa X-20 (Becton Dickinson).

Generation of classically activated (M1) and alternatively activated (M2) mouse and human macrophages.

Peritoneal macrophages from 8-12 week old mice (WT and $\alpha_D^{-/-}$, n = 3 mice per group) were harvested by lavage of the peritoneal cavity with 5 ml of sterile PBS 3 days after intraperitoneal (IP) injection of 4% thioglycollate (TG; 0.5ml). The cells were washed twice with PBS and resuspended in complete RPMI media. The cell suspension was transferred into 100mm petri dishes and incubated for 2h at 37°C in humidified air containing 5% CO_2 atmosphere. Nonadherent cells were washed out with RPMI media, and the adherent macrophages were replenished with RPMI media. The macrophages were differentiated to M1 and M2 phenotypes by treatment with recombinant mouse interferon-γ (IFN-γ) (100 U/ml, Thermo Fisher) and interleukin 4 (IL-4) (2nM, Thermo Fisher), respectively, for 4 days. Medium with IFN-γ and IL-4 were changed every 2 days or as required. The M1 phenotype macrophages from WT and $\alpha_D^{-/-}$ were labeled with red fluorescent marker PKH26 and green fluorescent marker PKH67, respectively, according to the manufacturer's instructions (Sigma-Aldrich). The fluorescently-labeled cells were dissociated from the plates using 5mM EDTA in PBS and used for the experiments thereafter.

Cell adhesion assay.

The adhesion assay was performed as described previously [22] with modifications. Briefly, 96-well plates (Immulon 2HB, Cambridge, MA) were coated with different concentrations of fibrinogen or Matrigel for 3 h at 37 °C. The wells were post-coated with 0.5% polyvinyl alcohol for 1 h at 37 °C. Mouse peritoneal macrophages or HEK 293 cells transfected with $\alpha_M\beta_2$, or $\alpha_D\beta_2$ integrins were labeled with 10 µM Calcein AM (Molecular Probes, Eugene, OR) for 30 min at 37 °C and washed with DMEM and resuspended in the same medium at a concentration of 1×10^6 cells/mL. Aliquots (50 µL) of the labeled cells were added to each well. For inhibition experiments, cells were mixed with antibodies and incubated for 15 minutes at 22 °C before they were added to the coated wells. After 30 minutes of incubation at 37 °C in a 5% CO_2 humidified atmosphere, the

68

nonadherent cells were removed by washing with HBSS. The fluorescence was measured in a Synergy H1 fluorescence plate reader (BioTek, Winooski, VT), and the number of adherent cells was determined from a labeled control.

Migration of macrophages in 3D fibrin gel and matrigel.

The migration assay was performed as described previously [25]. WT and $\alpha_D^{-/-}$ or WT and $\alpha_M^{-/-}$ peritoneal macrophages activated to M1 or M2 phenotype as described above were labeled with PKH26 red fluorescent dye and PKH67 green fluorescent dye, respectively. Cell migration assay was performed for 24 hours at 37°C in 5% CO_2 in a sterile condition. An equal number of WT and $\alpha_D^{-/-}$ macrophages was evaluated by cytospin of mixed cells before the experiment and at the starting point before migration. Labeled WT (1.5×10^5) and $\alpha_D^{-/-}$ (1.5×10^5) activated macrophages were plated on the membranes of transwell inserts with a pore size of 8 µm and 6.5 mm in diameter (Costar, Corning, NY) precoated with fibrinogen (Fg). Fibrin gel (100 µl/sample) was made by 0.75mg/ml Fg containing 1% FBS and 1% P/S and activated by 0.5 U/ml thrombin. Matrigel (50%) was diluted by RPMI-1640 supplemented with 1% FBS and 1% P/S. 30 nM of MCP-1 (or 100 nM FMLP) were added on the top of the gel to initiate the migration. Migrating cells were detected by Leica Confocal microscope (Leica-TCS SP8) and the results were analyzed and reconstructed using IMARIS 8.0 software.

Adoptive transfer in the model of resolution of peritoneal inflammation.

Adoptive transfer was performed as described previously [23]. Briefly, fluorescently-labeled WT (red PKH26 dye) and $\alpha_D^{-/-}$ or $\alpha_M^{-/-}$ (green PKH67 dye) M1- or M2-activated macrophages were mixed in a 1:1 ratio and further injected intraperitoneally into wildtype mice at 4 days after thioglycollate (TG)-induced inflammation. 3 days later, peritoneal macrophages were harvested with 5 ml PBS supplemented with 5 mM EDTA. The percentages of red and green fluorescent macrophages in the peritoneal exudate were assessed by fluorescence microscopy, multi-color flow cytometer (Fortessa X-20) and imaging flow cytometry (ImageStream Mark II, Amnis).

The PKH26 and PKH67 dyes were switched in one experiment to verify the effect of dye on cell migration. We did not detect any difference between two dyes. The quantification of the data was analyzed by using Image Analysis Software (EVOS, Thermo Fisher).

Adoptive transfer in the model of diet-induced diabetes.

The approach is based on previously published method [26] with some modifications. Monocytes were isolated from the bone marrow progenitors of WT and α_D-deficient mice using magnetic bead separation kit (Miltenyi Biotec, Gaithersburg, MD). Monocytes were labeled with red, PKH26 (WT) or green, PKH67 ($\alpha_D^{-/-}$) fluorescent dyes. Red (1.5×10^6) and green (1.5×10^6) cells were mixed together and injected in tail vein of wild type C57BL6 mice fed high fat diet (45% kcal/fat) for 8 weeks. After 3 days adipose tissue was isolated, digested as described previously [26] and analyzed using FACS (Fortessa X-20, BD) and imaging flow cytometry (ImageStream Mark II, Amnis).

Glucose tolerance and insulin sensitivity tests.

Wild type and $\alpha_D^{-/-}$ mice fed a high fat diet for 16 weeks were fasted overnight in a new cage containing water but no food, (approximately 16 hours). The following morning mice were weighed, and an initial blood glucose level was measured using a glucometer and blood from the tail vein. Glucose (2 grams/kg body weight of 20% D-glucose) was administered IP and at 15, 30, 60, and 120 minutes post injection blood glucose was again measured.

For Insulin sensitivity test, Mice fed a high fat diet were fasted for 5 hours, starting at 7 AM (lights on). After fasting, mice were weighed, and the initial level of blood glucose measured as described above. Insulin (0.75mU/g) was injected I.P. and the level of blood glucose was evaluated at 15, 30, 45 and 60 min.

Quantitative RT-PCR

Cellular mRNA was extracted from macrophages using the Qiagen Oligotex mRNA Midi Kit. mRNA was reverse transcribed with the iScript cDNA Synthesis Kit (Bio-Rad Laboratories, Inc., Hercules, CA) and real-time quantitative PCR was performed using SYBR Green Supermix (Bio-Rad) on an MyIQ2 two color real-time PCR detection system (Bio-Rad), with the thermal cycler conditions suggested by the manufacturer. The sequences of integrin primers are shown below: α_D forward, 5'-GGAACCGAATCAAGGTCAAGTA-3', and reverse, 5'-ATCCATTGAGAGAGCTGAGCTG-3'. α_M forward, 5'-TCCGGTAGCATCAACAACAT-3' and reverse, 5'-GGTGAAGTGAATCCGGAACT-3'. α_4 forward, 5'-AAGGAAGCCAGCGTTCATATT-3', and reverse, 5'-TCATCATTGCTTTTGCTGTTG-3'. α_5

forward, 5′-CAAGGTGACAGGACTCAGCA-3′, and reverse, 5′-GGTCTCTGGATCCAACTCCA-3′. αx forward, 5'-CTGGATAGCCTTTCTTCTGCTG-3', and reverse, 5'-GCACACTGTGTCCGAACTCA-3'. GAPDH or 5S rRNA were used as an internal control (Ambion/Life Technologies, Grand Island, NY).

Statistical analysis

Statistical analyses were performed using Student's t-test or Student's paired t-tests where indicated in the text using SigmaPlot 13. A value of $p < 0.05$ was considered significant.

Results

Integrin $\alpha_D\beta_2$ is upregulated on M1 macrophages in vitro and in atherosclerotic lesions.

Despite a detected role of $\alpha_D\beta_2$(CD11d) in neutrophil accumulation, the role of $\alpha_D\beta_2$ in macrophage function seems to be more significant. This assumption is based on the critical role of macrophages in atherogenesis and on the dominant expression of $\alpha_D\beta_2$ on macrophages. Moreover, most of identified cytokines are expressed by macrophages and related to macrophage functions.

Various studies have highlighted IL-6 as an upstream inflammatory cytokine that plays an important role in the development of atherosclerosis [27]. The high level of IL-6 found in such conditions has multiple functions, including activation of endothelial cells, increased coagulation, and promotion of lymphocyte proliferation and differentiation. Fractalkine is a chemokine which is involved in macrophage recruitment during inflammation [28]. IL-12 contributes to atherosclerosis by mediating the differentiation of naive T cells into Th1 cells. It stimulates the production of IFN-γ and TNF-α from T cells and natural killer cells, and also reduces IL-4 mediated suppression of IFN-α [29]. Therefore, IL-12 is involved in classical, pro-inflammatory activation of macrophages (M1). In contrast, IL-13, which is upregulated in $\alpha_D^{-/-}$/ApoE$^{-/-}$ mice, is responsible for the alternative macrophage activation [30].

Taken together these data indicate a link between pro-inflammatory macrophages and $\alpha_D\beta_2$. Accordingly, we tested the regulation of $\alpha_D\beta_2$ expression on M1 and M2 macrophages and compared its expression with its related integrin α_M(CD11b). Peritoneal macrophages were incubated 3 days in the presence of 100 U/ml IFN-γ (M1) or 2 nM IL-4 (M2) and integrin

71

expression was evaluated by q-PCR. Macrophage polarization was verified by q-PCR using markers for M1 (iNOS) and M2 (Arg1) subsets (Data not shown). $\alpha_D\beta_2$ was significantly upregulated on mouse peritoneal macrophages activated to the M1 phenotype (Fig.3-1A), while the density of $\alpha_M\beta_2$ remained relatively unchanged. To confirm this result, $\alpha_D\beta_2$ and $\alpha_D\beta_2$ expressions on M1 macrophages were verified by FACS (Fig.3-1B). To demonstrate similar pattern of expression for human $\alpha_D\beta_2$, we also tested M1 and M2 activation of human monocyte-derived macrophages using 100 U/ml IFN-γ and 2 nM IL-13. We found that the generation of the M1 phenotype significantly upregulated $\alpha_D\beta_2$ expression, while the M2 phenotype markedly decreased the $\alpha_D\beta_2$ level. In contrast, the expression of $\alpha_M\beta_2$ was not affected by macrophage polarization (Fig.3-1C). These data clearly demonstrate the association of $\alpha_D\beta_2$ with pro-inflammatory M1 macrophages in both mice and humans.

The progression of chronic inflammation depends on excessive accumulation of M1 macrophages in the subendothelial space during atherogenesis [31]. We sought to test whether $\alpha_D\beta_2$ expression was elevated on macrophages in atherosclerotic lesions. Flow cytometry of digested mouse atherosclerotic aortas identified a high expression of $\alpha_D\beta_2$ on macrophages in the lesion and confirmed a moderate expression of $\alpha_M\beta_2$ [32] (Fig. 3-1D). Remarkably, this pattern of expression is specific to chronic inflammation, since the level of $\alpha_D\beta_2$ is similar or lower on other subsets of monocytes/macrophages compared to $\alpha_M\beta_2$ (Fig. 3-1E) [17]. Therefore, $\alpha_D\beta_2$ is upregulated on M1 macrophages and within the site of inflammation, while $\alpha_M\beta_2$ expression is not regulated by macrophage activation and is expressed at moderate levels at inflammatory sites.

These data demonstrate a dramatic difference in $\alpha_D\beta_2$ expression on monocytes and macrophages during inflammation and suggest a potential regulatory role of $\alpha_D\beta_2$ in migration/accumulation of M1 macrophages in tissue.
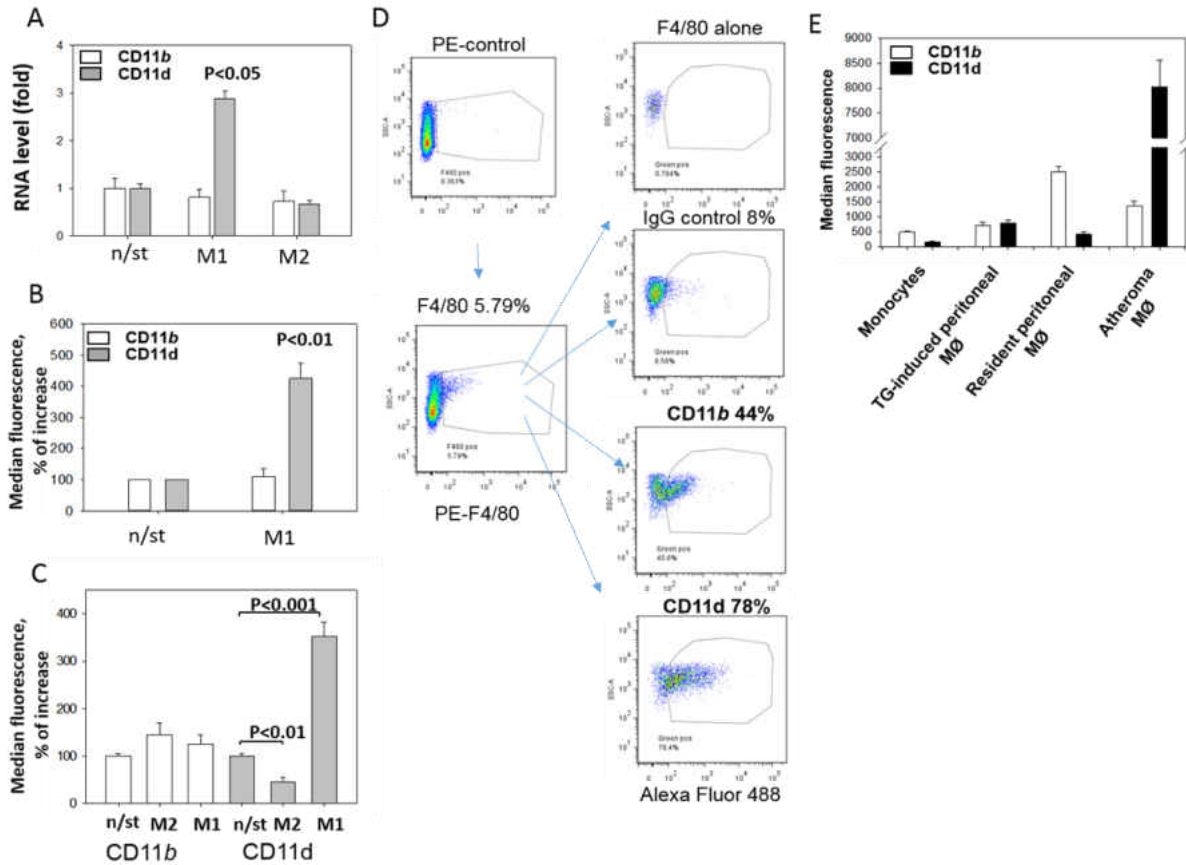
Fig.3-1 Integrin α_D(CD11d) is upregulated on M1 macrophages in vitro. Mouse peritoneal macrophages, isolated after the intraperitoneal injection of 4% thioglycollate, were plated and stimulated with 100 U/ml IFN-γ or 2 nM IL-4 for 3 days. After incubation integrin expression was evaluated by real-time quantitative PCR (**A**) and by FACS (**B**) (n=5). **C.** Human primary monocytes were stimulated with IFN-γ (M1) or IL-13 (M2) for 5 days and integrin expression was evaluated by FACS. Mean fluorescence values are plotted based on 5 independent experiments. **D.** Integrins α_D (CD11d) and α_M (CD11b) expression in atherosclerotic lesions. Aortas of ApoE$^{-/-}$ mice were isolated, digested and subjected to multi-color FACS with macrophage marker mAb F4/80 and integrin specific antibodies. Data are from a representative experiment of three with similar results. **E.** α_D and α_M expression on murine circulating monocytes; thioglycollate-induced peritoneal, resident peritoneal and atheroma macrophages. Data were plotted as the mean±SEM.

α$_D$ deficiency reduced macrophage accumulation in atherosclerotic lesions and does not have effects on macrophage apoptosis or proliferation.

The analysis of aorta sinuses with anti-macrophage Mac-3 antibody demonstrated an attenuated accumulation of macrophages in the atherosclerotic lesions of α$_D^{-/-}$/ApoE$^{-/-}$ mice that cannot be explained by reduced level of cholesterol in circulation or decreased foam cell formation and indicates a potential role of α$_D$ in macrophage migration (Fig.3-2A). However, the recent data demonstrate a significant role of apoptosis and proliferation on macrophage accumulations in the atherosclerotic lesions as well as on development of atherosclerosis. Our cytokine assay screening detected a reduced concentration of FAS ligand in α$_D^{-/-}$/ApoE$^{-/-}$ mice that indicates potential role of α$_D$ in apoptosis. The aorta root samples from ApoE$^{-/-}$ and α$_D^{-/-}$/ApoE$^{-/-}$ mice were stained with ApopTag peroxidase in Situ apoptosis kit (EMD Millipore), but demonstrated no difference between control and experimental groups (Fig.3-2B). In addition, to test the effect of CD11d-deficiency on macrophage apoptosis and proliferation, WT and α$_D^{-/-}$ peritoneal macrophages were isolated and incubated with oxidized lipids and GM-CSF for 5 days. There was no effect of α$_D$-deficiency on the macrophage number and survival using Annexin V apoptosis assay (Fig. 3-2C) and CyQuant direct proliferation assay (Fig. 3-2D).

Therefore, despite reduced concentration of Fas ligand we did not find changes in the apoptosis of α$_D^{-/-}$/ApoE$^{-/-}$ mice. These results are in agreement with published data that overexpression of Fas ligand during development of atherosclerosis increased lesion progression, but did not affect cell apoptosis. Rather, Fas ligand-mediated atherogenesis relates to increased lesion cellularity. Hence, α$_D$-mediated macrophage accumulation most likely depends on the regulation of macrophage migration.
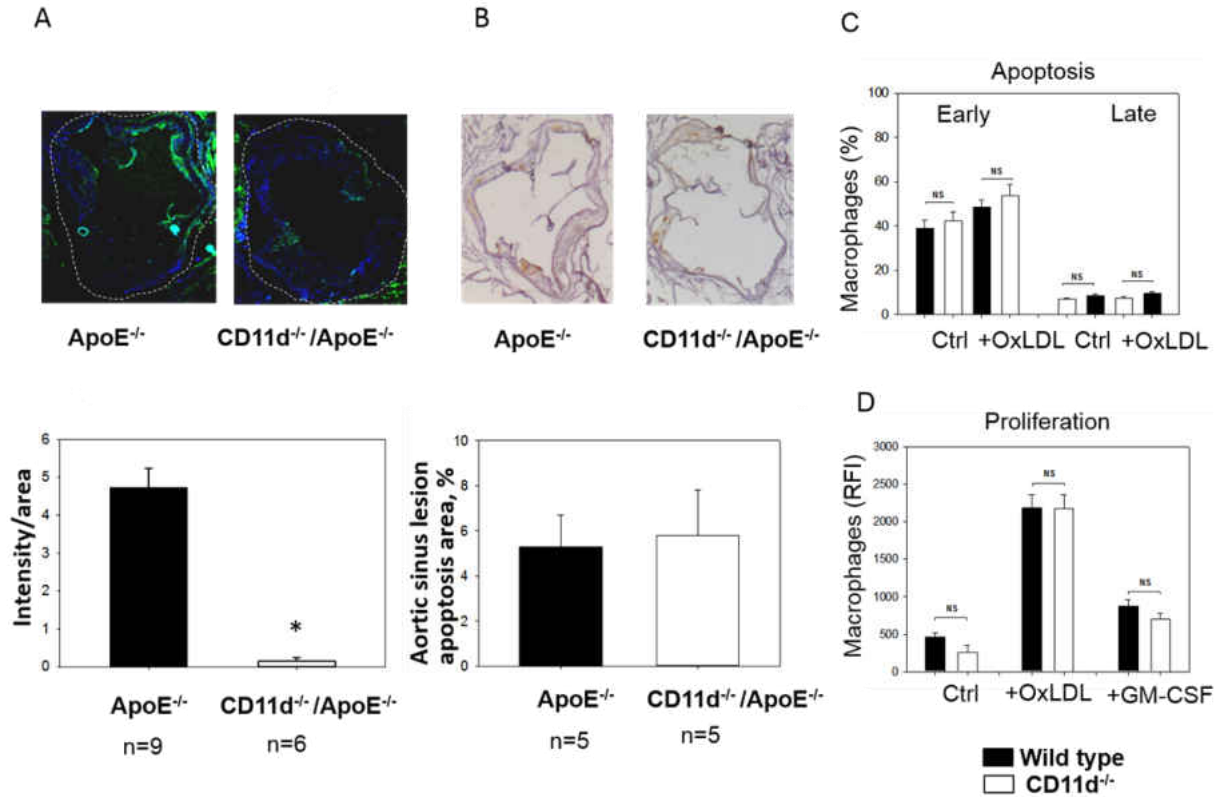
Fig. 3-2. Macrophage accumulation, apoptosis and proliferation in the mouse aortic sinus.

A. Macrophage staining in the aortic sinus from ApoE$^{-/-}$ and $\alpha_D$$^{-/-}$/ApoE$^{-/-}$ mice: Upper panel. Representative images of a cross section of the aortic sinus stained with Mac3 (40× magnification). The intima of vessel wall is surrounded by dash line. Lower panel, the graph represents the quantification of the surface area positive for Mac3. The data represent the mean ± SEM of Mac3 positive areas in 6 sections of each group. *p<0.05. Integrin α_D-deficiency does not affect macrophage apoptosis (**B, C**) or proliferation (**D**). **B.** Apoptosis was evaluated on aorta sinuses isolated from ApoE$^{-/-}$ and $\alpha_D$$^{-/-}$/ApoE$^{-/-}$ mice using ApopTag peroxidase in Situ apoptosis kit. **C.** Peritoneal macrophages were isolated from WT and $\alpha_D$$^{-/-}$ mice and incubated in vitro in different conditions. Macrophage apoptosis was assessed after 24 hours incubation on plates and an additional 18 hours incubation in the presence of 15 mg/ml OxLDL using Annexin V assay. **D.** Macrophage proliferation was evaluated after 5 days in culture in the presence of 50 mg/ml OxLDL or 60 ng/ml GM-CSF using CyQUANT® Direct proliferation assay kit. Black bars − wild type macrophages, open bars − α_D -deficient macrophages. Data were plotted as the mean ± SEM. Statistical analysis was performed using Student's t-test.

Strong adhesion of classically-activated (M1) macrophages is converted in weak migration in contrast to well-migrated, but low-adherent alternatively-activated (M2) macrophages.

To evaluate the adhesive and migratory properties of M1 and M2 macrophages, we stimulated thioglycollate-induced peritoneal macrophages with IFNγ (M1-activated) or IL-4 (M2-activated) and evaluated the adhesion of these cells to fibrinogen and their migration in 3D fibrin matrix. The adhesion assay revealed a much stronger attachment of M1 macrophages (28.68±5.33%) when compared to M2 macrophages (9.12±2.79%) (Fig.3-3A). Moreover, M1 and M2 adherent cells possess different morphologies. While M1 macrophages have a rounded, flat, pancake-like shape after adhesion assay, M2 macrophages were elongated and less spread out (Fig. 3-3B). The development of M1 and M2 phenotypes were verified by upregulation of iNOS and ArgI, respectively (Fig. 3-4A).

We tested how different adhesive properties affect macrophage cell migration (Fig.3-3C-F). Fluorescently labeled M1 (red, PKH26) and M2 (green, PKH67) macrophages were mixed in an equal number (Fig. 3-5A) and placed on a 3D fibrin gel where cell migration was stimulated via a MCP-1 gradient (Fig. 3-3C, E). After 48 hours, we detected a robust migration of M2 macrophages, which markedly exceeded the locomotion of M1 macrophages (Fig. 3-3D-F). It has been shown previously that M1 and M2 macrophages demonstrate a similar chemotaxis to MCP-1 in 2D transwell assay (no ligand coated on membrane) [33]. These data proved that the different migration of M1 and M2 macrophages in our 3D chemotaxis/haptokinesis assay does not regulated by different expression of CCR2 (chemotaxis), but by distinct adhesion-mediated migration (haptokinesis). To additionally verify it, the migration was repeated using a gradient of N-Formylmethionine-leucyl-phenylalanine (FMLP) and revealed similar results (Fig.3-5B), therefore the adhesive receptors are potential cause of different migratory properties of M1 and M2.
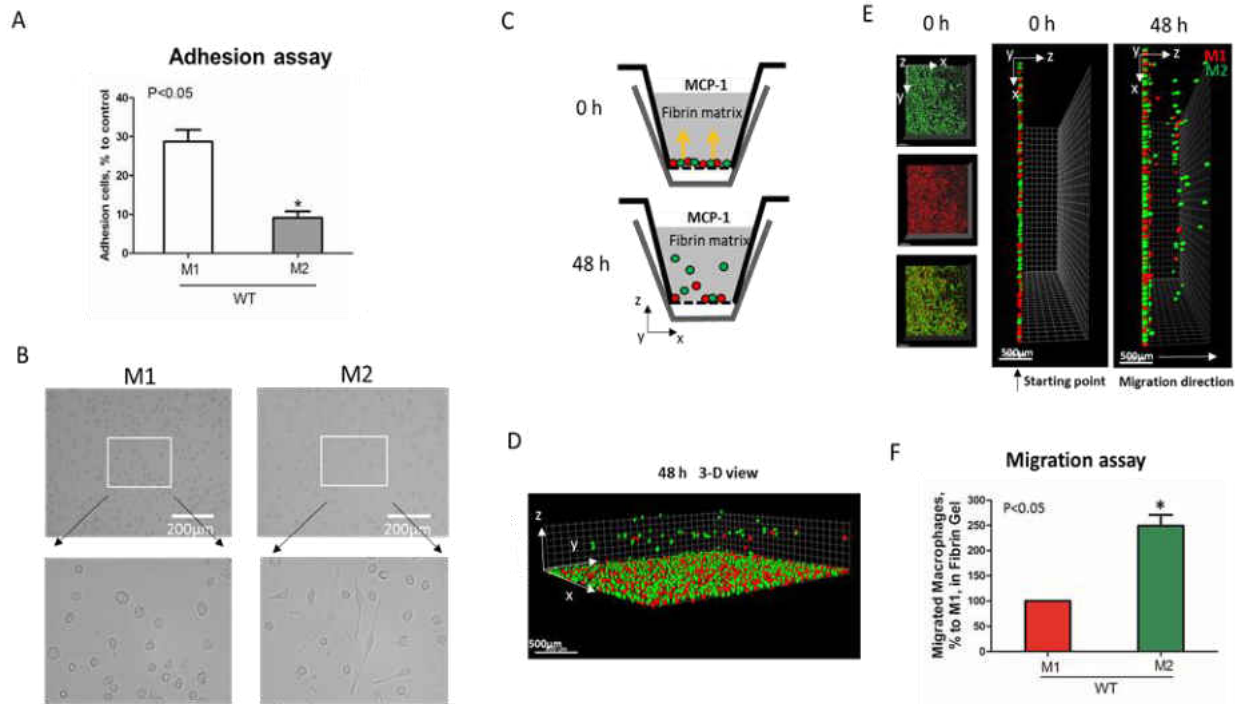
Fig.3-3. M1-activated macrophages demonstrate much stronger adhesive properties but weaker migration in comparison to M2-activated macrophages. A. Adhesion assay of WT M1 and M2-activated macrophages to Fg. 96-well plate was coated with 4 µg/ml Fg for 3 h at 37°C. Fluorescently labeled M1 and M2 macrophages were added to the wells and cell adhesion was determined after 30 min in a fluorescence plate reader. Data are presented as mean ± SEM. *, P < 0.05. **B.** Morphologies of M1 (**Left panel**) and M2 (**right panel**) activated macrophages, scale bar=200 µm. **C-F.** 3-D migration assay in Fibrin matrix using M1 and M2 activated macrophages labeled with PKH26 (Red) and PKH67 (Green) fluorescent dyes, respectively. **C.** Sketch diagram of the migrating cells in Boyden transwell chamber. Before migration (**upper panel**) and after 48h migration (**lower panel**). **D.** 3-D view of the migrating cells in Fibrin matrix after 48 hours. **E.** Labeled Cells were mixed in equal amounts and verified by scanning samples with confocal microscope before the initiation of migration (**E. left and middle panels**). Migration of macrophages was stimulated by 30 nM MCP-1 added to the top of the gel. After 48 hours, migrating cells were detected by a Leica Confocal microscope (**E. right panel**). **F.** The results were analyzed by IMARIS 8.0 software and statistical analyses were performed using Student's paired t-tests (n=4 per group). Scale bar= 500 µm. Data are presented as mean ± SEM. *, P < 0.05.
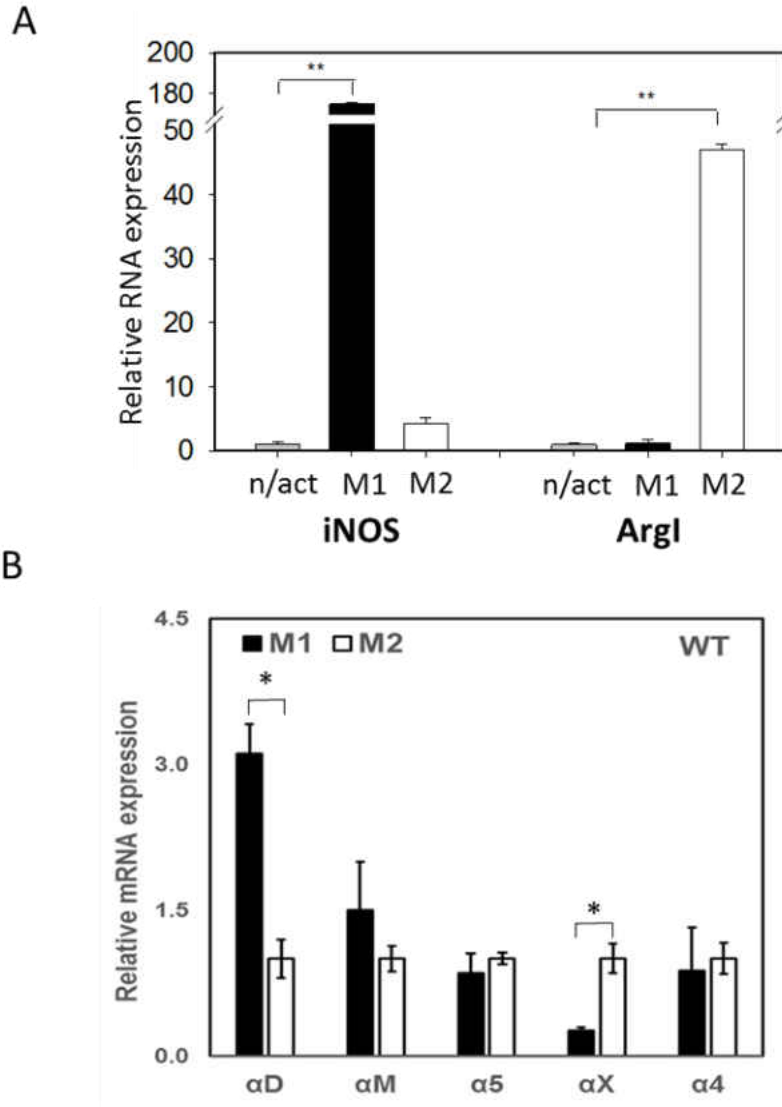
Fig.3-4. **The expression of markers and fibrin-binding integrins on M1 and M2 stimulated macrophages. A.**The expression of M1 (iNOS) and M2 (Arg I) markers on IFN-γ (M1) and IL-4 (M2) stimulated macrophages using Real Time-PCR. Statistical analyses were performed using paired Student t-tests (n=3 per group). Data are presented as mean ± SEM. **, P< 0.01, compared to non-activated (n/act). **B.** The expression of fibrin-binding integrins during M1 and M2 polarization. Open bars – non-activated; black bars M1-polarized, grey bars M2-polarized macrophages. Statistical analyses were performed using Student's paired t-tests (non-activated to activated) (n=3 per group). Data are presented as mean ± SEM. *, P < 0.05.
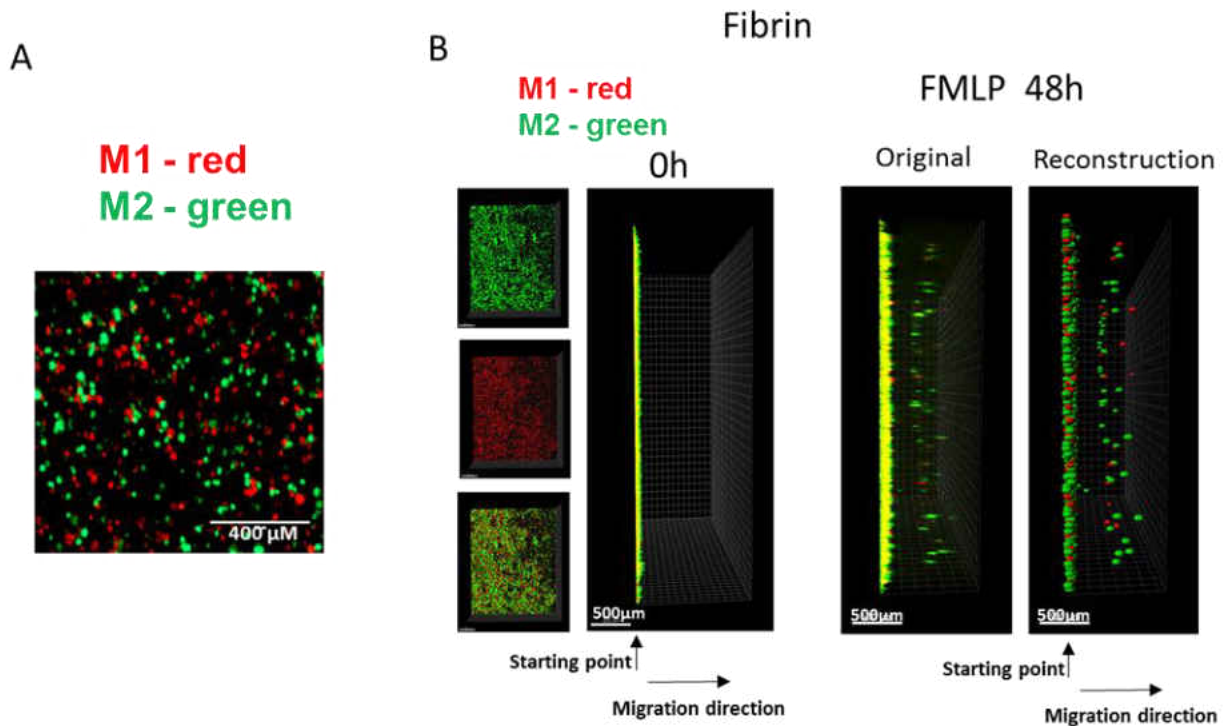
Fig.3-5. A-B. 3D migration assay of macrophages in Fibrin matrix. WT M1 and M2 macrophages were labeled with PKH26 and PKH67 fluorescent dyes, respectively. Cells were mixed in equal amounts before the experiment. Similar cell numbers were verified by cytospin of mixed cells (**A**) and by analysis of macrophage starting points before migration. The background fluorescence of fibrin gel was verified by scanning samples with confocal microscope before the initiation of migration (**B, left panel**). Migration of macrophages was stimulated by 100 nM FMLP added to the top of the gel. After 48 hours, migrating cells were detected by a Leica Confocal microscope (**B. middle panel-**original). The results were analyzed and reconstructed by IMARIS 8.0 software (**B, right panel**).

The levels of integrin expression determine the effects on macrophage migration.

Recently, we demonstrated that integrin α_D is upregulated on M1-polarized macrophages but does not change on M2-polarized macrophages [23]. We evaluated the potential changes in the expression of other fibrin-binding macrophage adhesive receptors during M1 and M2 polarization (Fig. 3-4A). The RT-PCR results demonstrated that α_D is the only adhesive receptor that upregulates during M1 macrophage activation to compare with M2 subset (Fig. 3-4B). We also detected the increased expression of integrin α_X on M2 macrophages; however, the total expression

of α_X on macrophages is very low [20], which quashes its potential effect on macrophage migration. Therefore, the upregulation of integrin α_D is the most significant modification that may affect the migratory properties of M1 and M2 macrophages.

Based on these data, further analysis was focused on integrin α_D and related integrin α_M, that possess similar ligand binding properties, but distinct surface expressions. The contributions of integrin α_D and α_M to M1 and M2 migration were evaluated using α_D- and α_M-deficient macrophages. α_D deficiency reduced the adhesion of M1 macrophages to fibrinogen (Fig. 3-6A), but significantly increased cell migration (Fig. 3-6C, left panel; 3E). In contrast, integrin α_M deficiency has very limited effect on adhesion, due to its moderate expression on M1 macrophages [23], (Fig.3-4B) and did not demonstrate a significant effect on cell locomotion (Fig. 3-6C right panel; 3-6E). Both integrins, α_D and α_M, have moderate expression on M2 macrophages [23], (Fig. 3-4B). The adhesion of M2 macrophages depends on both integrins, which is demonstrated in the presence of antibodies and integrin-deficient cells (Fig.3-6B). In parallel assays, the reduced migration of α_M- and α_D-deficient macrophages verified that both integrins help to support the mesenchymal migration of M2 macrophages (Fig.3-6D, F).

The deficiency of α_D or α_M may also modify the expression of other fibrin-binding integrins that can affect cell migration. To test this possibility, we evaluated the expression of α_4, α_5, α_X, and α_M on $\alpha_D^{-/-}$, as well as α_D on $\alpha_M^{-/-}$ macrophages activated to M1 and M2 phenotypes using RT-PCR. We did not detect any marked changes, except for the reduced expression of α_5 and α_X on α_D-deficient M1 macrophages (Fig.3-7). Clearly, these changes cannot significantly modify migration.
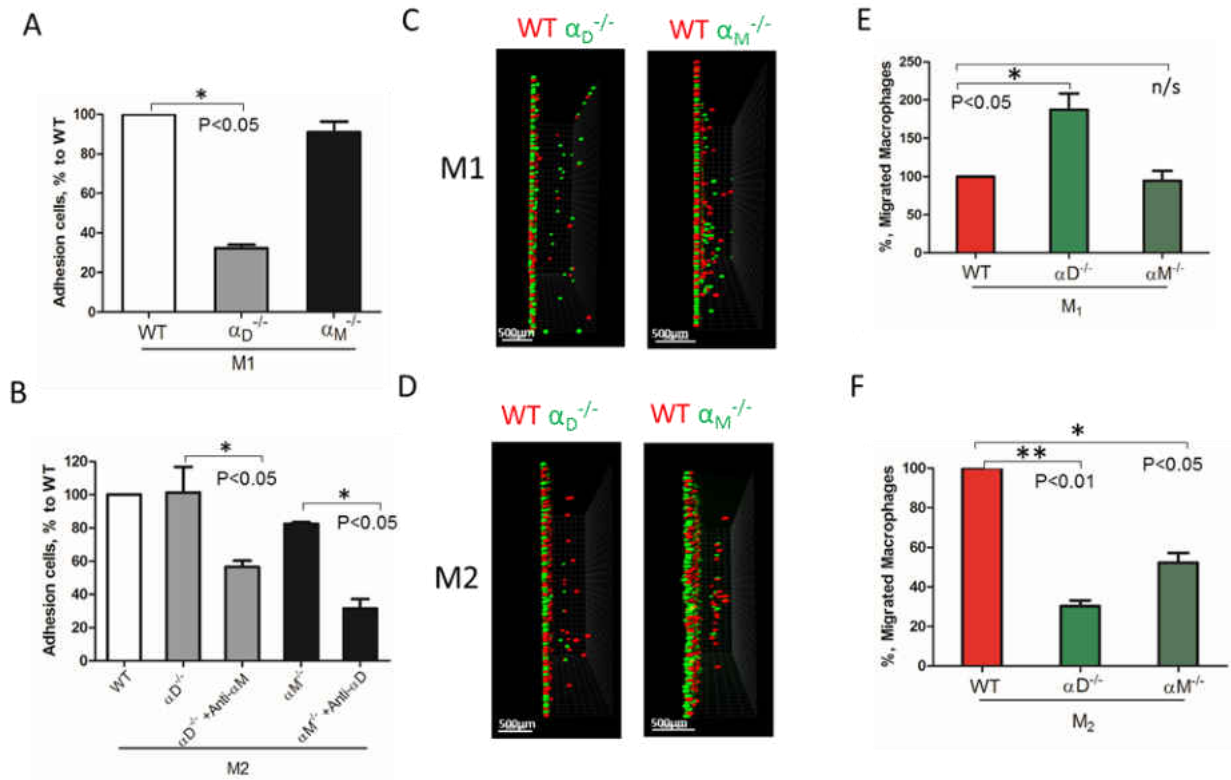
Fig.3-6. The level of integrin expression determines the effect on macrophage migration. A-B. Adhesion assay to fibrinogen of WT, $\alpha_D^{-/-}$ and $\alpha_M^{-/-}$ macrophages activated to M1 **(A)** and M2 **(B)** phenotypes. Some samples in **(B)** were pre-incubated with anti-α_M and anti-α_D blocking antibodies before the adhesion assay. Data are presented as mean ± SEM. *, P < 0.05. **C-D.** Migration assay of α_D- and α_M-deficiency M1 **(C)** and M2 **(D)** macrophages in 3D fibrin matrix. After 48 hours, migrating cells were detected by a Leica Confocal microscope and the results were analyzed by IMARIS 8.0 software, scale bar= 500 μm. **E-F.** Statistical analyses were performed using Student's paired t-test (n=4 per group). Data are presented as mean ± SEM. *, P < 0.05.
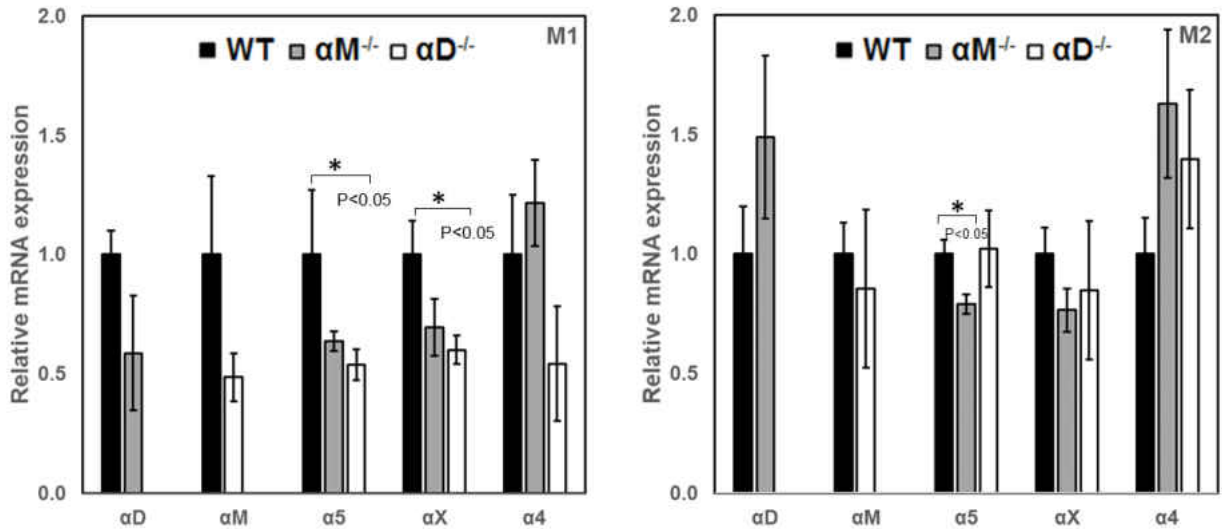
Fig.3-7. The expression of fibrin-binding integrins on $\alpha_D^{-/-}$ and $\alpha_M^{-/-}$ macrophages activated to M1 and M2 phenotypes using Real Time-PCR. Statistical analyses were performed using paired t-tests (n=3 per group). Data are presented as mean ± SEM. *, P< 0.05.

α_D-mediated adhesion is critical for the retention of M1 macrophages.

Inflamed extracellular matrix contains different β_2 ligands, including fibronectin, vitronectin, thrombospondin, fibrinogen and others. Moreover, we recently showed that oxidative stress during inflammation may form ECM protein modifications with carboxyethylpyrole, which is also a ligand for β_2 integrins [25]. To verify the role of α_D-mediated adhesion on cell migration, we performed macrophage migration in Matrigel, the model of basement membrane matrix, which consists of laminin, collagen IV and proteoglycans. Notably, these proteins are not ligands for integrin $\alpha_D\beta_2$ or $\alpha_M\beta_2$. To confirm this, we tested the adhesion of $\alpha_D\beta_2$- and $\alpha_M\beta_2$-transfected HEK293 cells to a plate coated with Matrigel (Fig. 3-8A). Both cell lines demonstrated strong adhesion to Matrigel, but this adhesion was independent of α_D and α_M, since anti-α_D and anti-α_M antibodies did not inhibit this binding. In contrast, the adhesion of $\alpha_M\beta_2$ and $\alpha_D\beta_2$-transfected cells to fibrinogen was significantly inhibited by these antibodies [21, 34] (Fig.3-8B). Apparently, the adhesion to Matrigel is mediated by integrins $\alpha_1\beta_1$ and $\alpha_2\beta_1$, which are receptors for laminin and collagen, and are expressed endogenously on HEK293 cells [35-37]. To verify this hypothesis, we evaluated the adhesion of MOCK-transfected HEK293 cells to Matrigel and fibrinogen. These cells did not support the adhesion to fibrinogen, but demonstrated the same level of adhesion to

Matrigel as $\alpha_D\beta_2$ and $\alpha_M\beta_2$ transfected cells (Fig.3-8A, B). Therefore, cells do not use $\alpha_D\beta_2$ for the adhesion to Matrigel. Accordingly, we detected a similar level of wild type and α_D-deficient macrophage migration through Matrigel, which is distinct to our data in α_D-dependent fibrin matrix. Therefore, this result is in agreement with our hypothesis regarding the critical role of α_D-mediated adhesion for macrophage retention during 3D migration (Fig.3-8C).

However, one of the mechanisms that affects mesenchymal migration is the secretion of MMPs that degrade Matrigel. To test the potential effect of α_M or α_D deficiency on MMP secretion, M1 and M2 macrophages were incubated in 48-well plates for 24 hours and the media was tested using gelatin zymography as we described previously [38] (Fig.3-8D). First, we found a much stronger secretion of MMPs (specifically MMP-9) in M2 macrophages in comparison to M1 macrophages. Second, we did not detect any significant effect of α_D- or α_M-knockout on MMPs secretion, particularly in regard to M1-polarized macrophages.

Interestingly, the robust secretion of collagen-specific MMP-9 by M2 macrophages can be responsible for the strong migration of these cells in Matrigel. The migration of M1 and M2 macrophages was performed in separate gels to avoid the effect of M2-released MMP-9 on the migration of M1 macrophages (Fig.3-9). In contrast, similar secretion of MMPs in WT and α_D-deficient M1 macrophages allowed us to compare these two cell types in one sample. Therefore, the similar migration of WT and α_D macrophages in Matrigel was not regulated by a different level of MMP secretion, but by the lack of α_D-mediated adhesion.
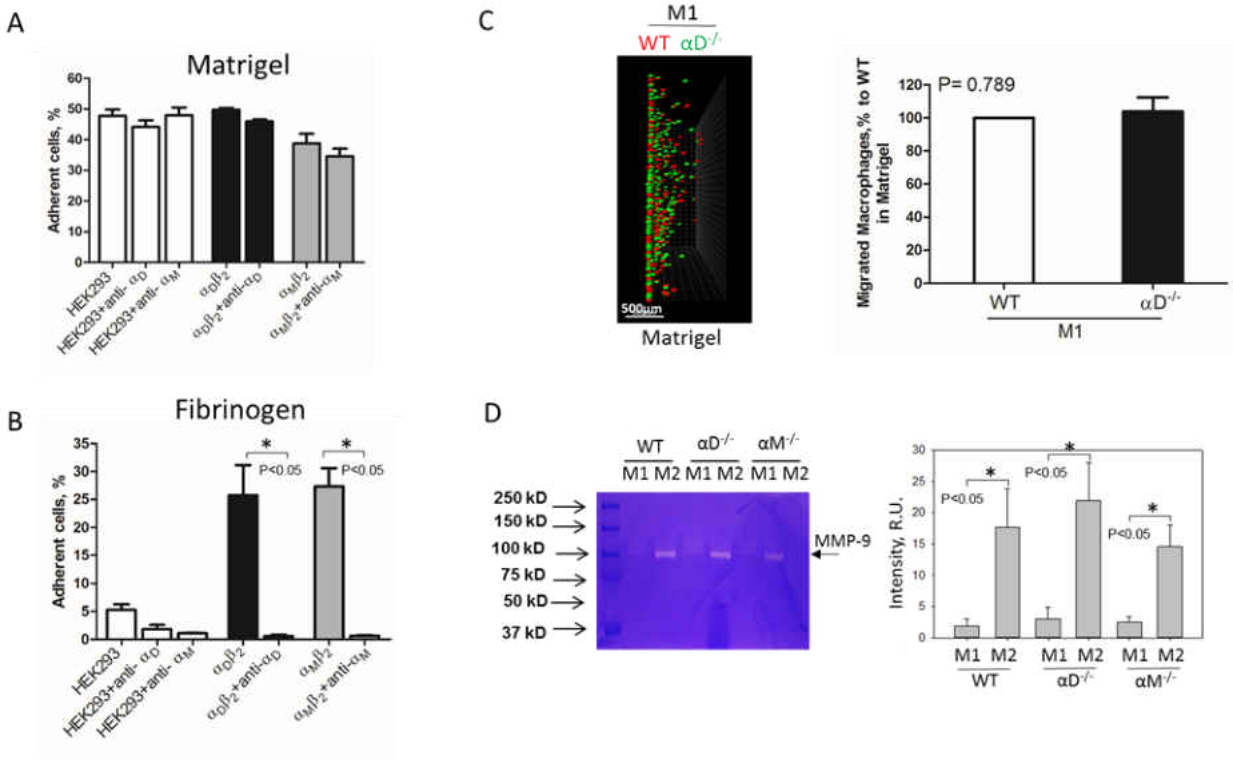
Fig.3-8. Matrigel does not support integrin αD-mediated adhesion and retention of M1 macrophages. **A-B.** Adhesion of $\alpha_D\beta_2$- and $\alpha_M\beta_2$-transfected and mock-transfected HEK293 cells to Matrigel **(A)** and fibrinogen **(B)**. The adhesion was performed as described above. Data are presented as mean ± SEM. *, P < 0.05. **C.** 3-D migration assay of WT and αD-deficient M1 macrophages in Matrigel. Migration was stimulated by 30 nM MCP-1 added to the top of the gel. After 48 hours, migrating cells were detected by a Leica Confocal microscope (Leica-TCS SP8) **(C, left panel)**. Scale bar= 500 μm. The results were analyzed by IMARIS 8.0 software. **(C, right panel)**. **D.** Evaluation of MMPs in culture media after macrophage adhesion. WT, $\alpha_D^{-/-}$ and $\alpha_M^{-/-}$ M1- and M2-activated macrophages were plated on fibrinogen. Media was collected after overnight incubation and analyzed by gelatin-zymography (**D, right pane**l). The intensity of gelatin degradation was evaluated by Fuji software (**D, left pane**l). Statistical analyses were performed using Student's paired t-tests (n=4 per group). Data are presented as mean ± SEM. *, P < 0.05.
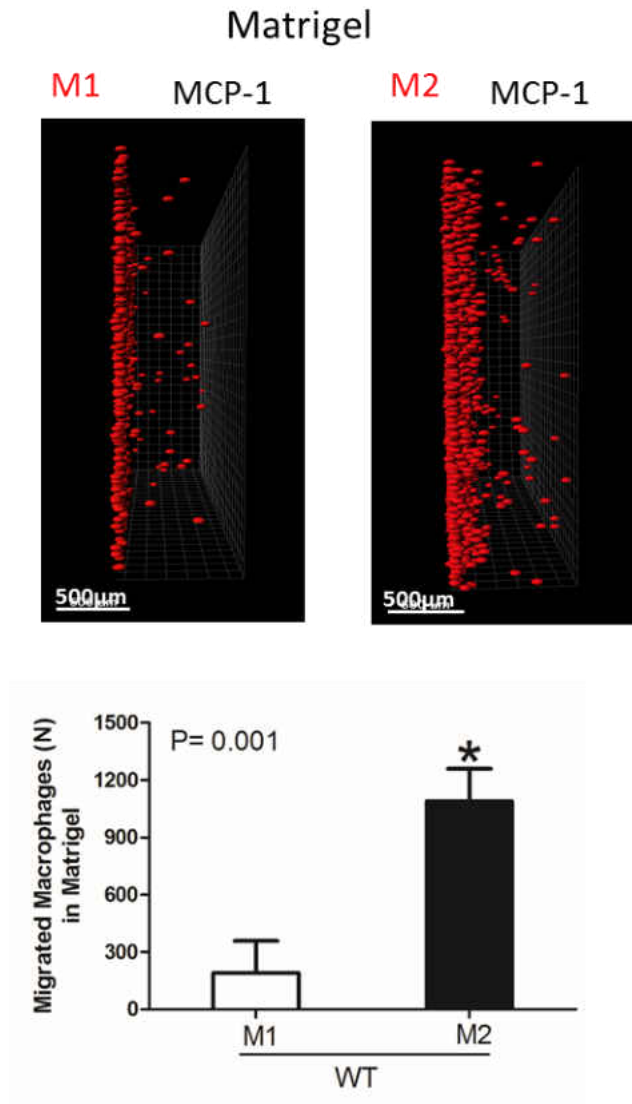
Fig.3-9. Migration of M1 and M2-activated macrophages in Matrigel. After 48 hours, migrating cells were detected by a Leica Confocal microscope and the results were analyzed by IMARIS 8.0 software, scale bar= 500 μm. Statistical analyses were performed using Student's paired t-tests (n=4 per group). Data are presented as mean ± SEM. *, P< 0.05.

A high expression of α_M on resident macrophages reduces their amoeboid migration.

To test the effect of high expression of other integrins on cell locomotion, we evaluated α_M-dependent migration of resident macrophages. α_M has a very high expression on peritoneal resident macrophages (Fig. 3-10A). A comparable analysis of 3D migration in fibrin matrix between WT and α_M-deficient resident peritoneal macrophages revealed a strong improvement in

the migration of the $\alpha_M^{-/-}$ subset (Fig. 3-10B, C right panel). Notably, α_D-deficiency, which has a very low expression on resident macrophages (Fig. 3-10A), did not affect macrophage migration (Fig. 3-10B, C left panel). These results demonstrated that α_M at high density on the cell surface can also prevent migration. It has been shown that resident macrophages apply the amoeboid migratory mode [24]. Accordingly, the migration of WT and $\alpha_M^{-/-}$ in the presence of ROCK inhibitor, the inhibitor of amoeboid migration [39], resulted in a dramatic reduction in both the number of migrated cells and migratory distance. Therefore, macrophage adhesion-independent amoeboid migration can be reduced by integrin-mediated strong adhesion.
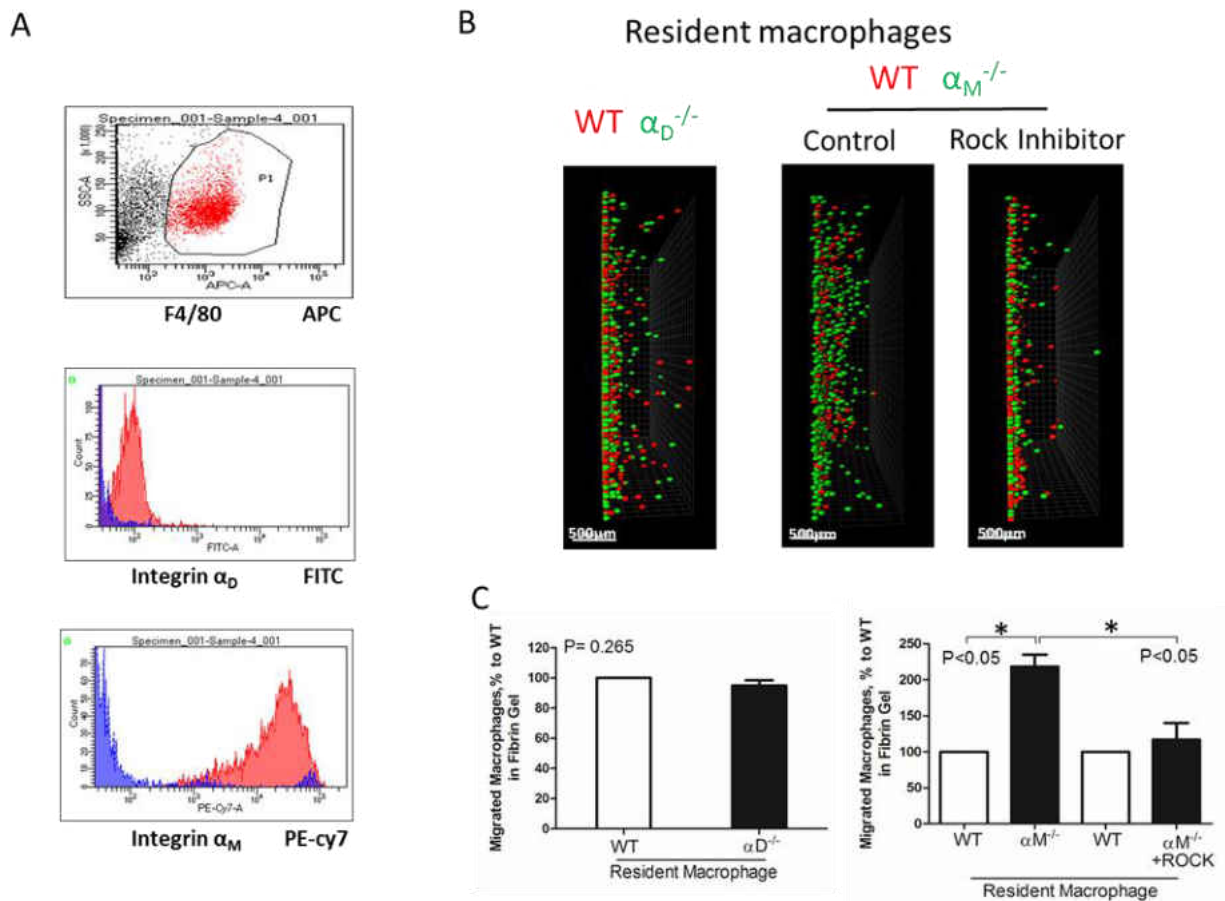
Fig.3-10. A high expression of α_M on resident macrophages reduces their amoeboid migration. A. The expression of integrin α_D and α_M on resident macrophages was detected with anti-α_D and anti-α_M antibodies, respectively, and tested by flow cytometry analysis. **B.** Migration of peritoneal resident macrophages in 3-D fibrin matrix. Migrating resident macrophages from WT and $\alpha_D^{-/-}$ mice are shown in the left panel. The middle and right panels represent the migrating resident macrophages from WT and $\alpha_M^{-/-}$ mice with or without Rock inhibitor (Y27632). Migrating cells

were detected by a Leica Confocal microscope (Leica-TCS SP8). Scale bar= 500 μm. **C.** The results were analyzed by IMARIS 8.0 software. Statistical analyses were performed using Student's paired t-tests (n=4 per group). Data are presented as mean ± SEM. *, P < 0.05.

***In vivo* migration of M1, M2 and resident macrophages confirmed the results of the 3D migration assays.**

To verify our *in vitro* results, we performed *in vivo* migration using the model of resolution of peritoneal inflammation as we have done previously [23]. After the development of thioglycollate-induced peritoneal inflammation, macrophages migrate to, and accumulate within, the peritoneal cavity. The resolution of inflammation is started after 96 hours and is characterized by the intensive emigration of macrophages from the peritoneal cavity to the lymphatics [40]. We injected adoptively transferred M1 and M2 macrophages to assess their migratory properties in the *in vivo* environment (Fig. 3-11A). *In vitro*-activated M1 and M2 macrophages were labeled with PKH26 and PKH67 fluorescent dyes, respectively. The recipient mice were first injected with thioglycollate and then, 96 hours later, with an equal number of fluorescently labeled M1 and M2 macrophages. After an additional 72 hours, the cells from the peritoneal cavity were collected and the number of M1 and M2 adoptively transferred macrophages was evaluated. The cytospin of harvested samples demonstrated the preferential accumulation of M1 macrophages (red fluorescence) in the peritoneal cavity (Fig. 3-11B and Fig. 3-12), which corresponds to our *in vitro* migration assays (Fig.3-3D-F). Our FACS data confirmed these results, since mostly M1 macrophages reside in the peritoneal cavity, while M2 macrophages emigrate during resolution (5.02±0.31% versus 2.57±0.41%) (Fig. 3-11C). The Amnis imaging flow cytometry verified the size and morphology of fluorescently labeled macrophages in the peritoneal cavity (Fig. 3-11D).

According to our *in vitro* results and previous data [23] we demonstrated that α_D-deficiency on an M1 background stimulated the emigration of macrophages from the peritoneal cavity, while α_M-knockout had no effect (Fig. 3-11E). In contrast, we detected an increased accumulation of α_M-deficient M2 macrophages in the cavity, which demonstrates the supportive role of α_M in the migration of M2 macrophages and remained consistent with our *in vitro* results. Surprisingly, we did not detect the same effect for $\alpha_D^{-/-}$ macrophages. The difference between the migrations of WT and $\alpha_D^{-/-}$ M2 macrophages was not significant (Fig. 3-11E, lower panel).

WT and $\alpha_M^{-/-}$ resident macrophages were isolated and tested using the same resolution of inflammation assay. After 72 hours, we detected predominantly wild type cells in the peritoneal cavity, while α_M-deficient macrophages emigrated (Fig. 3-13A). This result was verified by flow cytometry. The number of red-fluorescent WT cells isolated from the peritoneal cavity significantly exceeded the number of green-fluorescent $\alpha_M^{-/-}$ cells (Q4 versus Q1), (Fig. 3-13B). Based on this result, we suggest that α_M serves for the supporting resident macrophage accumulation in the tissue, and α_M-deficiency increases the efflux of resident macrophages.

To confirm this conclusion, we evaluated the number of macrophages in the non-inflamed peritoneal cavity of wild type and $\alpha_M^{-/-}$ mice. Isolated peritoneal cells were stained with F4/80 antibodies and analyzed by flow cytometry to detect the percentage of macrophages. We found that α_M-deficiency resulted in a twofold reduction in the number of resident macrophages in the cavity (Fig. 3-13C). In contrast, α_D-deficiency on resident peritoneal macrophages did not affect macrophage number. These data are in agreement with our *in vitro* and *in vivo* migration assays.
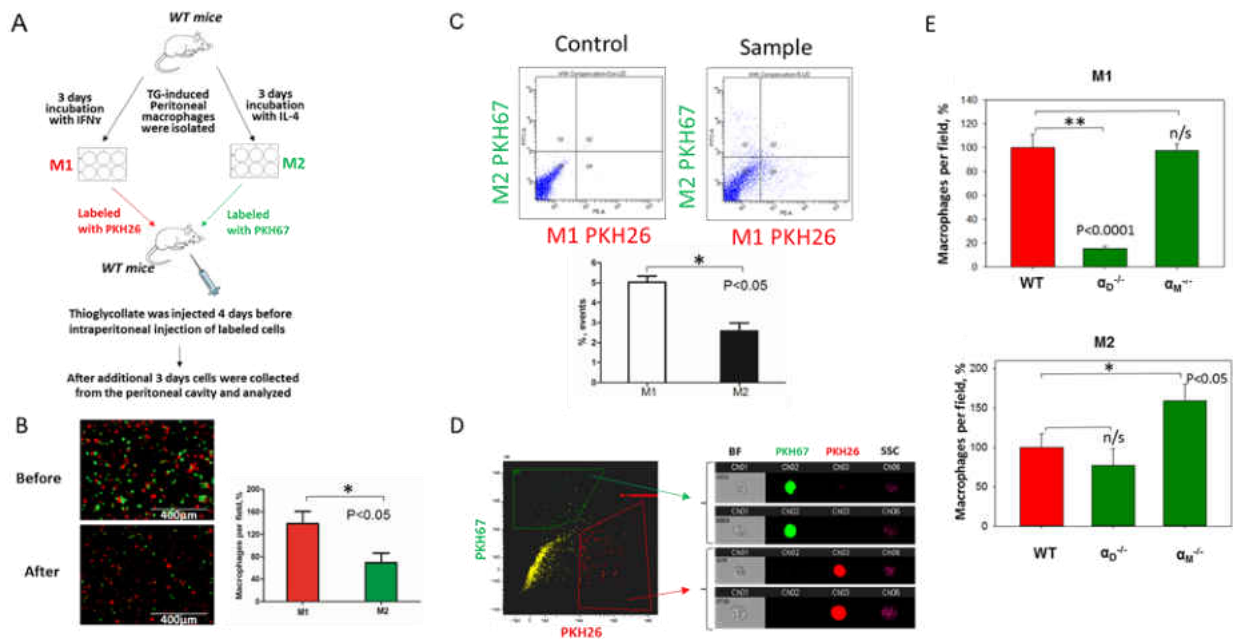
Fig.3-11. *In vivo* **migration of M1 and M2 macrophages confirmed the results of the 3D migration assays. A.** The model of *in vivo* resolution of peritoneal inflammation. Peritoneal macrophages were isolated from WT mice at 3 days after injection of thioglycollate (TG) and placed on petri dish for 3 days incubation with 100U/ml IFNγ or 2nM IL-4 to generate M1 and M2 activated macrophages, respectively. Collected M1 and M2 macrophages were labeled with

PKH26 or PKH67 fluorescent dyes. Labeled M1 and M2 macrophages were mixed in a 1:1 ratio and further injected intraperitoneally into WT mice with 4 days predisposed TG-induced peritoneal inflammation. **B.** The equal ratio of red and green macrophages before the injection was verified by sample cytospin preparation (**B, upper panel**). 3 days later, peritoneal macrophages were harvested, and the percentages of red and green fluorescent macrophages were assessed by cytospin (**B, lower panel**) and flow cytometry (**C, D**). The quantification of the data was analyzed by using Image Analysis Software (EVOS, Thermo Fisher) at least 4 fields of view per sample (n=4) (**B, right panel**). **C.** Flow cytometry. Live isolated cells were selected with live/dead kit and analyzed using 488 and 567 channels (Fortessa X-20). The results were analyzed with Diva software and statistical analysis was performed using Student's t-test. Data are presented as mean ± SEM. *, $P < 0.05$. **D.** Imaging flow cytometer. The population of single, alive cells was analyzed on red and green channels and individual cells were evaluated in green and red positive areas (ImageStream Mark II, Amnis). Channel 1- Brightfield (BF). Channel 2- 488 wavelength (PKH67). Channel 3 – 566 wavelength (PKH26), channel 6 – side scattering (SSC). **E.** M1- and M2-activated macrophages in the peritoneal cavity during the resolution of peritoneal inflammation. The quantification of the data was analyzed by using Image Analysis Software (EVOS, Thermo Fisher) 4-6 fields of view per sample (n=4). Data are presented as mean ± SEM. *, $P < 0.05$.
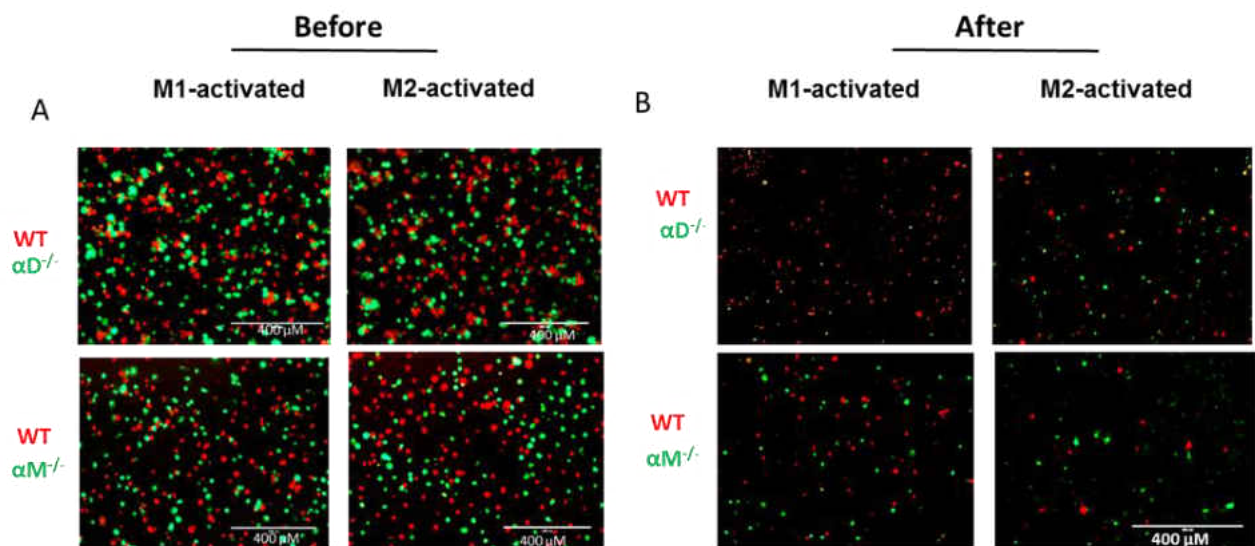
Fig.3-12. Adoptive transfer assay to test the resolution of peritoneal inflammation using WT, $\alpha_D^{-/-}$ or $\alpha_M^{-/-}$ macrophages activated to M1 and M2 phenotypes. A. The equal number of labeled

red and green cells were verified by cytospin of the mixed cells before intraperitoneal injection to the recipient mice. **B**. After 3 days, peritoneal macrophages were harvested and cytospun, and the percentages of red and green fluorescent macrophages were assessed by fluorescence microscopy. The quantification of the data was analyzed by using Image Analysis Software (EVOS, Thermo Fisher) at least 4 fields of view per sample (n=4) and presented on Fig. 3-9E.
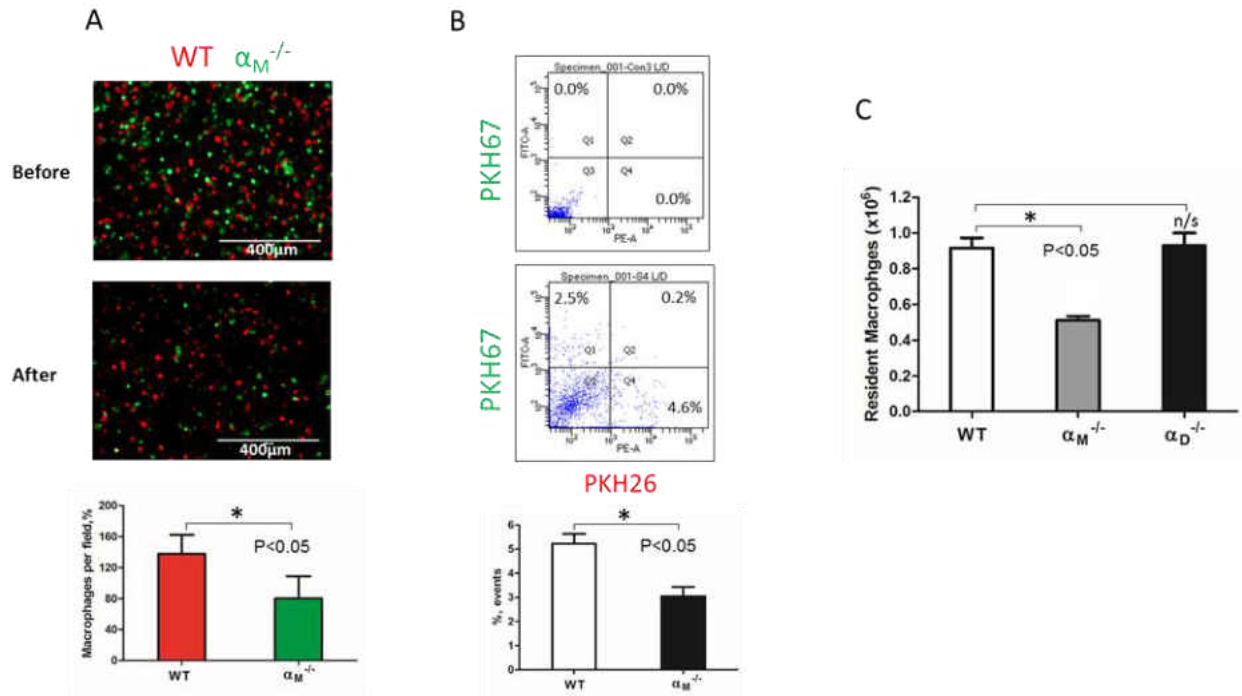
Fig.3-13. α_M deficiency improve efflux of resident macrophages. A. Fluorescently-labeled resident peritoneal macrophages isolated from WT and $\alpha_M^{-/-}$ mice were mixed in equal numbers and confirmed by cytospin (**A, upper panel**). Labeled cells were injected introperitoneally into WT mice four days after TG-induced inflammation. After 3 days, the harvested peritoneal cells were cytospun (**A, middle panel**). The quantification of the data was analyzed using t-test at least 4 fields of view per sample (n=4) by Image Analysis Software (EVOS, Thermo Fisher) (**A, lower panel**). Data are presented as mean ± SEM. *, P < 0.05. **B.** The harvested macrophages were also assessed by flow cytometry and the percentages of red (Q4) and green (Q1) fluorescent cells were assessed. Data are presented as mean ± SEM. *, P < 0.05. **C.** The amount of resident WT, $\alpha_M^{-/-}$ and $\alpha_D^{-/-}$ macrophages was evaluated by assessing the number and percentage of macrophages in non-inflamed peritoneal cavity of mice. Isolated peritoneal cells were counted and the number of WT, $\alpha_M^{-/-}$ and $\alpha_D^{-/-}$ resident macrophages were calculated based on the percentage of F4/80 positive population in flow cytometry analysis. Data are presented as mean ± SEM. *, P < 0.05.

αD deficiency reduces macrophage accumulation in adipose tissue and improves metabolic parameters.

To further confirm the contribution of $\alpha_D\beta_2$ to macrophage retention in the site of chronic inflammation, we used the model of diet-induced diabetes. The accumulation of pro-inflammatory (M1-like macrophages) in the inflamed adipose tissue is a hallmark of the inflammatory component of diabetes [26]. It has been shown that α_D is upregulated in the adipose tissue during diet-induced obesity [41], which concurs with the upregulation of α_D on M1-activated macrophages *in vitro* and in atherosclerotic lesions [23]. We also detected a strong expression of $\alpha_D\beta_2$ on adipose tissue macrophages of C57BL6 mice after 8 weeks of a high fat diet (45 kcal% fat). (Fig.3-14A,B). To assess the role of $\alpha_D\beta_2$ and $\alpha_M\beta_2$ in macrophage migration during chronic inflammation, monocytes isolated from WT and $\alpha_D^{-/-}$ (or $\alpha_M^{-/-}$) mice were labeled with red (PKH26) or green (PKH67) dyes, respectively, mixed in equal number and injected intravenously into mice on a high fat diet (Fig. 3-14C). The accumulation of adoptively transferred WT and integrin-deficient macrophages in the adipose tissue of these mice was evaluated after 3 days. The isolated adipose tissue was digested and analyzed by multi-color FACS. We detected a 3-fold decrease in the number of α_D-deficient macrophages (in comparison to WT) in the visceral adipose tissue (Fig.3-15A,B). The result was verified by Imaging flow cytometry that confirmed the presence of labeled cells in the digested adipose tissue (Fig.3-15C). More importantly, it also demonstrates the maturation of labeled macrophages, since migrated cells expressed macrophage receptor F4/80 (Fig.9C, Lower panels), while injected monocytes lack this expression (Fig. 3-15C, Upper panel). Interestingly, the deficiency of integrin α_M, which did not significantly upregulate on M1 macrophages [23] (Fig.3-4B) had no effect on macrophage accumulation in adipose tissue (Fig. 3-15A, Lower panel). Our previous data demonstrate that α_D deficiency does not affect monocyte recruitment from circulation during inflammation [23]. Therefore, these results are in agreement with our *in vitro* and *in vivo* experiments and with recently published data that α_M deficiency does not affect the accumulation of macrophages during diet-induced obesity [42, 43].

The assessment of metabolic parameters of α_D-knockout and WT mice after 16 weeks on a high fat diet confirm the physiological significance of our results by showing that a reduced number of macrophages in the adipose tissue of $\alpha_D^{-/-}$ improved glucose tolerance and insulin sensitivity (Fig.3-15D). On the other hand, the recently published data did not reveal a change in

glucose tolerance test of α_M-deficient mice in comparison to WT control after 20 weeks of high-fat diet, but detected decreased insulin sensitivity in skeletal muscle and liver [37].

Taken together, these results provide the link between integrin expression and potential pathophysiological functions. Apparently, the same integrin can support or inhibit 3D migration in tissue depending on the macrophage subset and the level of integrin expression on the cell surface.
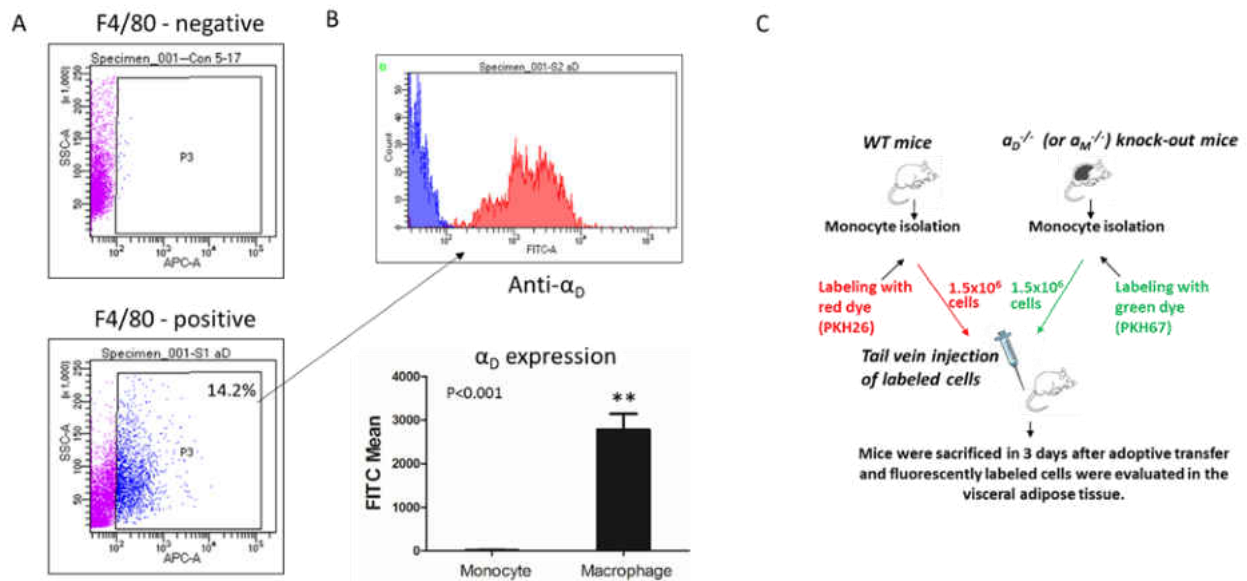
Fig. 3-14. The population of adipose tissue macrophages in adoptive transfer assay A. The population of adipose tissue macrophages was detected in digested visceral adipose tissue using F4/80 antibody conjugated to allophycocyanin (APC). **B.** The expression of integrin αD on monocytes (blue) and adipose tissue macrophages (red) were detected by FACS. Statistical analyses were performed using t-test, Data are presented as mean ± SEM. **p<0.001. **C.** Schematic representation of adoptive transfer assay using bone marrow monocyte progenitors isolated from WT and $\alpha_D^{-/-}$ (or $\alpha_M^{-/-}$) mice. The isolated WT and $\alpha_D^{-/-}$ (or $\alpha_M^{-/-}$) monocyte progenitors will be labeled with PKH26 and PKH67, respectively, and intravenously injected into WT mice fed on a high fat diet for 8 weeks. After 3 days, the mice were sacrificed and fluorescently labeled cells were isolated from visceral adipose tissue and evaluated by FACS and Imaging Flow cytometry as shown on Fig. 3-11.
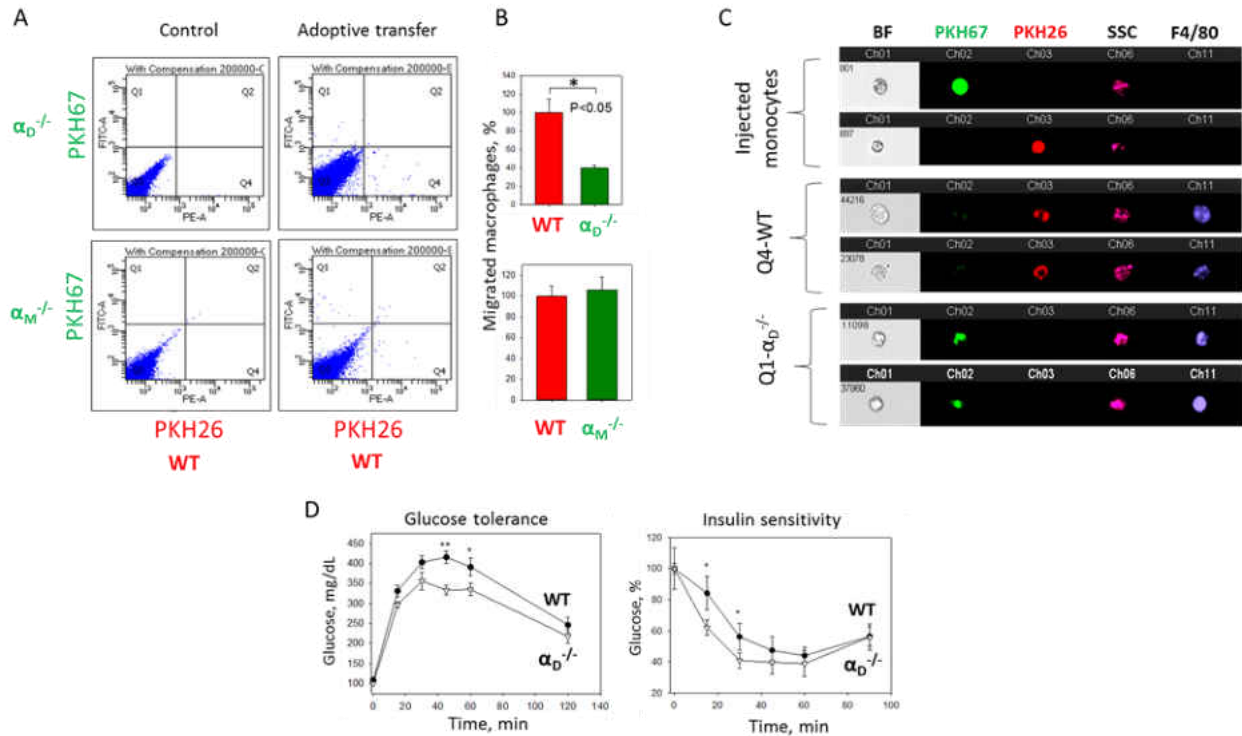
Fig. 3-15. α_D **deficiency reduces accumulation of monocyte-derived macrophages in adipose tissue and improves metabolic parameters during diet-induced diabetes. A.** WT and $\alpha_D^{-/-}$(or $\alpha_M^{-/-}$) monocytes were isolated from bone marrow, labeled with red (WT) or green ($\alpha_D^{-/-}$) fluorescent dyes, respectively, mixed in an equal amount and injected into the tail vein of WT mice fed for 8 weeks with high fat diet (45% kcal/fat). After 3 days visceral adipose tissue was isolated, digested and analyzed using flow cytometry. **B.** Statistical analyses were performed using Student's paired t-tests (n=4 per group). Data are presented as mean ± SEM. *, P < 0.05. **C.** Imaging flow cytometry. Upper panel represents the injected monocytes, isolated from WT and $\alpha_D^{-/-}$ (or $\alpha_M^{-/-}$) mice, labeled with red and green fluorescent dyes, respectively. Middle (Q4) and lower(Q1) panels represent the labeled cells in digested adipose tissue. Channel 11- F4/80 represents macrophage staining. **D.** WT mice (black circles) and α_D-knockout mice (white triangles) were fed with high fat diet for 16 weeks and glucose intolerance (**left panel**) and insulin resistance (**right panel**) were evaluated. n=6 for $\alpha_D^{-/-}$ and n=9 for WT per group. A statistical analysis was performed using Student's t-test. Data are presented as mean ± SEM. *, P < 0.05; **, P<0.01, compared to $\alpha_D^{-/-}$ group.

Discussion

The accumulation of macrophages at the site of inflammation is a complex physiological process that is critical for the development and resolution of inflammation. Macrophage apoptosis, proliferation and chemokine stimulation are important components of this mechanism, but the adhesive receptors that regulate the macrophage accumulation via cell migration and cell retention are the critical factors that generate the final outcome.

During the last decade, the role of adhesive receptors, particularly integrins, in the three-dimensional migration of immune cells in tissue has been questioned due to a new mechanism, the amoeboid mode of migration, being suggested [12, 44]. However, recent data demonstrate that some immune cells, particularly macrophages, utilize adhesion-mediated mesenchymal migration in 3D matrices [13, 45]. It has been shown that the migratory mode of macrophages depends on the environment and density of matrix [39]. Previously, based on 2D models, it was suggested that cell migration is regulated by cell-substratum adhesiveness, which depends on substrate concentration, adhesive receptor density and affinity [15]. This theory postulates that an intermediate level of adhesiveness (or intermediate expression of the adhesive receptors) is optimal for cell migration, while very low adhesiveness does not support cell locomotion and very high adhesiveness inhibits migration due to the prevention of the detachment of adhered cells. However, this theory was not evaluated during 3D migration in the tissue, which has more complex regulatory mechanisms and much stronger physiological implications. In this project, we tested integrins $\alpha_M\beta_2$ and $\alpha_D\beta_2$ as physiologically relevant models for studying the role of adhesive receptors during the migration of different subsets of macrophages. We discussed resident peritoneal macrophages and two subsets of monocyte-derived activated macrophages - classically activated (called M1), which can be generated by IFNγ/LPS or TNFα stimulation; and alternatively activated, which are produced by stimulation with IL-4 and/or IL-13 (called M2a) [7]. For simplicity, we are calling the latter group M2. We realize that M1 and M2 activated macrophages are simplified models; and macrophages in the atherosclerotic lesion and adipose tissue may represent "mixed phenotypes". However, these two subsets characterize the most variable difference in macrophage functional properties, and therefore, are an appropriate model for analyzing β_2 integrin expression and functions in different macrophage subsets.

Our experimental approach is based on several observations. First, α_D and α_M share similar ligands [21, 22]; second, these two integrins form a complex with the same β_2 subunit, thus leading to

similar integrin-mediated outside-in signaling during the interaction with the ligand; and third, the expressions of α_D and α_M are distinct on M1-polarized, M2-polarized and resident macrophages. We demonstrated that α_D is upregulated on M1 macrophages, while the expression of α_M is moderate (Fig.3-4)[23]. In contrast to these observations, the resident macrophages express a low level of α_D, but have a high density of α_M (Fig.3-10). At the same time, the expressions of both α_D and α_M integrins on M2 macrophages are intermediate (Fig.3-4).

Using these three subsets of macrophages, we found that 1) M2 macrophages possess much stronger migratory ability within 3D matrix in comparison with M1. 2) Integrins $\alpha_D\beta_2$ and $\alpha_M\beta_2$ are important receptors that regulate cell migration. 3) Similar to the 2D migration, integrins can support mesenchymal 3D cell migration at the intermediate density and prevent mesenchymal and amoeboid cell migration at high levels of expression. 4) Even the adhesion-independent amoeboid mode can be negatively-regulated by a high expression of β_2 integrins.

In this project, we show that strong adhesion via integrins is critical for cell retention that defines the different migratory properties of M1 and M2 macrophages. (Figs.3-6,3-10). The analysis of α_M, α_X, α_D, α_5, α_4, integrins demonstrates that the upregulation of α_D on M1 macrophages is a major change in integrin expression during M1 activation. Therefore, $\alpha_D\beta_2$-mediated adhesion is crucial for the prevention of M1 macrophage migration. In a parallel line of evidence, we found that the lack of α_D-dependent substrate (exemplified in Matrigel) eliminates the effect of α_D on cell migration in this matrix (Fig.3-8). Importantly, α_D-deficiency does not significantly change the expression of other macrophage integrins and the levels of MMP expression, which rules out the possibility for an indirect effect of α_D knockout on M1 macrophage migration.

Taken together, these results propose that the accumulation of M1 macrophages at the site of inflammation is mediated by strong adhesion which promotes cell retention and the progression of chronic inflammation. In agreement with that, α_D-deficiency prevents the accumulation of adoptively transferred fluorescently-labeled macrophage accumulation in adipose tissue during diabetes. The reduced number of macrophages is associated with reduced inflammation and improved glucose tolerance and insulin sensitivity in α_D-knockout mice. These data correspond to our previous results, that α_D-deficiency reduced macrophage accumulation in atherosclerotic lesions and the development of atherosclerosis [23]. Therefore, the upregulation of α_D on pro-inflammatory macrophages during diabetes [41] or atherosclerosis [23] demonstrates a similar outcome,

which is manifested in the macrophage retention at the site of inflammation and disease development. Interestingly, α_M deficiency has pro-atherogenic effect on female and no effect on male mice [46]. In agreement with this result, it has been recently shown that α_M deficiency elevates glucose level and decreased insulin sensitivity after 16 weeks on a high fat diet. Taken together, these data confirm the opposite role of $\alpha_D\beta_2$ and $\alpha_M\beta_2$ on pro-inflammatory M1 macrophages.

In contrast, the stronger migratory properties of M2 macrophages indicate that these cells more easily leave the tissue toward the lymphatics. The increased phagocytic properties of M2 macrophages, coupled with their high migratory abilities, confirm the major function of anti-inflammatory macrophages – phagocytosis followed by efflux from the tissue. α_D and α_M support the motility of M2 macrophages, and therefore promote the emigration of M2 macrophages from the inflamed tissue. Interestingly, the role of α_M in macrophage efflux during resolution was proposed previously [47].

The published data demonstrates that M2 macrophages may apply both locomotion modes, amoeboid and mesenchymal, which is supported by our observations regarding the α_M and partially α_D-mediated mesenchymal migration of M2 macrophages (Fig.3-6). In contrast, resident macrophages use preferentially amoeboid motility. Using ROCK inhibitor, we confirmed the preferential amoeboid migration of resident macrophages, but also demonstrated that amoeboid migration can be increased after the knockout of α_M integrin, which has a high density on these cells (Fig.3-10). Therefore, these data propose an anchoring role for integrin $\alpha_M\beta_2$ for resident macrophages in tissue. This mechanism may be important for the normal homeostasis and mobilization the initial immune defense, which is mediated by resident macrophages. We showed that α_M-deficiency reduced macrophage numbers in the non-inflamed peritoneal cavity (Fig.3-10). Therefore, the different immune pathologies associated with α_M-deficiency can be at least partially related to the impaired resident macrophage number. Most importantly, since integrins can block (or reduce) amoeboid migration, it suggests the potential role of integrins in the regulation (particularly, inhibition) of 3D migration of other immune cells that use only amoeboid movement (for example neutrophils or dendritic cells).

In summary, our study demonstrates the important contribution of $\alpha_D\beta_2$ and $\alpha_M\beta_2$ to the locomotion of distinct macrophage subsets and proposes a β_2-integrin dependent mechanism of macrophage retention in the tissue and efflux during the resolution of inflammation.

Acknowledgments：

References

1. Tobias P, Curtiss LK. Thematic review series: The immune system and atherogenesis. Paying the price for pathogen protection: toll receptors in atherogenesis. J Lipid Res 2005;46:404-11.

2. Bouloumie A, Curat CA, Sengenes C, Lolmede K, Miranville A, Busse R. Role of macrophage tissue infiltration in metabolic diseases. Curr Opin Clin Nutr Metab Care 2005;8:347-54.

3. Alexandraki K, Piperi C, Kalofoutis C, Singh J, Alaveras A, Kalofoutis A. Inflammatory process in type 2 diabetes: The role of cytokines. Ann N Y Acad Sci 2006;1084:89-117.

4. Ouchi N, Kihara S, Funahashi T, Matsuzawa Y, Walsh K. Obesity, adiponectin and vascular inflammatory disease. Curr Opin Lipidol 2003;14:561-6.

5. Eming SA, Wynn TA, Martin P. Inflammation and metabolism in tissue repair and regeneration. Science 2017;356:1026-30.

6. Subramanian S, Chait A. The effect of dietary cholesterol on macrophage accumulation in adipose tissue: implications for systemic inflammation and atherosclerosis. Curr Opin Lipidol 2009;20:39-44.

7. Gordon S. Macrophage heterogeneity and tissue lipids. J Clin Invest 2007;117:89-93.

8. Gordon S. Alternative activation of macrophages. Nat Rev Immunol 2003;3:23-35.

9. Mestas J, Ley K. Monocyte-endothelial cell interactions in the development of atherosclerosis. Trends Cardiovasc Med 2008;18:228-32.

10. McIntyre TM, Prescott SM, Weyrich AS, Zimmerman GA. Cell-cell interactions: leukocyte-endothelial interactions. Curr Opin Hematol 2003;10:150-8.

11. Herter J, Zarbock A. Integrin Regulation during Leukocyte Recruitment. J Immunol 2013;190:4451-7.

12. Lammermann T, Bader BL, Monkley SJ, Worbs T, Wedlich-Soldner R, Hirsch K, et al. Rapid leukocyte migration by integrin-independent flowing and squeezing. Nature 2008;453:51-5.

13. Bouissou A, Proag A, Bourg N, Pingris K, Cabriel C, Balor S, et al. Podosome Force Generation Machinery: A Local Balance between Protrusion at the Core and Traction at the Ring. ACS Nano 2017;11:4028-40.

14. DiMilla PA, Stone JA, Quinn JA, Albelda SM, Lauffenburger DA. Maximal migration of human smooth muscle cells on fibronectin and type IV collagen occurs at an intermediate attachment strength. J Cell Biol 1993;122:729-37.

15. Palecek SP, Loftus JC, Ginsberg MH, Lauffenburger DA, Horwitz AF. Integrin-ligand binding properties govern cell migration speed through cell-substratum adhesiveness. Nature 1997;385:537-40.

16. DiMilla PA, Barbee K, Lauffenburger DA. Mathematical model for the effects of adhesion and mechanics on cell migration speed. Biophys J 1991;60:15-37.

17. Yakubenko VP, Belevych N, Mishchuk D, Schurin A, Lam SC, Ugarova TP. The role of integrin alpha D beta2 (CD11d/CD18) in monocyte/macrophage migration. Exp Cell Res 2008;314:2569-78.

18. Clemetson KJ, Clemetson JM. Integrins and cardiovascular disease. Cell Mol Life Sci 1998;54:502-13.

19. Hogg N, Patzak I, Willenbrock F. The insider's guide to leukocyte integrin signalling and function. Nat Rev Immunol 2011;11:416-26.

20. Wu H, Gower RM, Wang H, Perrard XY, Ma R, Bullard DC, et al. Functional role of CD11c+ monocytes in atherogenesis associated with hypercholesterolemia. Circulation 2009;119:2708-17.

21. Yakubenko VP, Yadav SP, Ugarova TP. Integrin alphaDbeta2, an adhesion receptor up-regulated on macrophage foam cells, exhibits multiligand-binding properties. Blood 2006;107:1643-50.

22. Yakubenko VP, Lishko VK, Lam SCT, Ugarova TP. A molecular basis for integrin $a_M b_2$ in ligand binding promiscuity. J Biol Chem 2002;277:48635-42.

23. Aziz MH, Cui K, Das M, Brown KE, Ardell CL, Febbraio M, et al. The Upregulation of Integrin alphaDbeta2 (CD11d/CD18) on Inflammatory Macrophages Promotes Macrophage Retention in Vascular Lesions and Development of Atherosclerosis. J Immunol 2017;198:4855-67.

24. Cougoule C, Van GE, Le C, V, Lafouresse F, Dupre L, Mehraj V, et al. Blood leukocytes and macrophages of various phenotypes have distinct abilities to form podosomes and to migrate in 3D environments. Eur J Cell Biol 2012;91:938-49.

25. Yakubenko VP, Cui K, Ardell CL, Brown KE, West XZ, Gao D, et al. Oxidative modifications of extracellular matrix promote the second wave of inflammation via beta2 integrins. Blood 2018.

26. Oh DY, Morinaga H, Talukdar S, Bae EJ, Olefsky JM. Increased macrophage migration into adipose tissue in obese mice. Diabetes 2012;61:346-54.

27. Szekanecz, Z., M. R. Shah, W. H. Pearce, and A. E. Koch. 1994. Human atherosclerotic abdominal aortic aneurysms produce interleukin (IL)-6 and interferon-gamma but not IL-2 and IL-4: the possible role for IL-6 and interferon-gamma in vascular inflammation. *Agents Actions* 42: 159-162.

28. Lesnik, P., C. A. Haskell, and I. F. Charo. 2003. Decreased atherosclerosis in CX3CR1-/- mice reveals a role for fractalkine in atherogenesis. *J. Clin. Invest* 111: 333-340.

29. Uyemura, K., L. L. Demer, S. C. Castle, D. Jullien, J. A. Berliner, M. K. Gately, R. R. Warrier, N. Pham, A. M. Fogelman, and R. L. Modlin. 1996. Cross-regulatory roles of interleukin (IL)-12 and IL-10 in atherosclerosis. *J. Clin. Invest* 97: 2130-2138.

30. Gordon, S. 2003. Alternative activation of macrophages. *Nat. Rev. Immunol.* 3: 23-35.

31. Khallou-Laschet, J., A. Varthaman, G. Fornasa, C. Compain, A. T. Gaston, M. Clement, M. Dussiot, O. Levillain, S. Graff-Dubois, A. Nicoletti, and G. Caligiuri. 2010. Macrophage plasticity in experimental atherosclerosis. *PLoS. ONE.* 5: e8852.

32. Gray, J. L., and R. Shankar. 1995. Down regulation of CD11b and CD18 expression in atherosclerotic lesion- derived macrophages. *Am. Surg.* 61: 674-679.

33. Xuan W, Qu Q, Zheng B, Xiong S, Fan GH. The chemotaxis of M1 and M2 macrophages is regulated by different chemokines. J Leukoc Biol 2015;97:61-9.

34. Yakubenko VP, Solovjov DA, Zhang L, Yee VC, Plow EF, Ugarova TP. Identification of the binding site for fibrinogen recognition peptide g383-395 within the a_M I-domain of integrin a_Mb_2 . J Biol Chem 2001;275:13995-4003.

35. Elices MJ, Hemler ME. The human integrin VLA-2 is a collagen receptor on some cells and a collagen/laminin receptor on others. Proc Natl Acad Sci U S A 1989;86:9906-10.

36. Tawil NJ, Houde M, Blacher R, Esch F, Reichardt LF, Turner DC, et al. Alpha 1 beta 1 integrin heterodimer functions as a dual laminin/collagen receptor in neural cells. Biochemistry 1990;29:6540-4.

37. Lishko V.K., Yakubenko VP, Ugarova TP. The interplay between Integrins a_Mb_2 and a_5b_1 during cell migration to fibronectin. Exp Cell Res 2003; 283:116-26.

38. Yakubenko VP, Lobb RR, Plow EF, Ugarova TP. Differential induction of gelatinase B (MMP-9) and gelatinase A (MMP-2) in T-lymphocytes upon a_4b_1-mediated adhesion to VCAM-1 and the CS-1 peptide of fibronectin. Exp Cell Res 2000;260:73-84.

39. Maridonneau-Parini I. Control of macrophage 3D migration: a therapeutic challenge to limit tissue infiltration. Immunol Rev 2014;262:216-31.

40. Bellingan GJ, Caldwell H, Howie SE, Dransfield I, Haslett C. In vivo fate of the inflammatory macrophage during the resolution of inflammation: inflammatory

macrophages do not die locally, but emigrate to the draining lymph nodes. J Immunol 1996;157:2577-85.

41.   Thomas AP, Dunn TN, Oort PJ, Grino M, Adams SH. Inflammatory phenotyping identifies CD11d as a gene markedly induced in white adipose tissue in obese rodents and women. J Nutr 2011;141:1172-80.

42.   Robker RL, Collins RG, Beaudet AL, Mersmann HJ, Smith CW. Leukocyte migration in adipose tissue of mice null for ICAM-1 and Mac-1 adhesion receptors. Obes Res 2004;12:936-40.

43.   Wolf D, Bukosza N, Engel D, Poggi M, Jehle F, Anto MN, et al. Inflammation, but not recruitment, of adipose tissue macrophages requires signalling through Mac-1 (CD11b/CD18) in diet-induced obesity (DIO). Thromb Haemost 2017;117:325-38.

44.   Renkawitz J, Schumann K, Weber M, Lammermann T, Pflicke H, Piel M, et al. Adaptive force transmission in amoeboid cell migration. Nat Cell Biol 2009;11:1438-43.

45.   Wiesner C, Le-Cabec V, El AK, Maridonneau-Parini I, Linder S. Podosomes in space: macrophage migration and matrix degradation in 2D and 3D settings. Cell Adh Migr 2014;8:179-91.

46.   Szpak D, Izem L, Verbovetskiy D, Soloviev DA, Yakubenko VP, Pluskota E. alphaMbeta2 Is Antiatherogenic in Female but Not Male Mice. *J Immunol* 2018 April 1;200(7):2426-38.

47.   Cao C, Lawrence DA, Strickland DK, Zhang L. A specific role of integrin Mac-1 in accelerated macrophage efflux to the lymphatics. Blood 2005;106:3234-41.

CHAPTER 4

INHIBITION OF MACROPHAGE ADHESION MEDIATED BY INTEGRIN αDβ2 PREVENTS MACROPHAGE ACCUMULATION DURING INFLAMMATION

Kui Cui[1], Nataly P. Podolnikova[2], William Bailey[1], Eric Szmuc[1], Eugene A. Podrez[3], Tatiana V. Byzova,[3] Valentin P. Yakubenko[1]

[1]Department of Biomedical Sciences, Quillen College of Medicine, East Tennessee State University;
[2]Center for Metabolic and Vascular Biology, School of Life Sciences, Arizona State University. [3] Lerner Research Institute, Cleveland Clinic.

Running title: *Inhibition of integrin αDβ2-mediated macrophage accumulation*

Correspondence to Dr. Valentin Yakubenko, Department of Biomedical Sciences,

Quillen College of Medicine, East Tennessee State University, PO Box 70582, Johnson City, Email: yakubenko@etsu.edu, Phone: (423) 439-8511.

Keywords: macrophage, adhesion, migration, integrin αDβ2

Abstract

A critical step in the development of chronic inflammatory diseases is the accumulation of pro-inflammatory macrophages in the extracellular matrix (ECM) of peripheral tissues. The adhesion receptor, integrin $\alpha_D\beta_2$ promotes the development of atherosclerosis and diabetes by supporting macrophage retention in inflamed tissue. We recently found that the end-product of DHA oxidation, 2-(ω-carboxyethyl)pyrrole (CEP), serves as a ligand for $\alpha_D\beta_2$. CEP adduct with ECM is generated during inflammation-mediated lipid peroxidation. The goal of this project was to identify a specific inhibitor for $\alpha_D\beta_2$-CEP interaction, that can prevent macrophage accumulation.

Using a specially designed peptide library, biacore detected protein-protein interaction and adhesion of integrin-transfected HEK293 cells, we identified a sequence (called P5-peptide), which significantly and specifically inhibited α_D-CEP binding. In the model of thioglycollate-induced peritoneal inflammation, the injection of cyclic P5 peptide reduced 3-folds the macrophage accumulation into WT mice, but had no effect in α_D-deficient mice. The tracking of adoptively transferred fluorescently-labeled WT and $\alpha_D^{-/-}$ monocytes in the model of peritoneal inflammation, and in vitro two-dimensional and three-dimensional migration assays demonstrated that P5 peptide does not affect monocyte transendothelial migration or macrophage efflux from the peritoneal cavity, but regulates macrophage migration through the ECM. Moreover, the injection of P5 peptide into WT mice on a high-fat diet prevents macrophage accumulation in adipose tissue in $\alpha_D\beta_2$-dependent manner.

Taken together, these results demonstrate the importance of $\alpha_D\beta_2$-mediated macrophage adhesion for the accumulation of infiltrating macrophages in the inflamed ECM and propose P5 peptide as a potential inhibitor of atherogenesis and diabetes.

Introduction

Chronic inflammation is an essential mechanism during the development of cardiovascular and metabolic diseases. Monocyte recruitment and subsequent macrophage accumulation in the damaged tissue are critical steps that regulate inflammatory response and disease progression [1, 2].

While monocyte recruitment during acute inflammatory response may have a protective effect, the excessive accumulation of macrophages at the site of inflammation can lead to strong pro-inflammatory signaling, damage to healthy tissue and development of chronic inflammation [3]. Leukocyte integrins are adhesive receptors that significantly contributes to the monocyte/macrophage migration and accumulation [4]. Integrin $\alpha_D\beta_2$ (CD11d/CD18) is the most recently discovered leukocyte integrin with unique expression pattern and specific role in inflammation. Recently, we and others demonstrated that $\alpha D\beta 2$ has a relatively low expression on neutrophils and monocytes in circulation, but upregulates on tissue macrophages, particularly in atherosclerotic lesions and adipose tissue during diabetes [5-7]. We revealed that high expression of $\alpha_D\beta_2$ on cell surface promotes a strong adhesion to ECM proteins that leads to the retention of pro-inflammatory macrophages in inflamed tissue and supports atherogenesis and insulin resistance [8,9].

Interestingly, $\alpha_D\beta_2$ shares a high level of homology and ligand binding properties with related integrin $\alpha_M\beta_2$ (CD11b/CD18, Mac-1)[10]. $\alpha_M\beta_2$ is well studied leukocyte receptor, which is involved in the regulation of many acute and chronic inflammatory diseases [11-14]. $\alpha_D\beta_2$ and $\alpha_M\beta_2$ shares many extracellular matrix ligands such as fibronectin, fibrinogen and vitronectin, however, the expression of these integrins is markedly different on distinct subsets of macrophages [8]. Particularly, $\alpha_D\beta_2$ has a low expression on resident and alternatively activated (M2) macrophages, but dramatically upregulates on classically activated (M1) macrophages. $\alpha_M\beta_2$ demonstrates a high expression on resident macrophages, but is expressed moderately on M1 and M2 macrophages. This difference determines the distinct role of $\alpha_D\beta_2$ and $\alpha_M\beta_2$ in macrophage migration/retention and contribution to the development of inflammatory diseases [9]. Particularly, recent data demonstrated that $\alpha_M\beta_2$ has a protective effect on the development of atherosclerosis and diabetes, which is opposite to the pathological role of $\alpha_D\beta_2$ in chronic inflammation [13,15].

Ligand recognition, followed by specific intracellular signaling, is a critical step that determines integrin-mediated leukocyte migration and cellular responses. Most recently, we found that the end-product of DHA oxidation, 2-(ω-carboxyethyl)pyrrole (CEP) serves as a specific inflammatory ligand for integrins $\alpha_D\beta_2$ and $\alpha_M\beta_2$ [16]. CEP is formed during the oxidation of DHA that leads to the formation of CEP adducts with ECM proteins [17,18]. These CEP-modified proteins support $\alpha_M\beta_2$- and $\alpha_D\beta_2$-mediated macrophage migration to the site of inflammation. CEP is formed mostly during the inflammation and was abundantly detected in the atherosclerotic lesions

and adipose tissue during diabetes [19]. Based on $\alpha_D\beta_2$-specific pattern of expression on M1 macrophages, we hypothesized that CEP can be a critical ligand for $\alpha_D\beta_2$-mediated macrophage retention at the site of inflammation. Particularly because the affinity of α_D to CEP surpasses the affinity to natural ECM proteins [16,20].

Therefore, the inhibition of $\alpha_D\beta_2$-mediated adhesion of macrophages to CEP-modified proteins in the ECM may have a strong anti-inflammatory effect. However, the overlapping ligand binding properties of $\alpha_M\beta_2$ and $\alpha_D\beta_2$ complicate the development of an effective inhibitor [10,21].

In this project, we developed a strategy to identify the amino acid sequences, which are specific only for integrin $\alpha_D\beta_2$ and has no effect on $\alpha_M\beta_2$. Using in vitro approaches, we selected the peptide, called P5, with strong blocking ability against $\alpha_D\beta_2$-CEP interaction. Applying the model of peritoneal inflammation, we demonstrated that P5 peptide significantly reduced the accumulation of macrophage in the peritoneal cavity and this effect directly related to the $\alpha_D\beta_2$-dependent migration via ECM. Moreover, P5 does not interfere with monocyte transmigration through endothelium or macrophage efflux from the peritoneal cavity. Finally, using the model of diet induced diabetes, we demonstrated that P5 peptide markedly inhibits the accumulation of macrophages in the adipose tissue of mice, which demonstrates the effect of P5 on the development of chronic inflammation.

Taken together, these data confirm the significant role of integrin $\alpha_D\beta_2$ during the inflammatory response, support the concept of $\alpha_D\beta_2$ as important anti-inflammatory target and propose P5 sequence as a potential inhibitor of inflammation.

Materials and Method

Reagents

Reagents were purchased from Sigma-Aldrich (St. Louis, MO) and Thermo Fisher Scientific (Waltham, MA). Human fibrinogen and thrombin were obtained from Enzyme Research Laboratories (South Bend, IN). The synthesis of peptides P-con - WNGRTSTADYAMFKV, P3 – AGHLNGVYYQGGTYSKAS P4 – TGTTEFWLGNEKIHL, P5 –GDAFDGFDFGDDPSD was ordered from Peptide 2.0 Inc (Chantilly, VA). Recombinant mouse IFNγ was purchased from

Thermo Fisher Scientific. Phorbol Myristate Acetate (PMA) was purchased from Sigma. Recombinant Murine JE/MCP-1 (CCL2) was purchased from Pepro Tech (Rocky Hill, NJ). Anti-human α_D mAb (clone 240I) was generously provided by Eli Lilly Corporation (Indianapolis, IN). Mouse FITC- and APC- conjugated anti-α_M mAb (clone M1/70) and F4/80 mAbs were from eBioscience (San Diego, CA). The conformation-dependent antibody mAb 24 against β_2 integrin was from Hycult Biotechnology (The Netherlands). The mAb 44a directed against the human α_M integrin subunit was purified from the conditioned media of the hybridoma cell line obtained from American Type Culture Collection (ATCC, Manassas, VA) using protein A agarose (GE Healthcare, Piscataway, NJ). PKH26 (red) and PKH67 (green) fluorescent dyes were purchased from Sigma (St. Louis, MO).

Animals

Wild type (C57BL/6J), integrin α_D-deficient (B6.129S7-*Itgad^{tm1Bll}*/J) and integrin α_M-deficient (B6.129S4-*Itgam^{tm1Myd}*/J) mice were bought from Jackson Laboratory (Bar Harbor, ME). α_D-deficient and α_M-deficient mice have been backcrossed to C57BL/6 for at least ten generations. To develop insulin resistant mice C57BL/6 WT mice were fed a high fat diet with 45% kcal from fat (TD08811, Envigo) for 8 weeks. All procedures were performed according to animal protocols approved by East Tennessee State University IACUC.

Expression and isolation of recombinant α_D and α_M I domains in active and non-active conformation.

The construct for α_D I domains, α_M I domains were generated and recombinant proteins were isolated as described in our previous papers[10,16]. Briefly, α_D in non-active conformation (Pro^{128}-Ala^{323}), α_M in active conformation (E^{123}-K^{315}) were inserted into a PGEX4T-1 vector. In "active" α_M I domains, the unpaired Cys^{128} was substituted to Ser to prevent I domain dimerization. Proteins were expressed in E. Coli and purified using affinity chromatography on glutathione agarose and its fusion part removed by thrombin. α_D in active conformation (Pro^{128}-Lys^{314}) was inserted in pET15b vector, expressed in E. Coli as a His-tag fusion protein and purified using affinity chromatography on Ni-chelating agarose (Qiagen Inc., Valencia, CA).

Analyses of the αDI-domain binding to CEP, Fg and P5 peptide by surface plasmon resonance and Bio-Layer Interferometry.

The interaction between I domains and CEP or fibrinogen in the presence of P3, P4, and P5 peptides was measured using surface plasmon resonance (Biacore3000 instrument, Biacore, Uppsala, Sweden) as we described previously [10,19]. Fibrinogen and CEP conjugated to albumin and were immobilized on the CM5 biosensor chip using the standard amine coupling chemistry (1000 RU/flow cell). Steady-state experiments were performed at room temperature in 10 mM HEPES (pH 7.4) buffer containing 150 mM NaCl, 1 mM $MgCl_2$, 1 mM $CaCl_2$ and 0.005% surfactant P20 at a flow rate of 20 μl/min. SPR sensograms were obtained by injecting various concentrations of $α_D$ and $α_M$ I domains. In some samples, analytes were preincubated with blocking peptides for 15 min at room temperature. All data were corrected for the response obtained using a blank reference flow cell that was activated with N-ethyl-N′-(dimethylaminopropyl) carbodiimide/N-hydroxysuccinimide and then blocked with ethanolamine. Nonspecific binding to the blank flow cell was subtracted. The chip surfaces were regenerated by injecting a short pulse of 25 mM NaOH. The resulting sensorgrams were analyzed in overlay plots using BIAevaluation software (version 4.01, GE Healthcare).

The interaction between the αDI-domain (in active and non-active conformation) and P5 peptide was measured using Bio-Layer Interferometry (ForteBio, Fremont, CA). N-terminal biotinylated P5 peptide was immobilized on streptavidin biosensor. Different concentrations of the I-domains in 20 mM HEPES (pH 7.4) buffer containing 150 mM NaCl, 1 mM $MgCl_2$, 1 mM $CaCl_2$ and 0.05% Tween 20 were added to immobilized P5 peptide. For some experiments Mg^{2+} and Ca^{2+} was exchanged for 5 mM EDTA. All data were corrected for the response obtained using a blank reference biosensor. The biosensor surface was regenerated using 2 M NaCl and 50 mM NaOH. Data were analyzed using the ForteBio Data Analysis 11.0 program (ForteBio, Fremont, CA).

Synthesis of cellulose-bound peptide library

The γ-module of fibrinogen-derived peptide library assembled on a single cellulose membrane support was prepared by parallel spot synthesis as described previously [22,23]. The libraries were synthesized as 9-mer overlapping peptides with a three-amino acid offset. Peptides

were C-terminally attached to the cellulose via a (β-Ala)$_2$ spacer and were acetylated N-terminally. The membrane-bound peptides were tested for the ability to bind the α_MI-domain and α_DI-domain. In brief, membranes were blocked with 1% BSA and incubated with 5 µg/mL ^{125}I-labeled α_M I-domain or α_D I-domain in TBS containing 1 mM MgCl$_2$, 0.1% BSA, and 2 mM dithiothreitol. Membranes were washed with TBS containing 0.05% Tween 20 and dried, and α_M- and α_D- I-domain binding was visualized by autoradiography and analyzed by densitometry.

Flow cytometry analysis

Flow cytometry analysis was performed to assess the expression and activation of receptors on the surface of the cells transfected with $\alpha_D\beta_2$, $\alpha_M\beta_2$, $\alpha_L\beta_2$ integrins and to evaluate the number of fluorescently labeled mouse macrophages isolated from the peritoneal cavity or adipose tissue. HEK 293 transfected cells were incubated with anti-α_D (clone 240I), anti-α_M (clone M1/70) and anti-β_2 (clone IB4) antibodies and analyzed using a Fortessa X-20 (Beckton Dickinson) as described[10,21]. The isolated pre-labeled WT (red PKH26) bone marrow derived macrophages, peritoneal macrophages or adipose tissue macrophages (WT-red and $\alpha_D^{-/-}$-green) were washed with PBS, counted and analyzed by flow cytometry (Fortessa X-20) and imaging flow cytometry (ImageStream Mark II, Amnis). Macrophage numbers were calculated based on the percentage of F4/80 positive population in flow cytometry.

Cell adhesion assay

The adhesion assay was performed as described previously with modifications [10,21]. Briefly, 96-well plates (Immulon 2HB, Cambridge, MA) were coated with fibrinogen, CEP, P5 or vitronectin for 3 h at 37 °C. The wells were post-coated with 0.5% polyvinyl alcohol for 1 h at 37 °C. HEK 293 cells transfected with $\alpha_M\beta_2$, $\alpha_X\beta_2$ or $\alpha_D\beta_2$ integrins were labeled with 10 µM Calcein AM (Molecular Probes, Eugene, OR) for 20 min at 37 °C and washed with DMEM and resuspended in the same medium at a concentration of 1×10^6 cells/ml. Aliquots (50 µl) of the labeled cells were added to each well. For inhibition experiments, cells were mixed with various concentration of peptides (P3, P4, and P5) and incubated for 20 minutes at 37 °C before they were added to the ligand-coated wells. After 30 minutes of adhesion at 37 °C in a 5% CO$_2$ humidified atmosphere, the nonadherent cells were removed by washing with HBSS. The fluorescence was

measured in a Synergy H1 fluorescence plate reader (BioTek, Winooski, VT), and the number of adherent cells was determined from a labeled control.

Isolation of peritoneal macrophage and activation of M1 macrophages

WT and $\alpha_D^{-/-}$, 8-week-old, mice were intraperitoneally injected with 1ml of 4% thioglycollate (TG), 3 days later, peritoneal cells were harvested with 5 ml of sterile PBS by lavage of the peritoneal cavity. The cells were washed with PBS and resuspended in RPMI media. The cell suspension was transferred into 100mm Petri dishes and incubated for 2h at 37^oC in humidified air containing 5% CO_2 atmosphere. Non-adherent cells were washed out with RPMI media, and the adherent macrophages were replenished with RPMI media. The macrophages were differentiated to M1 phenotype by treatment with recombinant mouse interferon-γ (IFN-γ) (100 U/ml, Thermo Fisher) for 4 days. Medium with IFN-γ was changed every 2 days or as required. The M1 phenotype macrophages from WT and $\alpha_D^{-/-}$ mice were labeled with red fluorescent marker PKH26 and green fluorescent marker PKH67, respectively, according to the manufacturer's instructions (Sigma-Aldrich). The fluorescently-labeled cells were dissociated from the plates using 5mM EDTA in PBS and used for the experiments thereafter.

Adoptive transfer in the recruitment of macrophages to the peritoneal cavity

The approach is based on our previous publication with some modifications [8]. Bone marrow monocytes were isolated from WT mice using magnetic bead separation kit (Miltenyi Biotec, Gaithersburg, MD). Monocytes were labeled with red, PKH26 (WT) fluorescent dyes. Recipient WT mice were intraperitoneally injected with 100 µg/mouse P5 peptide. After 20 min, 1 ml of 4% thioglycollate was intraperitoneally injected to all mice to induce inflammation. Then fluorescently labeled WT (red PKH26 dye) bone marrow monocytes were injected into the tail vein of the recipient mice. After 72 hours, the peritoneal macrophages were harvested and assessed by fluorescence microscopy and flow cytometry (BD Fortessa X-20).

Adoptive transfer in macrophage efflux from the peritoneal cavity

The adoptive transfer was performed as described previously with some modifications [8]. Briefly, recipient and donor WT mice were intraperitoneally injected with 4% thioglycollate. After 48 hours, macrophages were isolated from the peritoneal cavity of donor mice, labeled with PKH26 red fluorescent dye and injected into the peritoneal cavity of the recipient mice ($1x10^6$ cells per mouse). Immediately, the recipient mice were intraperitoneally injected with 200 µg/ml P5 peptide or control. After an additional 24 hours, macrophages were harvested from the peritoneal cavity, counted and the number of fluorescently labeled macrophages was assessed by fluorescence microscopy and flow cytometry (BD Fortessa X-20).

Adoptive transfer in the model of diet-induced diabetes

The adoptive transfer was performed as described previously [9]. Briefly, WT and $\alpha_D^{-/-}$ bone marrow monocytes were isolated and purified by magnetic bead separation kit (Miltenyi Biotec, Gaithersburg, MD), labeled with red PKH26 (WT) or green PKH67 ($\alpha_D^{-/-}$) fluorescent dyes, respectively, mixed in an equal amount ($1x10^6$ cells per color per mouse) and injected into the tail vein of WT mice fed a high fat diet (45% kcal/fat) for 8 weeks. The experimental group were intraperitoneally injected with 200 µg/ml P5 peptide 20min before the injection of labeled cells. After 3 days, visceral adipose tissue was isolated, digested and analyzed using flow cytometry (Fortessa X-20) and imaging flow cytometry (ImageStream Mark II, Amnis).

Trans-endothelial migration assay

Human umbilical vein endothelial cells (HUVEC) were seeded at 10^5 cells per well in the upper chamber of Transwell inserts (diameter: 6.5 mm, pore size: 5.0 µm, Corning), labeled with PKH67 green fluorescence and cultured overnight in Vascular Cell Basal Medium with VEGF (ATCC). On the next day, isolated bone marrow monocytes were labeled with PKH26 red fluorescent dye and added to the top of endothelial cells, MCP-1 was added to the lower chamber of the wells to stimulate the migration of monocytes. In some experiments, the monocytes were pre-incubated with 200 µg/ml P5 peptide for 20 min. After 3h incubation at 37°C, the number of

migrated cells was determined by Leica Confocal Microscope and the results were reconstructed and analyzed using IMARIS 8.0 software.

Migration of macrophages in 3D fibrin gel

Migration assay was performed as described previously [9,22]. WT and $\alpha_D^{-/-}$ peritoneal non-activated macrophages were labeled with PKH26 red fluorescent dye and PKH67 green fluorescent dye, respectively. Cell migration assay was performed for 48 hours at 37°C in 5% CO_2 in a sterile condition. An equal number of WT and $\alpha_D^{-/-}$ macrophages was evaluated by cytospin of mixed cells before the experiment and at the starting point before migration. Labeled WT (1.5×10^5) and $\alpha_D^{-/-}$ (1.5×10^5) activated macrophages were plated on the membranes of transwell inserts with a pore size of 8 μm and 6.5 mm in diameter (Costar, Corning, NY) precoated with fibrinogen (Fg). Fibrin gel (100 μl/sample) was generated by mixing 0.75mg/ml Fg containing 1% FBS and 1% P/S and 0.5 U/ml thrombin. 30 nM of MCP-1 was added on the top of the gel to initiate the migration. Migrating cells were detected by Leica Confocal microscope (Leica-TCS SP8) and the results were analyzed and reconstructed using IMARIS 8.0 software.

Statistical analysis

Statistical analyses were performed using Student's t-test or Student's paired t-tests where indicated in the text using SigmaPlot 13. A value of $p < 0.05$ was considered significant.

Results

Screening the peptide library for the binding to α_D and α_M I-domains.

To identify the sequences, which are unique for the $\alpha_D\beta_2$ binding and have no cross-reactivity with $\alpha_M\beta_2$ binding, we synthesized a peptide library on the cellulose membrane spanning the sequence of γ-module of fibrinogen (Fig. 4-1). It has been shown that γ-module of fibrinogen contains multiple binding sites for $\alpha_M\beta_2$ integrin [22] and is critical for the $\alpha_D\beta_2$ binding to fibrinogen [10]. The peptide library consisting of 9-mer peptides with a 3-residue offset was tested for binding

of ^{125}I-labeled active αDI- domain as described previously for αMI-domain [24] (Fig. 4-2). We detected 3 sequences, which are specific only for the binding of αD I-domain – (spots 27-29, 49-51, and 67-70). The identified sequences AGHLNGVYYQGGTYSKAS, TGTTEFWLGNEKIHL, GDAFDGFDFGDDPSD were synthesized as soluble peptides and named P3, P4 and P5, correspondingly.

1.	VQIHDITGK	5481.32		46.	YAYFAGGDA	6090.85
2.	HDITGKDCQ	12879.24		47.	FAGGDAGDA	15712.64
3.	TGKDCQDIA	12189.18		48.	GDAGDAFDG	21063.70
4.	DCQDIANKG	12609.41	49.		GDAFDGFDF	16708.48
5.	DIANKGAKQ	4404.64	50. P5		FDGFDFGDD	22059.54
6.	NKGAKQSGL	75.42	51.		FDFGDDPSD	23249.53
7.	AKQSGLYFI	-2992.55		52.	GDDPSDKFF	15106.72
8.	SGLYFIKPL	-3797.58		53.	PSDKFFTSH	4275.41
9.	YFIKPLKAN	-6064.43		54.	KFFTSHNGM	-1043.98
10.	KPLKANQQF	-2875.97		55.	TSHNGMQFS	3683.10
11.	KANQQFLVY	-2975.53		56.	NGMQFSTWO	6434.77
12.	QQFLVYCEI	1464.55		57.	QFSTWDNDN	12387.87
13.	LVYCEIDGS	9021.67		58.	TWDNDNDKF	14769.36
14.	CEIDGSGNG	14661.79		59.	NDNDKFEGN	15733.18
15.	DGSGNGWTV	9780.55		60.	DKFEGNCAE	12670.80
16.	GNGWTVFQK	-758.15		61.	EGNCAEQDG	18250.09
17.	WTVFQKRLD	-3202.77		62.	CAEQDGSGW	12750.44
18.	FQKRLDGSV	-486.21		63.	QDGSGWWMN	7118.20
19.	RLDGSVDFK	4675.03		64.	SGWWMNKCH	-1282.61
20.	GSVDFKKNW	746.17		65.	WMNKCHAGH	1340.79
21.	DFKKNWIQY	-1809.67		66.	KCHAGHLNG	4171.45
22.	KNWIQYKEG	-1429.90	67.		AGHLNGVYY	1869.30
23.	IQYKEGFGH	2602.74	68. P3		LNGVYYQGG	2189.25
24.	KEGFGHLSP	4594.52	69.		VYYQGGTYS	81.44
25.	FGHLSPTGT	4279.08	70.		QGGTYSKAS	1599.56
26.	LSPTGTTEF	5874.89		71.	TYSKASTPN	480.19
27.	TGTTEFWLG	4541.07		72.	KASTPNGYD	6670.50
28. P4	TEFWLGNEK	4469.51		73.	TPNGYDNGI	9674.11
29.	WLGNEKIHL	1797.56		74.	GYDNGIIWA	5928.38
30.	NEKIHLIST	2665.99		75.	NGIIWATWK	-3227.74
31.	IHLISTQSA	2049.25		76.	IWATWKTRW	-10078.13
32.	ISTQSAIPY	808.51		77.	TWKTRWYSM	-9799.57
33.	QSAIPYALR	-3760.97		78.	TRWYSMKKT	-10689.99
34.	IPYALRVEL	-2596.93		79.	YSMKKTTMK	-7807.28
35.	ALRVELEDW	6510.05		80.	KKTTMKIIP	-6993.37
36.	VELEDWNGR	8703.34		81.	TMKIIPFNR	-7489.32
37.	EDWNGRTST	7375.39		82.	IIPFNRLTI	-5701.98
38.	NGRTSTADY	4428.34		83.	FNRLTIGEG	1013.94
39.	TSTADYAMF	5150.58		84.	LTIGEGQQH	8170.15
40.	ADYAMFKVG	2293.77		85.	GEGQQHHLG	10801.01
41.	AMFKVGPEA	2075.78		86.	QQHHLGGAK	4035.94
42.	KVGPEADKY	5666.37		87.	HLGGAKQAG	3976.26
43.	PEADKYRLT	2860.15		88.	GAKQAGDVA	7785.60
44.	DKYRLTYAY	-3988.20		89.	QAGDVAAAA	9737.16
45.	RLTYAYFAG	-5749.55		90.	DVAAAAFAL	6049.73

P3 - AGHLNGVYYQGGTYSKAS

P4 - TGTTEFWLGNEKIHL

P5 - GDAFDGFDFGDDPSD

Control peptide 38-40 –
WNGRTSTADYAMFKV

Fig. 4-1 Synthetized peptide library based on the sequence of γ-module of fibrinogen. The peptide sequences identified as positive for the αDI-domain binding are shown in green.
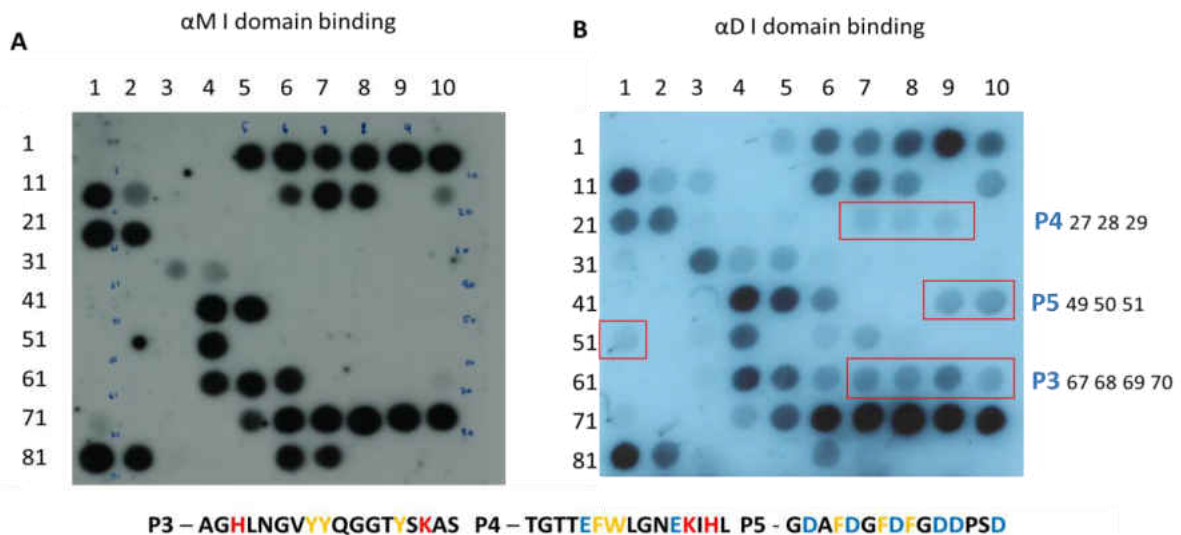

P3 – AGHLNGVYYQGGTYSKAS P4 – TGTTEFWLGNEKIHL P5 - GDAFDGFDFGDDPSD

Fig.4-2. Screening the peptide library for the binding to α_D and α_M I-domains. Peptide library was synthetized on the cellulose membrane spanning the sequence of γ-module of fibrinogen. The library was incubated with ^{125}I-labeled α_D I-domain or α_M I-domain and binding was visualized by autoradiography. The numbers on the left and above each panel indicate the peptide (spot) numbers. The peptide numbers correspond to the numbering of spots in the panel. Spot-analysis indicates three peptides, called P3, P4, and P5 as unique sequences to bind to $\alpha_D\beta_2$.

Evaluation of inhibitory abilities of identified sequences by surface plasmon resonance and adhesion assay.

The abilities of detected peptides to inhibit α_D I-domain binding to CEP was tested applying a surface plasmon resonance (Biacore 3000) (Fig. 4-3A, B). α_D I-domain and α_M I-domain were pre-incubated with 200 µg/ml P3, P4 and P5 peptides and added to the immobilized CEP using previously detected concentrations[16]. Two peptides (P4 and P5) demonstrated marked inhibition of α_D I-domain binding, while inhibition of α_M I-domain was not significant. To extend this result, we tested peptides in the adhesion assay using $\alpha_D\beta_2$ and $\alpha_M\beta_2$-transfected HEK 293 cells (Fig. 4-3C). CEP was immobilized on the 96-well plate and integrin transfected cell lines were pre-incubated with 200 µg/ml of peptides. Similar to direct protein-protein assay, P3 peptide does not have a blocking effect. However, the inhibitory ability of P4 peptide was reduced to compare with direct protein-protein interaction assay (Fig. 4-3A). Apparently, the binding region for the P4 peptide is only exposed on isolated I-domain, but it is partially blocked on $\alpha_D\beta_2$ heterodimer, which is expressed on the cell surface. Therefore, P4 binding site is not natural region for the $\alpha_D\beta_2$-CEP interaction. In contrast to these data, P5 peptide inhibits 50% of $\alpha_D\beta_2$ adhesion to CEP that is similar to the biacore results. The effect of P5 peptide on adhesion of $\alpha_M\beta_2$ cells was not significant. We tested different concentration of P5 peptide in adhesion assay and find concentration-dependent inhibition of $\alpha_D\beta_2$ binding to CEP (Fig. 4-3D).

Integrin $\alpha_D\beta_2$ and $\alpha_M\beta_2$ are multiligand receptors [10,21]. It has been shown that several integrin ligands have overlapping binding sites within I-domain [21,25-27]. Based on this information, we tested if P5 peptide can inhibit $\alpha_D\beta_2$-mediated cell adhesion to other ligands. First, we evaluated the adhesion of $\alpha_D\beta_2$- and $\alpha_M\beta_2$-transfected HEK 293 cells to fibrinogen in the presence of P5 peptide. We found that P5 peptide blocked only the adhesion of $\alpha_D\beta_2$ (Fig. 4-3E) in concentration-

dependent manner (Fig.4-4A). Since integrin $\alpha_X\beta_2$, which is also expressed on macrophages, has high homology with α_D and interacts with Fg, we tested this receptor in inhibition assay. The adhesion of $\alpha_X\beta_2$ transfected cells to immobilized fibrinogen was not affected in the presence of P5 peptide (Fig. 4-4B), that confirmed the specificity of selected inhibitor for integrin α_D.

We also tested the ability of P5 to block the adhesion of $\alpha_D\beta_2$ and $\alpha_M\beta_2$ to another ligand, vitronectin and received the similar result. Namely, P5 inhibits the adhesion of $\alpha_D\beta_2$-transfected cells, but has no effect on adhesion of $\alpha_M\beta_2$-transfected cells (Fig.4-3F). Taken together these data showed that P5 peptide can prevent the binding of $\alpha_D\beta_2$ to different ECM ligands without affecting the function of other macrophage integrins.
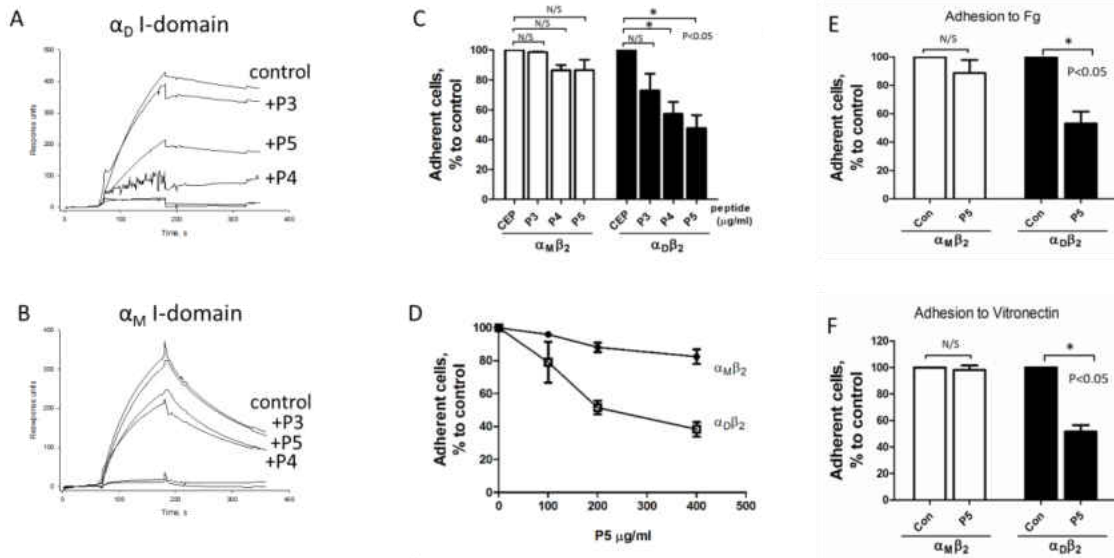
Fig.4-3. P5 peptide is a specific inhibitor for integrin $\alpha_D\beta_2$. A, B. Representative profiles of the surface plasmon resonance measured by Biacore for α_D **(A)** and α_M **(B)** binding to the CEP-BSA coupled to the CM5 chip in the presence of 200µg/ml P3, P4 and P5 peptides. **C-E.** Adhesion assay of $\alpha_D\beta_2$ and $\alpha_M\beta_2$ HEK 293 transfected cells in the presence of inhibitory peptides. **C.** 96-well plate was coated with CEP for 3 h at 37°C. Calcein AM labeled HEK293 transfected $\alpha_M\beta_2$ and $\alpha_D\beta_2$ cells were added to the wells and cell adhesion was determined after 30 min in a

fluorescence plate reader. Some samples were pre-incubated with P3, P4 or P5 peptide for 20 min before the adhesion assay. Data are presented as mean ± SEM. *, P<0.05. **D.** Adhesion of HEK293 transfected $\alpha_M\beta_2$ and $\alpha_D\beta_2$ cells to CEP in the presence of different concentrations of P5 peptide. Data are presented as mean ± SEM. *, P<0.05. **E, F.** Adhesion of HEK293 transfected $\alpha_M\beta_2$ and $\alpha_D\beta_2$ cells to fibrinogen **(E)** and vitronectin **(F)**, some samples were pre-incubated with P5 peptide before the adhesion assay. Data are presented as mean ± SEM. *, P<0.05.
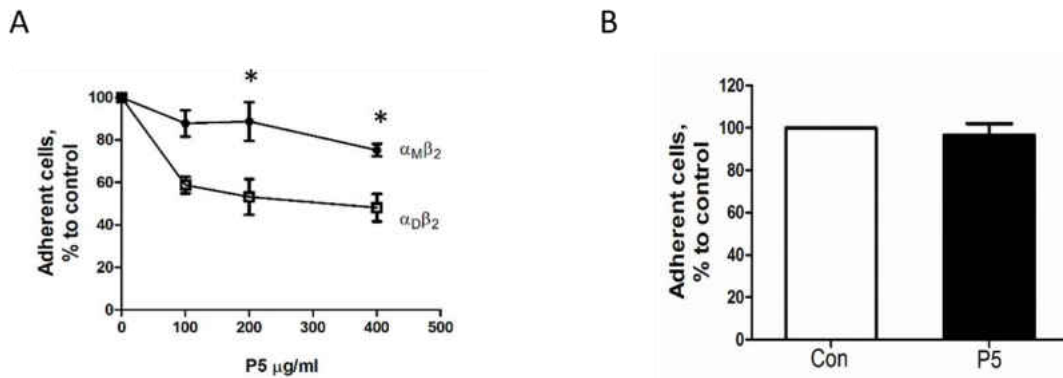
Fig. 4-4. Adhesion assay of HEK293 transfected cells in the presence of P5 peptide. A. Adhesion of $\alpha_M\beta_2$ and $\alpha_D\beta_2$ - HEK293 transfected cells to fibrinogen in the presence of different concentration of P5. **B.** Adhesion of $\alpha_X\beta_2$ -HEK293 transfected cells to fibrinogen in the presence of 200μg/ml P5 peptide. Data are presented as mean ± SEM. *, P < 0.05. The experiment was repeated 3 times with the similar result.

P5 peptide supports direct adhesion of $\alpha_D\beta_2$ cells and prevents receptor activation on the cell surface.

The blocking peptide can bind directly to the binding site within α_D or may have an allosteric effect. To detect the mechanism of P5 inhibition, we tested the direct binding of $\alpha_D\beta_2$ to P5 peptide. Using immobilized P5 in adhesion assay (Fig.4-5A), we found that P5 peptide can support a direct binding to $\alpha_D\beta_2$, while $\alpha_M\beta_2$ does not have this ability. The adhesion of both cell lines to Fg was used as positive control (Fig.4-5A).

The role of α_D I-domain conformation for the binding to P5 peptide was assessed using Bio-interferometry. Particularly, we tested the interaction of α_D I-domain in active and non-active conformation to the biotinylated P5 peptide, which was immobilized on streptavidin biosensor. We found that active form of α_D I-domain has a similar binding to P5 in the presence of 1mM Mg^{2+} and 5 mM EDTA. At the same time, a non-active conformation of α_D I-domain cannot interact with P5 (Fig. 4-5B).

In parallel experiment, we tested how binding of P5 peptide affect the change in the conformation of entire $\alpha_D\beta_2$ heterodimer on the cell surface. Using activation-dependent antibody mAb24, we found that pre-incubation with P5 peptide, significantly reduced $\alpha_D\beta_2$ activation (Fig.4-5C). Therefore, the binding of P5 peptide is not required a fully active conformation of $\alpha_D\beta_2$ and can prevent a conformational change from intermediate to the active stage. In agreement with our other data, P5 peptide did not have an effect on the activation of $\alpha_M\beta_2$ cells.
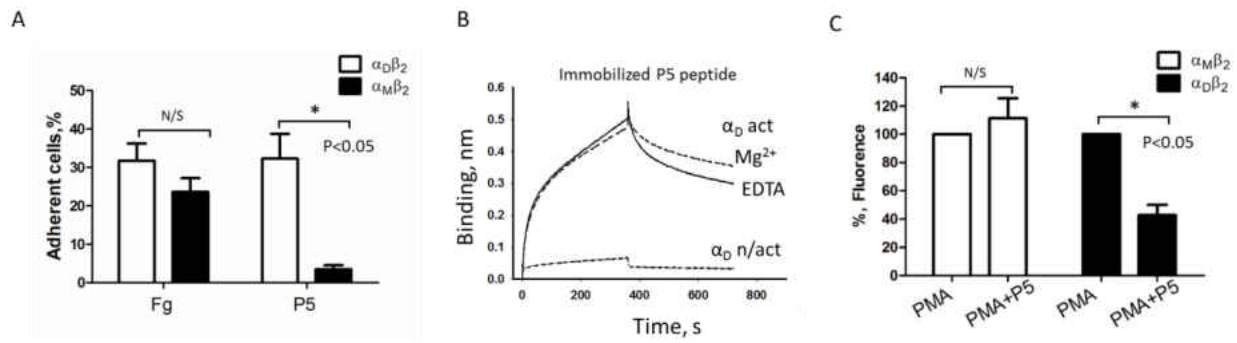
Fig.4-5. Characterization of P5 peptide binding to integrin $\alpha_D\beta_2$. A. Direct adhesion of HEK293 transfected $\alpha_M\beta_2$ and $\alpha_D\beta_2$ cells to immobilized P5 peptide. Cells were added to the 96-well plate coated with P5 peptide or with fibrinogen (Fg) as control and adhesion was performed as described in Fig.2. **B. Analysis of the activation stage of α_D I-domain for the binding to P5 peptide**. A representative binding curves of α_D I-domain binding to P5 peptide measured by Bio-interferometry (ForteBio). N-terminally biotinylated P5 peptide was immobilized on streptavidin biosensor. 2 μM of α_D I-domain in active conformation (solid line) and non-active conformation (dotted line) in the presence of 1 mM Mg^{2+} or α_D I-domain in active conformation in the presence of 5 mM EDTA (dash line) were incubated with immobilized P5. The binding was analyzed using ForteBio Data Analysis 11.0 software. The experiment was

repeated 3 times with the similar result. **C. P5 peptide inhibits the activation of integrin $\alpha_D\beta_2$ on the cell surface.** $\alpha_D\beta_2$ and $\alpha_M\beta_2$ transfected HEK 293 cells were pre-incubated with P5 peptide for 30 min at 37°C, then cells were incubated with 100 nM PMA for 30 min at 37°C to induce integrin activation. The activation stage of integrins were assessed using activation-dependent antibody mAb24. Fluorescently labeled cells were detected by FACS. Data are presented as mean ± SEM. *, $P< 0.05$.

Effect of P5 peptide on the macrophage accumulation in the peritoneal cavities of WT, $\alpha_D^{-/-}$ and $\alpha_M^{-/-}$ mice.

The blocking effect of P5 peptide on $\alpha_D\beta_2$-mediated cell adhesion might interfere with macrophage migration in vivo. We used the model of thioglycollate-induced peritoneal inflammation to evaluate changes in macrophage migration after P5 treatment. WT mice were injected intraperitoneally with P5 peptide or control peptide 30 min before the injection of thioglycollate and the number of peritoneal macrophages was detected after 72 hours. We selected a control peptide from the same γ-module sequence based on the absence of binding to $\alpha_D\beta_2$ and $\alpha_M\beta_2$ and presence of negatively and positively charged amino acids. Accordingly, the sequence (WNGRTSTADYAMFKV), which corresponds to spots 37-40, was synthetized and tested. The adhesion assay in the presence of control peptide confirmed the lack of its effect on $\alpha_D\beta_2$-mediated adhesion (Fig. 4-6A). The injection of cyclic P5 peptide to WT mice reduced 3 folds the accumulation of macrophages in the peritoneal cavity, while the treatment with control peptide or PBS had no effect (Fig. 4-6B). Interestingly, the injection of P5 to α_M-deficient mice demonstrated a reduction of macrophages in the peritoneal cavity similar to WT mice, while α_D-deficiency completely eliminated a blocking effect of P5 peptide (Fig. 4-6C). These results demonstrate the specificity of P5 peptide in vivo.
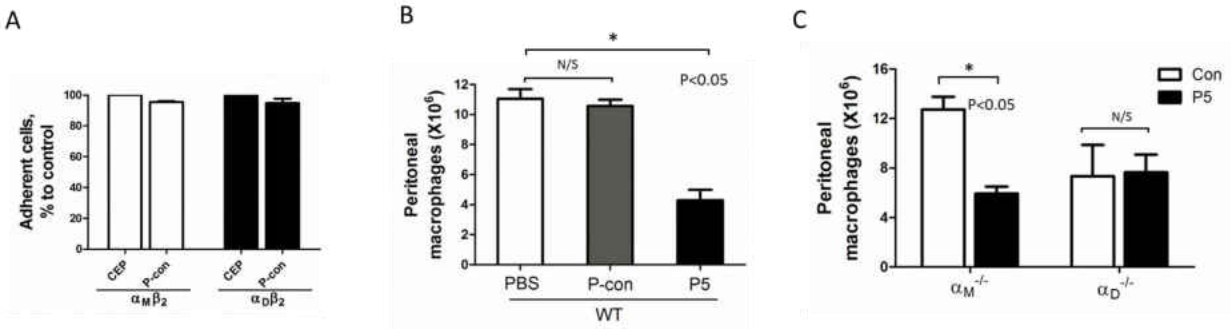
Fig. 4-6. P5 peptide inhibits the accumulation of macrophages in the peritoneal cavity during sterile inflammation. A. Adhesion of $\alpha_D\beta_2$ and $\alpha_M\beta_2$ transfected cells to CEP in the presence of 200 μg/ml control peptide. **B-C.** WT (**B**), $\alpha_M^{-/-}$ and $\alpha_D^{-/-}$ (**C**) mice were intraperitoneally injected with 200 μg/ml cyclic P5 peptide, control peptide or PBS. 20 min later, 4% thioglycollate was injected intraperitoneally to all mice to induce inflammation. After 3 days, the amount of WT, $\alpha_M^{-/-}$ and $\alpha_D^{-/-}$ macrophages was evaluated by assessing the number and percentage of macrophages in the inflamed peritoneal cavity of mice. Isolated peritoneal cells were counted and the number of WT, $\alpha_M^{-/-}$ and $\alpha_D^{-/-}$ macrophages were calculated based on the percentage of F4/80 positive population in flow cytometry analysis. Data are presented as mean ± SEM. *, P < 0.05.

Mechanism of P5 peptide inhibition during peritoneal inflammation.

The model of peritoneal inflammation is a well-described model of acute inflammation, which is commonly used to evaluate monocyte/macrophage recruitment. Macrophage accumulation in the peritoneal cavity depends on several factors including monocyte progenitor translocation to the blood stream, monocyte transmigration via endothelium monolayer, macrophage migration through the interstitium to the peritoneal cavity, and efflux from the cavity to the lymphatic. We sought to detect what step of macrophage accumulation is interfered by P5 peptide.

To clarify this question, we developed several assays. First, we isolated monocyte progenitors from WT mice, labeled cells with PKH26 red fluorescent dye and injected intravenously to the mice with initiated peritoneal inflammation (Fig.4-7A). One group of mice was treated with P5 peptide, second with the control. After 72 hours cells were isolated from the peritoneal cavity and the number of red-fluorescent adoptively transferred macrophages was

evaluated by FACS (Fig.4-7B). We found that according to our previous observations (Fig.4-6B) the total number of macrophages was significantly reduced after P5 treatment (Fig. 4-7C, left panel). More interestingly, the number of labeled macrophages was also significantly decreased (Fig.4-7C, right panel). This result demonstrated that the effect of P5 peptide on macrophage recruitment. But, clearly, P5 does not affect translocation from bone marrow, since labeled cells were injected to the blood stream. Also, this result shows that the effect of P5 is mediated by monocyte-derived macrophages and is not related to the proliferation of resident macrophages.
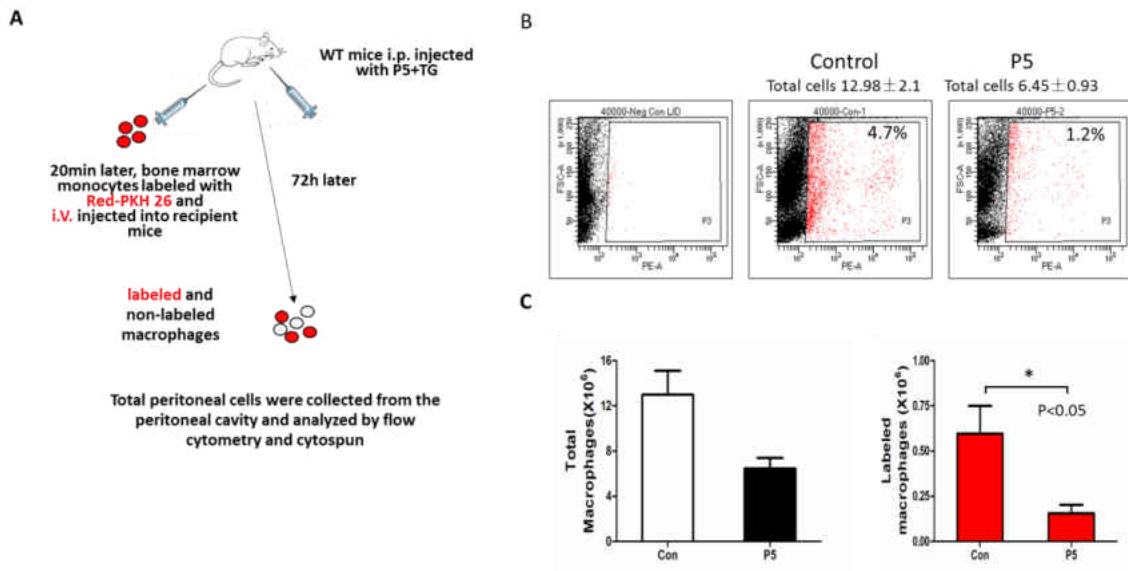
Fig.4-7. P5 peptide regulates the recruitment of macrophages. A. Schematic representation of experiment**.** WT mice were intraperitoneally injected with P5, 20 min later, TG were intraperitoneally injected to all the mice to induce inflammation, then fluorescently labeled WT bone marrow monocytes were injected into the tail vein of the recipient mice. After 72h, the harvested macrophages (labeled macrophages and total macrophages) were also assessed by flow cytometry (**B**) and the percentages of red fluorescent cells were assessed (**C**). Macrophages were calculated based on the percentage of F4/80 positive population in flow cytometry analysis. Data are presented as mean ± SEM. *, P < 0.05.

Second, we tested the potential role of P5 in the macrophage efflux from the peritoneal cavity (Fig. 4-8A). Macrophages were isolated at 72 hours after thioglycollate injection and labeled with PKH 26 fluorescent dye. The labeled macrophages were injected intraperitoneally to the mice

at 48 hours after thioglycollate-induced inflammation. One group was treated immediately with P5 peptide, another with control. After an additional 24 hours, cells from the peritoneal cavity were collected and the number of labeled macrophages was compared in both groups using FACS (Fig.4-8B) and cytospin (Fig. 4-9). Again, the number of recipient macrophages was affected by P5 peptide (Fig. 4-8C). However, the amount of fluorescently-labeled macrophages in the peritoneal cavity was not changes in the presence of P5 peptide that demonstrates that P5 treatment did not affect efflux of macrophage during peritoneal inflammation (Fig. 4-8C).

Based on these experiments, we concluded that P5 interferes with the recruitment of monocyte/macrophages from the bloodstream to the peritoneal cavity. Therefore, the contribution of P5 peptide may affect endothelial transmigration or migration through the ECM.
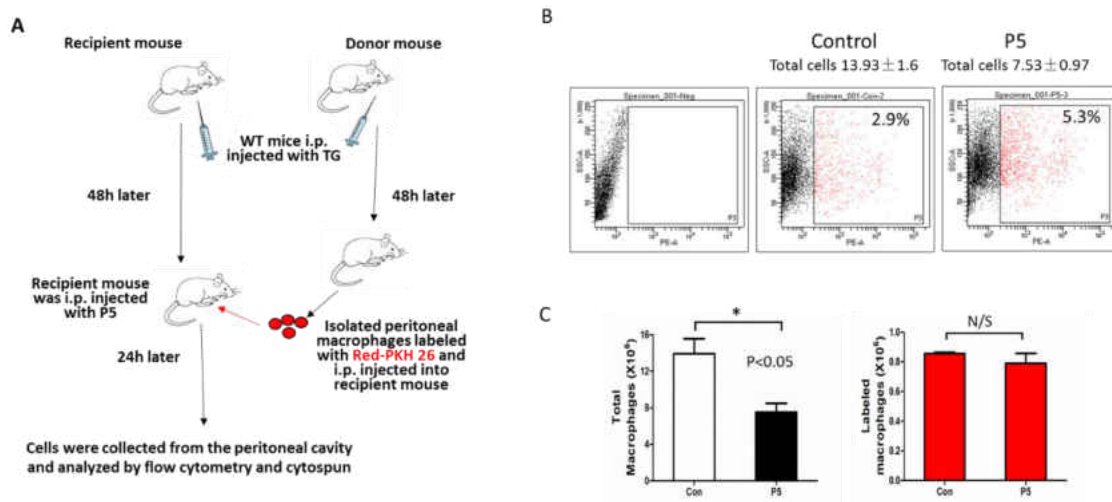
Fig.4-8. P5 peptide does not affect the efflux of macrophages from the peritoneal cavity. A. Schematic representation of experiment**.** Recipient and donor mice WT mice were intraperitoneally injected with thioglycollate (TG). After 48 hours, macrophages were isolated from the peritoneal cavity of donor mice and labeled with red fluorescent dye (PKH26). The recipient mice were intraperitoneally injected with labeled macrophages and P5 peptide. After additional 24h, the total macrophage number and percentage of labeled macrophages were evaluated by flow cytometry as described for Fig.4-7. (**B,C**). Data are presented as mean ± SEM. *, P < 0.05.
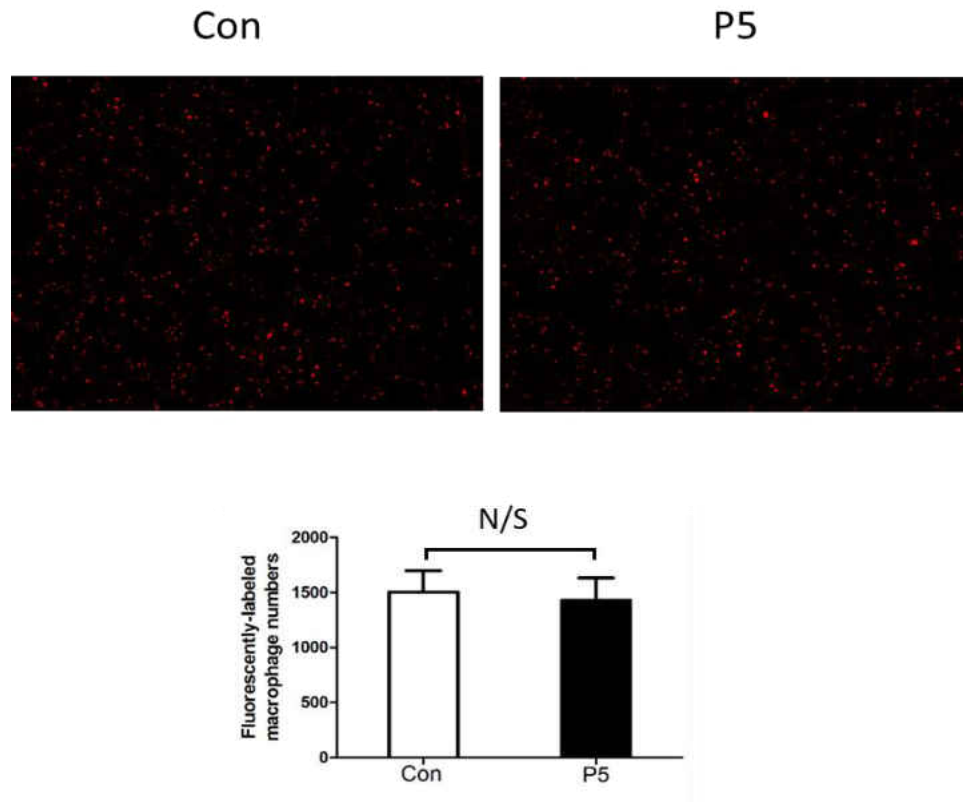
Fig.4-9. P5 peptide does not affect the efflux of macrophages from the peritoneal cavity. The experiments were performed as described in Fig. 4-8. The harvested peritoneal cells were cytospun and evaluated using fluorescent microscope (**upper panel**). The quantification of the data was analyzed using t-test at least 9 fields of view per sample (n=3) by Image Analysis Software (EVOS, Thermo Fisher) Data are presented as mean ± SEM. *, P < 0.05 (**lower panel**).

P5 peptide has no effect on 2D trans-endothelial migration but inhibits 3D migration in the matrix.

Accordingly, we tested the role of P5 in monocyte transmigration via endothelial monolayer in vitro. Boyden chamber was coated overnight with HUVEC cells, which were labeled with green PKH67 fluorescent dye. Monocytes, labeled with red fluorescence (PKH26), were added to the upper chamber (Fig. 4-10A). Monocyte migration was stimulated with MCP-1 added to the lower chamber. One group of monocytes was pre-treated with P5 peptide 20 min before the experiment. The transmigration was evaluated after 3 hours by confocal microscopy and analyzed

by IMARIS software (Fig.4-10B). We did not detect the effect of P5 on transmigration that corresponds to the relatively low level of integrin $\alpha_D\beta_2$ on the circulatory monocytes (Fig.4-10C).
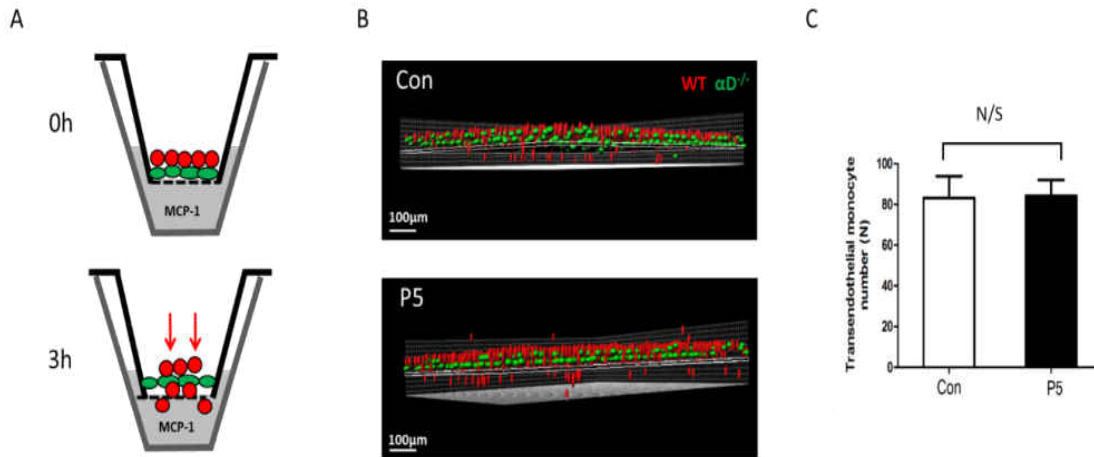
Fig.4-10. P5 peptide does not affect the trans-endothelial migration of monocytes A. PKH67-fluorescently labeled (green) HUVEC cells were coated on the membrane of the upper chamber of transwell. Monocytes were labeled with PKH26 red fluorescent dye and added on the top of endothelial cells. MCP-1 was added to the lower chamber of the transwells to stimulated monocyte migration. After 3h, monocyte transmigration was detected by the Leica Confocal microscope. **B.** Side view of the transwell. In P5 group, the monocytes were preincubated with P5 peptide for 20 min. The results were analyzed by IMARIS 8.0 software and plotted (**C**). Statistical analyses were performed using Student's paired t-tests (n=5 per group). Scale bar= 100 μm. Data are presented as mean ± SEM. *, P<0.05.

To test a contribution of P5 peptide to macrophage migration in the matrix, we used in vitro 3D migration assay in fibrin gel (Fig. 4-11A). Thioglycollate-induced peritoneal macrophages were isolated from WT and $\alpha_D^{-/-}$ mice and labeled with green (PKH67) or red (PKH26) fluorescent dyes, respectfully. The equal number of cells was loaded on one side of 3D fibrin gel and MCP-1 was added to the opposite side to stimulate the migration. One group of samples was pretreated with P5 peptide. P5 was also added to the fibrin matrix. The migration was evaluated after 48 hours by confocal microscopy (Fig.4-11B, C). The pre-incubation with P5 peptide markedly reduced

migration of non-polarized macrophages. Therefore, this experiment confirmed that P5 peptide affects migration of macrophages through ECM during acute peritoneal inflammation.

Usually, the further development of inflammation promotes the polarization of macrophages to the pro-inflammatory M1 phenotype. We recently showed that expression of $\alpha_D\beta_2$ is upregulated on M1-polarized macrophages and $\alpha_D\beta_2$'s high expression generates a strong adhesion, following by macrophage retention [8,9]. Therefore, we hypothesized that P5 peptide treatment may have the opposite effect on the migration of M1-activated macrophages. WT and $\alpha_D^{-/-}$ peritoneal macrophages were stimulated with IFN-γ for 4 days and tested in 3D migration assay in the fibrin matrix. As we have shown previously, M1-polarized WT macrophages demonstrate significantly lower migration to compare with non-activated macrophages, however, $\alpha_D^{-/-}$ M1 macrophages demonstrates enhanced migration to compare with WT (Fig. 4-11D, left panel). Accordingly, the addition of P5 peptide improved migratory properties of WT M1 macrophages (Fig. 4-11D, right panel). Apparently, P5-mediated inhibition of $\alpha_D\beta_2$ adhesion releases macrophage migration. Notably, the migration of $\alpha_D^{-/-}$ macrophages is not significantly changed after P5 peptide treatment, which is in agreement with our previous observations (Fig. 4-6C). Based on these results we can predict that the effect of P5 peptide on the development of chronic inflammation would be more complex and will include the inhibition of macrophage migration to the site of inflammation and inhibition of macrophage retention at the site of inflammation.
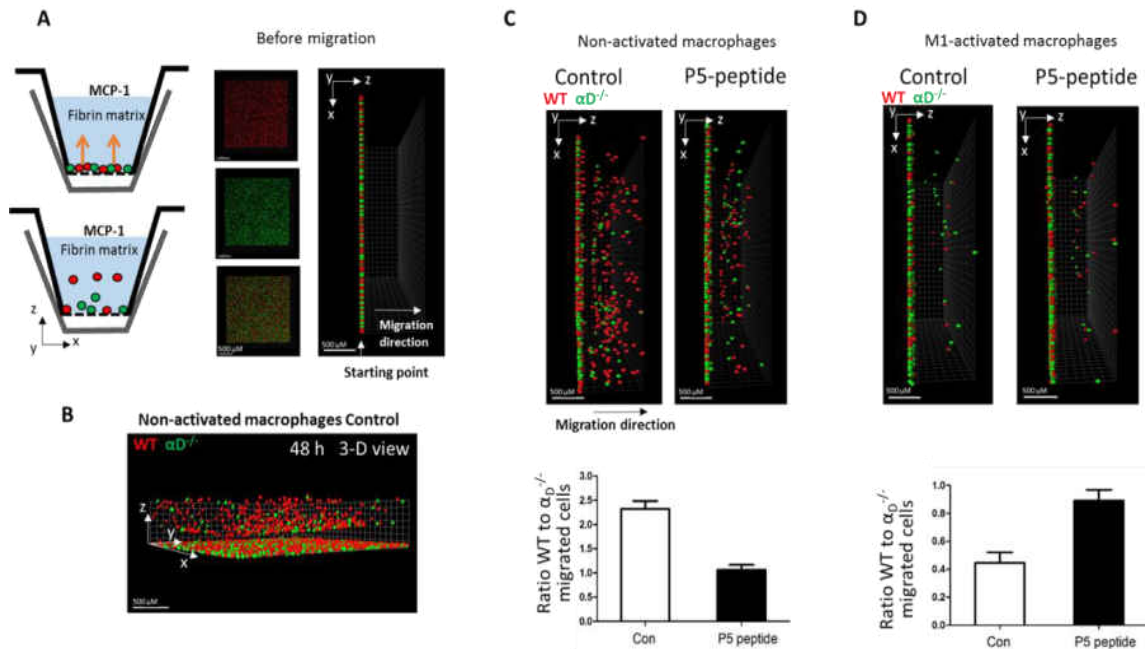
Fig.4-11. 3D migration of macrophages was regulated by P5 peptide. A. Schematic representation of experiment. Labeled cells were mixed in equal amounts and added to the transwell. Before the initiation of migration, the background was verified by scanning samples with confocal microscope. The migration was stimulated by the adding 30 nM MCP-1 to the opposite side of fibrin gel. **B.** After 48 hours the migration was evaluated using Leica Confocal microscope. 3-D view of the migrating cells in Fibrin matrix. **C-D.** Side view of migration of non-activated **(C)** and M1-activated **(D)** macrophages. The results were analyzed and reconstructed by IMARIS 8.0 software. Statistical analyses were performed using Student's paired t-tests (n=4 per group). Scale bar= 500 μm. Data are presented as mean ± SEM. *, P<0.05.

Inhibition of macrophage accumulation in the adipose tissue of diabetic mice by P5 peptide.

To test P5 effect on chronic inflammation, we analyzed an accumulation of macrophages in adipose tissue of pre-diabetic mice. Mice after 8 weeks on a high-fat diet were injected with fluorescently labeled WT (PKH26 red) and $\alpha_D^{-/-}$(PKH67 green) monocytes. One group was injected with cyclic P5 peptide, another with control. After 48 hours the number of red and green-labeled macrophages in the adipose tissue was evaluated using classical FACS (Fig. 4-12A) and imaging flow cytometry (Fig. 4-12B). We have previously shown that α_D-deficiency reduced

125

macrophage accumulation in the adipose tissue. Now, we demonstrate that P5 peptide possesses a similar effect on WT macrophages. The accumulation of P5 treated WT macrophages was reduced by 2.5 folds. Interestingly, the migration of $\alpha_D^{-/-}$ macrophages was not affected. Specifically, the ratio of WT to $\alpha_D^{-/-}$ macrophages in adipose tissue of control mice was 3 folds, while this ratio was reduced to 1 after P5 peptide treatment (Fig. 4-12C, D).
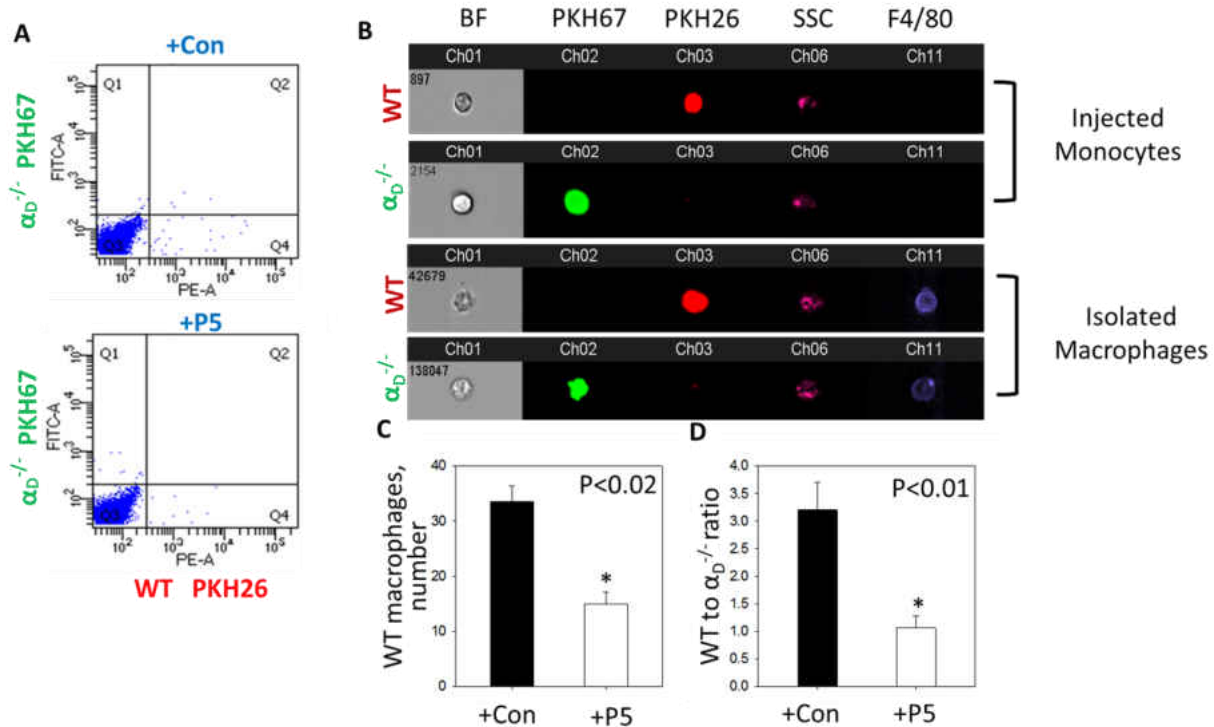
Fig. 4-12. P5 peptide inhibited accumulation of macrophages in adipose tissue of mice during diet-induced diabetes. Isolated WT and $\alpha_D^{-/-}$ bone marrow monocytes were labeled with red PKH26 (WT) or green PKH67 ($\alpha_D^{-/-}$) fluorescent dyes, respectively, mixed in an equal amount and injected into the tail vein of WT mice fed a high fat diet (45% kcal/fat) for 8 weeks. Experimental groups were intraperitoneally injected with 200 µg/ml P5 peptide 20 min before the injection of labeled cells. After 3 days, visceral adipose tissue was isolated, digested and analyzed using flow cytometry. A. Q1 and Q4 quadrants represent the labeled cells in digested adipose tissue. Statistical analyses were performed using Student's paired t-tests (n=5 for con, n=4 for P5 group). Data are presented as mean ± SEM. *, P<0.05. B. Imaging flow cytometry. The upper panels represent the injected monocytes, isolated from WT and $\alpha_D^{-/-}$ mice, labeled with red and green

fluorescent dyes, respectively. The lower panels represent macrophages isolated from adipose tissue. The population of single, alive cells was analyzed on red and green channels. Channel 1- Brightfield (BF). Channel 2- 488 wavelength (PKH67). Channel 3 – 566 wavelength (PKH26), channel 6 – side scattering (SSC). Channel 11- F4/80 represents macrophage staining. C. Macrophage number was calculated based on flow cytometry data and presented as mean ± SEM. *, P < 0.05. D. The ratio of WT and $\alpha_D^{-/-}$ macrophage in each mouse was calculated and presented as mean ± SEM. *, P<0.05.

Discussion

Our previous results demonstrated that modification of ECM proteins with the product of DHA oxidation, CEP, generates new inflammation-specific substrates in the tissue [16]. We found that CEP is a ligand for $\alpha_D\beta_2$ and $\alpha_M\beta_2$-mediated macrophage adhesion and migration [16]. Importantly, we and others detected CEP modified proteins in different inflamed tissues such as atherosclerotic lesions, pathological angiogenesis, adipose tissue during diabetes and peritoneal tissue during sterile inflammation [16,19,28,29]. Our other recent results demonstrated that the upregulation of integrin $\alpha_D\beta_2$ at the site of inflammation promotes strong adhesion of macrophages to the substrate, related macrophage retention and disease progression [8].

The proposed study was designed to develop the inhibitor of $\alpha_D\beta_2$-medited adhesion of macrophages to the inflamed ECM, focusing on CEP as an inflammation-specific ligand. Since $\alpha_M\beta_2$ and $\alpha_D\beta_2$ have a different, rather opposite role during chronic inflammation [8,9,13,15], our goal was to identify the inhibitor that will work specifically only with integrin $\alpha_D\beta_2$. The lack of commercially available monoclonal antibodies against $\alpha_D\beta_2$ as well as focus on specific $\alpha_D\beta_2$ ligand led us to the search for the peptide-based inhibitor. Based on different affinities between CEP - α_D I-domain (K_D 1.81x10^{-7}) and CEP- α_M I domain (K_D 2.1x10^{-6})[16], we hypothesized that ligand binding sites for CEP within $\alpha_D\beta_2$ and $\alpha_M\beta_2$ have a different structure.

We selected γ-module of fibrinogen for the generation of a cellulose-bound peptide library, based on our earlier finding that γ-module contains several independent sites that can be recognized by integrin $\alpha_M\beta_2$ [22]. We also showed that $\alpha_D\beta_2$ interacts with fibrinogen, via γ-module [10]. Utilizing this library, we identify 3 unique peptides, which are specific only for binding to integrin $\alpha_D\beta_2$ (Fig. 4-2). The inhibitory abilities of identified sequences were tested in the protein-binding assay (surface plasmon resonance) and adhesion assay, that narrowed our search to one peptide, called

P5 (Fig. 4-3). P5 peptide has a strong negative charge due to 6 aspartic acids. Since the critical molecular group of CEP is a carboxyl group [18], P5 peptide mimics the multiple CEP modifications on a protein surface. We cannot exclude that some other peptides with strong negative charge may have a similar effect on $\alpha_D\beta_2$-mediated macrophage adhesion. However, a number of tested peptides with several aspartic/glutamic acids in the structure do not interact with α_D I-domain (Fig. 4-1 and Fig. 4-2 spot 47, 48, 58 and 59).

$\alpha_D\beta_2$ is a multi-ligand receptor. The previous data demonstrated that binding sites within α_D for different ligands are overlapping [10]. Accordingly, we found that P5 peptide can also block the binding to vitronectin and fibrinogen that broads the inhibitory ability of P5. However, the K_D of α_D binding to CEP surpasses the binding to Fg or vitronectin [10,16,30], therefore during inflammation CEP-modified proteins will be preferential ligands for $\alpha_D\beta_2$. Moreover, the formation of adducts between CEP and natural ligands of $\alpha_D\beta_2$ will promote the $\alpha_D\beta_2$ interaction with these ligands via CEP binding site.

The integrin ligand binding requires the interaction of negatively charged amino acid of the ligand with the metal-ion-dependent adhesion site (MIDAS) in integrin I-domain structure [30]. MIDAS is a binding site for Mg^{2+}, which is coordinated by five side chains of amino acids from I-domain and acidic residue from the ligand. Such coordination stabilizes the active conformation of I-domain and promotes ligand binding[31]. The ability of P5 peptide to interact with α_D I-domain in the presence of EDTA demonstrates that P5 is not involved in the interaction with MIDAS via one of aspartic acid. Moreover, the lack of P5 peptide to interact with integrin α_M (Fig. 4-2,4-5), that contains the same MIDAS structure, confirms that P5 binding site is located in the separate part of I-domain. Further studies are required to localize the binding motif for P5 peptide within $\alpha_D\beta_2$. One of the potential explanations of P5 mechanism can be a prevention of $\alpha_D\beta_2$ activation since the pre-incubation of $\alpha_D\beta_2$-cells with P5 peptide inhibit following activation/conformational change of $\alpha_D\beta_2$ (Fig.4-5C). It has been shown that integrin can interact with ligands in the intermediate affinity [32]. The ligand docking can change integrin conformation to an active form and increase affinity of binding. Therefore, the effect of P5 peptide on $\alpha_D\beta_2$ binding to different ligands can be explained by prevention of conformational change from the intermediate to the active stage.

Mouse and human integrin α_D have a high level of homology (identity 71%; positive 80%). CEP formation is similar in human and mouse tissues[33]. P5 peptide inhibited the binding of CEP to human α_D I-domain, human $\alpha_D\beta_2$-transfected HEK 293 cells and mouse macrophages in vitro and in vivo. Therefore, P5 peptide represents the common inhibitor for human and mouse systems.

To evaluate the effect of P5 peptide in vivo, a mouse peritoneal model of inflammation was applied. Thioglycollate-induced peritoneal inflammation represents a sterile acute inflammation. In contrast to chronic inflammatory diseases, the expression of integrin $\alpha_D\beta_2$ on peritoneal macrophages is intermediate[7]. However, this model is commonly used to study the mechanism of neutrophil and macrophage migration and provided an important information regarding the effect of P5 peptide inhibition in vivo. The macrophage accumulation in the peritoneal cavity at 72 hours after injection of sterile thioglycollate allows tracking monocyte recruitment and macrophage efflux during inflammation [34-36]. We demonstrated the specificity of P5 peptide-mediated inhibition, since P5 peptide significantly blocked accumulation of WT and $\alpha_M^{-/-}$ macrophages, but had no effect on the accumulation of α_D-deficient macrophages in the peritoneal cavity (Fig. 4-6).

The monocyte/macrophage recruitment to and efflux from the peritoneal cavity is a complex process that can be divided into several stages: translocation of monocytes from bone marrow/spleen, monocyte transmigration through the endothelium, migration via ECM and efflux from the cavity to lymphatics. Since each step is regulated by leukocyte integrins, we tested a potential role of P5 on these processes. Using adoptively transferred macrophages, we found that P5 peptide has no effect on macrophage efflux from the peritoneal cavity (Fig. 4-9). It corresponds to the previous results that macrophage efflux is regulated by integrin $\alpha_4\beta_1$ [35,36] and $\alpha_M\beta_2$ [34]. In contrast, the injection of fluorescently labeled monocytes to the blood stream in the presence of P5 peptide significantly reduced the accumulation of labeled macrophages in the peritoneal cavity (Fig. 4-7). This result demonstrated that P5 peptide inhibits monocyte endothelial transmigration or/and migration via ECM (peritoneal wall) toward the cavity. Also, this result indicated that the P5 effect is not related to monocyte translocation from the bone marrow. These data are in agreement with the facts that $\alpha_D\beta_2$ has a low expression on monocyte progenitors that reduced potential contribution of $\alpha_D\beta_2$ to this step [37].

To further determine the role of P5 peptide in the recruitment, we tested P5 in monocyte transmigration (Fig. 4-10) and migration through the extracellular matrix in vitro (Fig. 4-11). We did not detect a difference in monocyte transmigration via endothelial monolayer in the presence of P5 peptide. It corresponds to the previous results that monocyte diapedesis depends on integrin $\alpha_L\beta_2$, $\alpha_4\beta_1$ and to some extend $\alpha_M\beta_2$ [38,39], [40]. It also in agreement with our previous data that α_D-deficiency do not change transmigration of monocytes during atherogenesis [8].

In contrast to these data, P5 had a strong effect on the migration of WT macrophages in 3D matrix. Macrophages can apply mesenchymal (adhesion-dependent) or amoeboid (adhesion-independent) migration mode in the 3D environment [41-45]. We recently found that integrin $\alpha_D\beta_2$ can regulate mesenchymal migration [9], and the density of $\alpha_D\beta_2$ on macrophage surface is important for the outcome. The interplay between integrin density and cell migration is based on the theory of cell migration, which postulates that intermediate adhesion supports migration, while very strong adhesion will inhibit cell locomotion [46,47]. In our current experiment, we used non-activated peritoneal macrophages, which have a moderate level of $\alpha_D\beta_2$ expression [7]. Clearly, α_D-deficiency reduced migration of non-activated macrophages (Fig. 4-11C, left panel ($\alpha_D^{-/-}$ green fluorescence versus WT red fluorescence)), that confirmed a supportive role of $\alpha_D\beta_2$ in migration. Accordingly, P5 peptide reduced the migration of WT non-activated macrophages (Fig. 4-11C, right panel), but does not have an effect on migration of α_D-deficient macrophages.

In our previous project, we found that high expression of $\alpha_D\beta_2$ on M1 macrophages serves to inhibit cell migration due to strong adhesion [8,9]. We verified this result by demonstrating a reduced migration of α_D-deficient M1-activated macrophages (green fluorescence) (Fig. 4-11D, left panel). Accordingly, the migration of WT M1-activated macrophages in the presence of P5 peptide was improved, since $\alpha_D\beta_2$-mediated adhesion was reduced (Fig.4-11D, right panel). The migration of α_D-deficient macrophages (green fluorescence) surpasses WT (red fluorescence) in the control sample but had a similar level after P5 treatment (Fig. 4-11C,D). These data demonstrate that P5 peptide may differently affect macrophage migration depending on subset of macrophages and level of $\alpha_D\beta_2$ expression on the surface. The obtained result is in agreement with our previous data that integrin $\alpha_D\beta_2$ has a different role during migration depending on receptor density on the cell surface [7,9]. The intermediate expression of $\alpha_D\beta_2$ during acute inflammation

supports macrophage migration to the site of inflammation, while upregulation of $\alpha_D\beta_2$ on pro-inflammatory macrophages promotes macrophage retention at the site of chronic inflammation.

To further confirm that P5 may affect macrophage accumulation during chronic inflammation we applied the model of diet-induced insulin resistance. Recently, we demonstrated that α_D-deficiency reduced glucose tolerance and insulin resistance in C57BL6 mice [9]. Using adoptive transfer of fluorescently labeled WT and $\alpha_D^{-/-}$ monocytes, we demonstrated that ratio WT to $\alpha_D^{-/-}$ macrophages in the adipose tissue reduced after P5 peptide treatment (Fig. 4-12). Macrophage accumulation in adipose tissue is a critical marker of inflammation and development of diabetes. This result confirmed the important role of integrin $\alpha_D\beta_2$ in the development of inflammation and proposes P5 peptide as a potential approach for the development of an anti-inflammatory treatment that can prevent macrophage accumulation and development of different inflammatory diseases, particularly type 2 diabetes.

References

1.   Alexandraki K, Piperi C, Kalofoutis C, Singh J, Alaveras A, Kalofoutis A. Inflammatory process in type 2 diabetes: The role of cytokines. *Ann N Y Acad Sci*. 2006;1084:89-117.

2.   Ouchi N, Kihara S, Funahashi T, Matsuzawa Y, Walsh K. Obesity, adiponectin and vascular inflammatory disease. *Curr Opin Lipidol*. 2003;14(6):561-566.

3.   Subramanian S, Chait A. The effect of dietary cholesterol on macrophage accumulation in adipose tissue: implications for systemic inflammation and atherosclerosis. *Curr Opin Lipidol*. 2009;20(1):39-44.

4.   Schittenhelm L, Hilkens CM, Morrison VL. beta2 Integrins As Regulators of Dendritic Cell, Monocyte, and Macrophage Function. *Front Immunol*. 2017;8:1866.

5.   Thomas AP, Dunn TN, Oort PJ, Grino M, Adams SH. Inflammatory phenotyping identifies CD11d as a gene markedly induced in white adipose tissue in obese rodents and women. *J Nutr*. 2011;141(6):1172-1180.

6.   Van der Vieren M, Le Trong H, St.John T, Staunton DE, Gallatin WM. A novel leukointegrin, a_db_2, binds preferentially to ICAM-3. *Immunity*. 1995;3:683-690.

7.   Yakubenko VP, Belevych N, Mishchuk D, Schurin A, Lam SC, Ugarova TP. The role of integrin alpha D beta2 (CD11d/CD18) in monocyte/macrophage migration. *Exp Cell Res*. 2008;314:2569-2578.

8.   Aziz MH, Cui K, Das M, et al. The Upregulation of Integrin alphaDbeta2 (CD11d/CD18) on Inflammatory Macrophages Promotes Macrophage Retention in Vascular Lesions and Development of Atherosclerosis. *J Immunol*. 2017;198(12):4855-4867.

9.   Cui K, Ardell CL, Podolnikova NP, Yakubenko VP. Distinct Migratory Properties of M1, M2, and Resident Macrophages Are Regulated by alphaDbeta2 and alphaMbeta2 Integrin-Mediated Adhesion. *Front Immunol*. 2018;9:2650.

10.   Yakubenko VP, Yadav SP, Ugarova TP. Integrin alphaDbeta2, an adhesion receptor up-regulated on macrophage foam cells, exhibits multiligand-binding properties. *Blood*. 2006;107:1643-1650.

11.   Shen D, Podolnikova NP, Yakubenko VP, et al. Pleiotrophin, a Multifunctional Cytokine and Growth Factor, Induces Leukocyte Responses through the Integrin Mac-1. *J Biol Chem*. 2017.

12.   Yakubenko VP, Bhattacharjee A, Pluskota E, Cathcart MK. aMb2 integrin activation prevents alternative activation of human and murine macrophages and impedes foam cell formation. *Circ Res*. 2011;108:544-554.

13.   Szpak D, Izem L, Verbovetskiy D, Soloviev DA, Yakubenko VP, Pluskota E. alphaMbeta2 Is Antiatherogenic in Female but Not Male Mice. *J Immunol*. 2018;200(7):2426-2438.

14.   Wolf D, Anto-Michel N, Blankenbach H, et al. A ligand-specific blockade of the integrin Mac-1 selectively targets pathologic inflammation while maintaining protective host-defense. *Nat Commun*. 2018;9(1):525.

15.   Wolf D, Bukosza N, Engel D, et al. Inflammation, but not recruitment, of adipose tissue macrophages requires signalling through Mac-1 (CD11b/CD18) in diet-induced obesity (DIO). *Thromb Haemost*. 2017;117(2):325-338.

16.   Yakubenko VP, Cui K, Ardell CL, et al. Oxidative modifications of extracellular matrix promote the second wave of inflammation via beta2 integrins. *Blood*. 2018.

17.   Wang H, Linetsky M, Guo J, et al. 4-Hydroxy-7-oxo-5-heptenoic Acid (HOHA) Lactone is a Biologically Active Precursor for the Generation of 2-(omega-Carboxyethyl)pyrrole (CEP) Derivatives of Proteins and Ethanolamine Phospholipids. *Chem Res Toxicol*. 2015;28(5):967-977.

18.   Gu X, Meer SG, Miyagi M, et al. Carboxyethylpyrrole protein adducts and autoantibodies, biomarkers for age-related macular degeneration. *J Biol Chem*. 2003;278(43):42027-42035.

19.   Kim YW, Yakubenko VP, West XZ, et al. Receptor-Mediated Mechanism Controlling Tissue Levels of Bioactive Lipid Oxidation Products. *Circ Res*. 2015;117(4):321-332.

20.   Biswas S, Xin L, Panigrahi S, et al. Novel phosphatidylethanolamine derivatives accumulate in circulation in hyperlipidemic ApoE-/- mice and activate platelets via TLR2. *Blood*. 2016;127(21):2618-2629.

21.   Yakubenko VP, Lishko VK, Lam SC-T, Ugarova TP. A molecular basis for integrin a_Mb_2 in ligand binding promiscuity. *J Biol Chem*. 2002;277:48635-48642.

22.   Lishko VK, Podolnikova NP, Yakubenko VP, et al. Multiple binding sites in fibrinogen for integrin alpha Mbeta 2 (Mac-1). *Journal of Biological Chemistry*. 2004;279:44897-44906.

23.   Podolnikova NP, Podolnikov AV, Haas TA, Lishko VK, Ugarova TP. Ligand recognition specificity of leukocyte integrin alphaMbeta2 (Mac-1, CD11b/CD18) and its functional consequences. *Biochemistry*. 2015;54(6):1408-1420.

24.   Lishko VK, Podolnikova NP, Yakubenko VP, et al. Multiple binding sites in fibrinogen for integrin alphaMbeta2 (Mac-1). *J Biol Chem*. 2004;279(43):44897-44906.

25.   Yakubenko VP, Solovjov DA, Zhang L, Yee VC, Plow EF, Ugarova TP. Identification of the binding site for fibrinogen recognition peptide g383-395 within the a_M I-domain of integrin $a_M b_2$. *J Biol Chem*. 2001;275:13995-14003.

26.   Ustinov VA, Plow EF. Delineation of the key amino acids involved in NIF binding to the I-domain supports a mosaic model for the capacity of integrin $a_M b_2$ to recognize multiple ligands. *J Biol Chem*. 2002;277:18769-18776.

27.   Zhang L, Plow EF. Amino acid sequences within the a subunit of integrin $a_M b_2$ (Mac-1) critical for specific recognition of C3bi. *Biochemistry*. 1999;38:8064-8071.

28.   West XZ, Malinin NL, Merkulova AA, et al. Oxidative stress induces angiogenesis by activating TLR2 with novel endogenous ligands. *Nature*. 2010;467(7318):972-976.

29.   Panigrahi S, Ma Y, Hong L, et al. Engagement of platelet toll-like receptor 9 by novel endogenous ligands promotes platelet hyperreactivity and thrombosis. *Circ Res*. 2013;112(1):103-112.

30.   Li R, Rieu P, Griffith DL, Scott D, Arnaout MA. Two functional states of the CD11b A-domain: correlations with key features of two Mn^{2+} - complexed crystal structures. *J Cell Biol*. 1998;143:1523-1534.

31.   Xiong J-P, Li R, Essafi M, Stehle T, Arnaout MA. An isoleucine-based allosteric switch controls affinity and shape shifting in integrin CD11b A-domain. *J Biol Chem*. 2000;275:38762-38767.

32.   Zhu J, Zhu J, Springer TA. Complete integrin headpiece opening in eight steps. *J Cell Biol*. 2013;201(7):1053-1068.

33.   Salomon RG. Carboxyethylpyrroles: From Hypothesis to the Discovery of Biologically Active Natural Products. *Chem Res Toxicol*. 2017;30(1):105-113.

34.   Cao C, Lawrence DA, Strickland DK, Zhang L. A specific role of integrin Mac-1 in accelerated macrophage efflux to the lymphatics. *Blood*. 2005;106:3234-3241.

35.   Bellingan GJ, Caldwell H, Howie SE, Dransfield I, Haslett C. In vivo fate of the inflammatory macrophage during the resolution of inflammation: inflammatory macrophages do not die locally, but emigrate to the draining lymph nodes. *J Immunol*. 1996;157(6):2577-2585.

36.   Bellingan GJ, Xu P, Cooksley H, et al. Adhesion molecule-dependent mechanisms regulate the rate of macrophage clearance during the resolution of peritoneal inflammation. *J Exp Med*. 2002;196:1515-1521.

37.   Noti JD. Expression of the myeloid-specific leukocyte integrin gene CD11d during macrophage foam cell differentiation and exposure to lipoproteins. *International Journal of Molecular Medicine*. 2002;10:721-727.

38.   Chuluyan HE, Issekutz AC. VLA-4 integrin can mediate CD11/CD18-independent transendothelial migration of human monocytes. *JClinInvest*. 1993;92:2768-2777.

39.   Shang XZ, Issekutz AC. Contribution of CD11a/CD18, CD11b/CD18, ICAM-1 (CD54) and -2 (CD102) to human monocyte migration through endothelium and connective tissue fibroblast barriers. *Eur J Immunol*. 1998;28:1970-1979.

40.   Meerschaert J, Furie MB. Monocytes use either CD11/CD18 or VLA-4 to migrate across human endothelium in vitro. *JImmunol*. 1994;152:1915-1926.

41.   Lammermann T, Bader BL, Monkley SJ, et al. Rapid leukocyte migration by integrin-independent flowing and squeezing. *Nature*. 2008;453:51-55.

42.   Bouissou A, Proag A, Bourg N, et al. Podosome Force Generation Machinery: A Local Balance between Protrusion at the Core and Traction at the Ring. *ACS Nano*. 2017;11(4):4028-4040.

43.   Cougoule C, Van GE, Le C, V, et al. Blood leukocytes and macrophages of various phenotypes have distinct abilities to form podosomes and to migrate in 3D environments. *Eur J Cell Biol*. 2012;91(11-12):938-949.

44.   Maridonneau-Parini I. Control of macrophage 3D migration: a therapeutic challenge to limit tissue infiltration. *Immunol Rev*. 2014;262(1):216-231.

45.   Wiesner C, Le-Cabec V, El AK, Maridonneau-Parini I, Linder S. Podosomes in space: macrophage migration and matrix degradation in 2D and 3D settings. *Cell Adh Migr*. 2014;8(3):179-191.

46.   Palecek SP, Loftus JC, Ginsberg MH, Lauffenburger DA, Horwitz AF. Integrin-ligand binding properties govern cell migration speed through cell-substratum adhesiveness. *Nature*. 1997;385:537-540.

47.   DiMilla PA, Stone JA, Quinn JA, Albelda SM, Lauffenburger DA. Maximal migration of human smooth muscle cells on fibronectin and type IV collagen occurs at an intermediate attachment strength. *J Cell Biol*. 1993;122:729-737.

CHAPTER 5

SUMMARY

The major findings of our research were:

1. CEP is not present in healthy tissues and its levels are dramatically increased at the sites of inflammation.

2. Inhibition of CEP does not affect the response of neutrophils to inflammation but prevents the consequent macrophage recruitment.

3. Neutrophil activation and migration through ECM results in the generation of CEP-modified proteins.

4. CEP-modified proteins promote macrophage adhesion and migration.

5. Integrins $\alpha_M\beta_2$ and $\alpha_D\beta_2$ are specific macrophage receptors for CEP-mediated adhesion and migration.

6. The expression of integrin $\alpha_D\beta_2$ was significantly upregulated on macrophages in atherosclerotic lesions and M1 macrophages *in vitro.*

7. αD-deficiency reduced macrophage accumulation in atherosclerotic lesions and does not have effects on macrophage apoptosis or proliferation.

8. Strong adhesion of M1-activated macrophages translates to weak 3D migration, while moderate adhesion of M2-activated macrophages generates dynamic motility.

9. The high expression of $\alpha_M\beta_2$ on resident macrophages prevents their amoeboid migration, which is markedly increased in α_M-deficient macrophages.

10. α_D deficiency prevents the retention of inflammatory macrophages in adipose tissue and improves metabolic parameters, while α_M deficiency does not affect macrophage accumulation.

11. P5 peptide is a specific inhibitor for integrin $\alpha_D\beta_2$.

12. P5 peptide inhibits the accumulation of macrophages in the peritoneal cavity.

13. P5 peptide inhibits the recruitment of non-activated macrophages to the peritoneal cavity.

14. P5 peptide neither affects trans-endothelial migration of monocytes nor the efflux of macrophages from the peritoneal cavity.

15. In vitro 3D migration of macrophages was inhibited by P5 peptide.

16. P5 peptide inhibits macrophage accumulation in the adipose tissue of diabetic mice.

Inflammation is a critical part of the body's immune response. Normally, inflammatory response is to protect our body from the bacteria or virus infection and to repair damaged tissues. Neutrophil recruitment is the first wave of immune response directed to fight inflammation. The followed migration of monocyte/macrophage to the inflamed sites are considered as second wave of immune response. However, the mechanisms controlling the transition between the first and second wave of inflammation are not fully understood. In chapter 2, we found a lipid oxidation product, called 2-(ω-carboxyethyl)pyrrolle (CEP) (Yakubenko et al. 2018), generated by neutrophils migration to the inflamed sites serves as a ligand for integrins $\alpha_M\beta_2$ and $\alpha_D\beta_2$ during the second wave of immune response, namely, the recruitment of macrophages. In this process, neutrophils seem to "pave the road" for future macrophage invasion by modifying ECM with CEP. We also detected the levels of CEP were markedly increased in the peritoneal tissues after 72 hours of the injection of thioglycolate to the peritoneal cavity. In addition, the blocking of CEP does not affect neutrophil extravasation, but significantly reduced the subsequent infiltration of macrophages. Using HEK293 cells transfected with β_2 integrins, we found that integrins $\alpha_M\beta_2$ and $\alpha_D\beta_2$ can bind to CEP, but not $\alpha_L\beta_2$. We also used 3D migration assay in vitro to investigate the migration of thioglycolate-induced peritoneal macrophages in the presence or absence of CEP. Interestingly, we found that in vitro 3D migration of neutrophils was not affected in the presence of CEP, however, β_2 integrin-mediated macrophages migration in fibrin matrix was strongly supported by CEP. In summary, CEP generation may have pro-inflammatory as well as protective functions, depending on type of inflammation. The information obtained in our studies not only establishes the foundation for a new model of inflammation but also provides a new strategy for treatment of chronic inflammatory diseases.

In the chapter 3, we are interested in how β_2 integrins, especially $\alpha_M\beta_2$ and $\alpha_D\beta_2$, are involved in the migration and retention of macrophages during chronic disease (Cui et al. 2018). In this study, we first stimulated TG-induced peritoneal macrophages into M1 and M2 macrophage phenotypes using IFN-γ and IL-4 respectively to study their adhesive and migratory properties. We used two methods which are adhesion assay and 3D migration assay and found M1-activated macrophages demonstrate much stronger adhesive properties but weaker migration in comparison to M2-activated macrophages. In addition, using WT, $\alpha_M^{-/-}$ and $\alpha_D^{-/-}$ mouse, we studied the adhesive and migratory properties of M1 and M2 activated or resident macrophages. We found that the level of integrin expression determines the effect on macrophage migration

and adhesion, namely, the high expression of integrin $\alpha_D\beta_2$ on M1 macrophage strongly reduced their migration through fibrin matrix, while the moderate expression of integrins $\alpha_M\beta_2$ and $\alpha_D\beta_2$ on M2 macrophage are both involved in their migration. In in vivo studies, we used the model of resolution of peritoneal inflammation to confirm our in vitro studies. We found that M1-activated macrophages perform a higher retention during the resolution of peritoneal inflammation compared to M2-activated macrophages. These results are corresponding to in vitro studies. We also found M1 macrophages may apply mesenchymal migratory mode, while M2 phenotypes utilize both locomotion modes, amoeboid and mesenchymal. In summary, this part of our study demonstrates the important contribution of $\alpha_M\beta_2$ and $\alpha_D\beta_2$ to the locomotion of distinct macrophage subsets and proposes a β_2-integrin dependent mechanism of macrophage retention in the tissue and efflux during the resolution of inflammation.

We recently found that CEP serves as a ligand for $\alpha_D\beta_2$ and strongly upregulated in the inflamed tissues in chapter 2. Integrin $\alpha_D\beta_2$, which also has a significant increased expression on pro-inflammatory macrophages and in atherosclerotic lesions, promotes the development of atherosclerosis and diabetes by supporting macrophage retention in inflamed tissue in chapter 3. In chapter 4, we were trying to identify a specific inhibitor for $\alpha_D\beta_2$-CEP interaction, which can prevent the excessive macrophage accumulation. Using a specially designed peptide library, biacore detected protein-protein interaction and adhesion of integrin-transfected HEK293 cells, we identified a sequence (called P5-peptide), which significantly and specifically inhibited α_D-CEP binding. The injection of cyclic P5 peptide reduced 3-folds the accumulation of macrophages at 72 hours after thioglycollate-induced peritoneal inflammation model into WT mice, but had no effect in α_D-deficient mice. The tracking of adoptively transferred fluorescently-labeled WT and $\alpha_D^{-/-}$ monocytes in the model of peritoneal inflammation, and in vitro two-dimensional and three-dimensional migration assays demonstrated that P5 peptide does not affect monocyte transendothelial migration or macrophage efflux from the peritoneal cavity, but regulates macrophage migration through the ECM. Moreover, the injection of P5 peptide into WT mice on a high-fat diet prevents macrophage accumulation in adipose tissue in $\alpha_D\beta_2$-dependent manner.

Taken together, we identify new inflammation-specific ligand for integrin $\alpha_D\beta_2$, carboxyethyl pyrrole (CEP). We demonstrate that $\alpha_D\beta_2$ promotes chronic inflammation by mediating strong macrophage adhesion to CEP at the site of inflammation. We identify the short

peptide, called P5, that can prevent $\alpha_D\beta_2$ binding to CEP, and as result, can prevent the development of chronic inflammation. Therefore, our studies propose a new therapeutic approach for the treatment of atherosclerosis and other chronic inflammatory diseases by focusing on inhibition of $\alpha_D\beta_2$-mediated adhesion to inflammatory substrate using short blocking peptide.

REFERENCES

Antonov AS, Antonova GN, Munn DH, Mivechi N, Lucas R, Catravas JD, Verin AD. 2011. Alphavbeta3 integrin regulates macrophage inflammatory responses via pi3 kinase/akt-dependent nf-kappab activation. Journal of cellular physiology. 226(2):469-476.

Apostolova LG. 2016. Alzheimer disease. Continuum. 22(2 Dementia):419-434.

Aurora AB, Porrello ER, Tan W, Mahmoud AI, Hill JA, Bassel-Duby R, Sadek HA, Olson EN. 2014. Macrophages are required for neonatal heart regeneration. The Journal of clinical investigation. 124(3):1382-1392.

Aziz MH, Cui K, Das M, Brown KE, Ardell CL, Febbraio M, Pluskota E, Han J, Wu H, Ballantyne CM et al. 2017. The upregulation of integrin alphadbeta2 (cd11d/cd18) on inflammatory macrophages promotes macrophage retention in vascular lesions and development of atherosclerosis. J Immunol. 198(12):4855-4867.

Baker BM, Chen CS. 2012. Deconstructing the third dimension: How 3d culture microenvironments alter cellular cues. J Cell Sci. 125(Pt 13):3015-3024.

Barczyk M, Carracedo S, Gullberg D. 2010. Integrins. Cell and tissue research. 339(1):269-280.

Baxter M, Hudson R, Mahon J, Bartlett C, Samyshkin Y, Alexiou D, Hex N. 2016. Estimating the impact of better management of glycaemic control in adults with type 1 and type 2 diabetes on the number of clinical complications and the associated financial benefit. Diabetic medicine : a journal of the British Diabetic Association. 33(11):1575-1581.

Bilsland CA, Diamond MS, Springer TA. 1994. The leukocyte integrin p150,95 (cd11c/cd18) as a receptor for ic3b. Activation by a heterologous beta subunit and localization of a ligand recognition site to the i domain. J Immunol. 152(9):4582-4589.

Bobryshev YV, Ivanova EA, Chistiakov DA, Nikiforov NG, Orekhov AN. 2016. Macrophages and their role in atherosclerosis: Pathophysiology and transcriptome analysis. BioMed research international. 2016:9582430.

Bories GFP, Leitinger N. 2017. Macrophage metabolism in atherosclerosis. FEBS Lett. 591(19):3042-3060.

Cao C, Lawrence DA, Strickland DK, Zhang L. 2005. A specific role of integrin mac-1 in accelerated macrophage efflux to the lymphatics. Blood. 106(9):3234-3241.

Charo IF, Taubman MB. 2004. Chemokines in the pathogenesis of vascular disease. Circ Res. 95(9):858-866.

Chavakis T. 2012. Leucocyte recruitment in inflammation and novel endogenous negative regulators thereof. European journal of clinical investigation. 42(6):686-691.

Chinetti-Gbaguidi G, Colin S, Staels B. 2015. Macrophage subsets in atherosclerosis. Nature reviews Cardiology. 12(1):10-17.

Chistiakov DA, Bobryshev YV, Orekhov AN. 2016. Macrophage-mediated cholesterol handling in atherosclerosis. Journal of cellular and molecular medicine. 20(1):17-28.

Ciano PS, Colvin RB, Dvorak AM, McDonagh J, Dvorak HF. 1986. Macrophage migration in fibrin gel matrices. Lab Invest. 54(1):62-70.

Coustan DR. 2013. Gestational diabetes mellitus. Clinical chemistry. 59(9):1310-1321.

Cruz-Guilloty F, Saeed AM, Duffort S, Cano M, Ebrahimi KB, Ballmick A, Tan Y, Wang H, Laird JM, Salomon RG et al. 2014. T cells and macrophages responding to oxidative damage cooperate in pathogenesis of a mouse model of age-related macular degeneration. PloS one. 9(2):e88201.

Cui K, Ardell CL, Podolnikova NP, Yakubenko VP. 2018. Distinct migratory properties of m1, m2, and resident macrophages are regulated by alphadbeta2 and alphambeta2 integrin-mediated adhesion. Frontiers in immunology. 9:2650.

de Ferranti SD, de Boer IH, Fonseca V, Fox CS, Golden SH, Lavie CJ, Magge SN, Marx N, McGuire DK, Orchard TJ et al. 2014. Type 1 diabetes mellitus and cardiovascular disease: A scientific statement from the american heart association and american diabetes association. Circulation. 130(13):1110-1130.

Devaraj S, Dasu MR, Jialal I. 2010. Diabetes is a proinflammatory state: A translational perspective. Expert review of endocrinology & metabolism. 5(1):19-28.

Ding ZM, Babensee JE, Simon SI, Lu H, Perrard JL, Bullard DC, Dai XY, Bromley SK, Dustin ML, Entman ML et al. 1999. Relative contribution of lfa-1 and mac-1 to neutrophil adhesion and migration. J Immunol. 163(9):5029-5038.

Doyle AD, Carvajal N, Jin A, Matsumoto K, Yamada KM. 2015. Local 3d matrix microenvironment regulates cell migration through spatiotemporal dynamics of contractility-dependent adhesions. Nature communications. 6:8720.

Driscoll MK, Danuser G. 2015. Quantifying modes of 3d cell migration. Trends Cell Biol. 25(12):749-759.

Dunne JL, Collins RG, Beaudet AL, Ballantyne CM, Ley K. 2003. Mac-1, but not lfa-1, uses intercellular adhesion molecule-1 to mediate slow leukocyte rolling in tnf-alpha-induced inflammation. J Immunol. 171(11):6105-6111.

el-Gabalawy H, Canvin J, Ma GM, Van der Vieren M, Hoffman P, Gallatin M, Wilkins J. 1996. Synovial distribution of alpha d/cd18, a novel leukointegrin. Comparison with other integrins and their ligands. Arthritis Rheum. 39(11):1913-1921.

Eming SA, Wynn TA, Martin P. 2017. Inflammation and metabolism in tissue repair and regeneration. Science. 356(6342):1026-1030.

Engin AB. 2017. Adipocyte-macrophage cross-talk in obesity. Advances in experimental medicine and biology. 960:327-343.

Evans R, Patzak I, Svensson L, De Filippo K, Jones K, McDowall A, Hogg N. 2009. Integrins in immunity. J Cell Sci. 122(Pt 2):215-225.

Even-Ram S, Yamada KM. 2005. Cell migration in 3d matrix. Curr Opin Cell Biol. 17(5):524-532.

Falk E. 2006. Pathogenesis of atherosclerosis. J Am Coll Cardiol. 47(8 Suppl):C7-12.

Friedl P, Borgmann S, Brocker EB. 2001. Amoeboid leukocyte crawling through extracellular matrix: Lessons from the dictyostelium paradigm of cell movement. J Leukoc Biol. 70(4):491-509.

Friedl P, Weigelin B. 2008. Interstitial leukocyte migration and immune function. Nature immunology. 9(9):960-969.

Frostegard J. 2013. Immunity, atherosclerosis and cardiovascular disease. BMC medicine. 11:117.

Getz GS, Reardon CA. 2016. Apoe knockout and knockin mice: The history of their contribution to the understanding of atherogenesis. Journal of lipid research. 57(5):758-766.

Glatigny S, Duhen R, Arbelaez C, Kumari S, Bettelli E. 2015. Integrin alpha l controls the homing of regulatory t cells during cns autoimmunity in the absence of integrin alpha 4. Scientific reports. 5:7834.

Graupera M, Guillermet-Guibert J, Foukas LC, Phng LK, Cain RJ, Salpekar A, Pearce W, Meek S, Millan J, Cutillas PR et al. 2008. Angiogenesis selectively requires the p110alpha isoform of pi3k to control endothelial cell migration. Nature. 453(7195):662-666.

Grayson MH, Van der Vieren M, Sterbinsky SA, Michael Gallatin W, Hoffman PA, Staunton DE, Bochner BS. 1998. Alphadbeta2 integrin is expressed on human eosinophils and functions as an alternative ligand for vascular cell adhesion molecule 1 (vcam-1). The Journal of experimental medicine. 188(11):2187-2191.

Groh L, Keating ST, Joosten LAB, Netea MG, Riksen NP. 2018. Monocyte and macrophage immunometabolism in atherosclerosis. Seminars in immunopathology. 40(2):203-214.

Guiet R, Van Goethem E, Cougoule C, Balor S, Valette A, Al Saati T, Lowell CA, Le Cabec V, Maridonneau-Parini I. 2011. The process of macrophage migration promotes matrix metalloproteinase-independent invasion by tumor cells. J Immunol. 187(7):3806-3814.

Haberka M, Skilton M, Biedron M, Szostak-Janiak K, Partyka M, Matla M, Gasior Z. 2019. Obesity, visceral adiposity and carotid atherosclerosis. Journal of diabetes and its complications. 33(4):302-306.

Hakkinen KM, Harunaga JS, Doyle AD, Yamada KM. 2011. Direct comparisons of the morphology, migration, cell adhesions, and actin cytoskeleton of fibroblasts in four different three-dimensional extracellular matrices. Tissue engineering Part A. 17(5-6):713-724.

Hanlon SD, Smith CW, Sauter MN, Burns AR. 2014. Integrin-dependent neutrophil migration in the injured mouse cornea. Experimental eye research. 120:61-70.

Herter J, Zarbock A. 2013. Integrin regulation during leukocyte recruitment. J Immunol. 190(9):4451-4457.

Hesse E, Hefferan TE, Tarara JE, Haasper C, Meller R, Krettek C, Lu L, Yaszemski MJ. 2010. Collagen type i hydrogel allows migration, proliferation, and osteogenic differentiation of rat bone marrow stromal cells. Journal of biomedical materials research Part A. 94(2):442-449.

Hilgendorf I, Swirski FK, Robbins CS. 2015. Monocyte fate in atherosclerosis. Arterioscler Thromb Vasc Biol. 35(2):272-279.

Huebsch N, Arany PR, Mao AS, Shvartsman D, Ali OA, Bencherif SA, Rivera-Feliciano J, Mooney DJ. 2010. Harnessing traction-mediated manipulation of the cell/matrix interface to control stem-cell fate. Nature materials. 9(6):518-526.

Jacquemet G, Hamidi H, Ivaska J. 2015. Filopodia in cell adhesion, 3d migration and cancer cell invasion. Curr Opin Cell Biol. 36:23-31.

Jenkins AJ, Joglekar MV, Hardikar AA, Keech AC, O'Neal DN, Januszewski AS. 2015. Biomarkers in diabetic retinopathy. The review of diabetic studies : RDS. 12(1-2):159-195.

Jenkins SJ, Ruckerl D, Cook PC, Jones LH, Finkelman FD, van Rooijen N, MacDonald AS, Allen JE. 2011. Local macrophage proliferation, rather than recruitment from the blood, is a signature of th2 inflammation. Science. 332(6035):1284-1288.

Jin J, Min H, Kim SJ, Oh S, Kim K, Yu HG, Park T, Kim Y. 2016. Development of diagnostic biomarkers for detecting diabetic retinopathy at early stages using quantitative proteomics. Journal of diabetes research. 2016:6571976.

Jing Y, Wu F, Li D, Yang L, Li Q, Li R. 2018. Metformin improves obesity-associated inflammation by altering macrophages polarization. Molecular and cellular endocrinology. 461:256-264.

Johnson AR, Milner JJ, Makowski L. 2012. The inflammation highway: Metabolism accelerates inflammatory traffic in obesity. Immunological reviews. 249(1):218-238.

Justus CR, Leffler N, Ruiz-Echevarria M, Yang LV. 2014. In vitro cell migration and invasion assays. Journal of visualized experiments : JoVE. (88).

Kawamoto E, Okamoto T, Takagi Y, Honda G, Suzuki K, Imai H, Shimaoka M. 2016. Lfa-1 and mac-1 integrins bind to the serine/threonine-rich domain of thrombomodulin. Biochem Biophys Res Commun. 473(4):1005-1012.

Kettle AJ, Gedye CA, Hampton MB, Winterbourn CC. 1995. Inhibition of myeloperoxidase by benzoic acid hydrazides. The Biochemical journal. 308 (Pt 2):559-563.

Kierdorf K, Prinz M, Geissmann F, Gomez Perdiguero E. 2015. Development and function of tissue resident macrophages in mice. Seminars in immunology. 27(6):369-378.

Kim YW, Yakubenko VP, West XZ, Gugiu GB, Renganathan K, Biswas S, Gao D, Crabb JW, Salomon RG, Podrez EA et al. 2015. Receptor-mediated mechanism controlling tissue levels of bioactive lipid oxidation products. Circ Res. 117(4):321-332.

Kleinman HK, Martin GR. 2005. Matrigel: Basement membrane matrix with biological activity. Seminars in cancer biology. 15(5):378-386.

Koelwyn GJ, Corr EM, Erbay E, Moore KJ. 2018. Regulation of macrophage immunometabolism in atherosclerosis. Nature immunology. 19(6):526-537.

Kumar R, Clermont G, Vodovotz Y, Chow CC. 2004. The dynamics of acute inflammation. Journal of theoretical biology. 230(2):145-155.

Kurosaka S, Kashina A. 2008. Cell biology of embryonic migration. Birth defects research Part C, Embryo today : reviews. 84(2):102-122.

Kutys ML, Doyle AD, Yamada KM. 2013. Regulation of cell adhesion and migration by cell-derived matrices. Exp Cell Res. 319(16):2434-2439.

Lammermann T, Bader BL, Monkley SJ, Worbs T, Wedlich-Soldner R, Hirsch K, Keller M, Forster R, Critchley DR, Fassler R et al. 2008. Rapid leukocyte migration by integrin-independent flowing and squeezing. Nature. 453(7191):51-55.

Lanir N, Ciano PS, Van de Water L, McDonagh J, Dvorak AM, Dvorak HF. 1988. Macrophage migration in fibrin gel matrices. Ii. Effects of clotting factor xiii, fibronectin, and glycosaminoglycan content on cell migration. J Immunol. 140(7):2340-2349.

Lavin Y, Mortha A, Rahman A, Merad M. 2015. Regulation of macrophage development and function in peripheral tissues. Nature reviews Immunology. 15(12):731-744.

Lejay A, Fang F, John R, Van JA, Barr M, Thaveau F, Chakfe N, Geny B, Scholey JW. 2016. Ischemia reperfusion injury, ischemic conditioning and diabetes mellitus. Journal of molecular and cellular cardiology. 91:11-22.

Ley K, Laudanna C, Cybulsky MI, Nourshargh S. 2007. Getting to the site of inflammation: The leukocyte adhesion cascade updated. Nature reviews Immunology. 7(9):678-689.

Li Z. 1999. The alphambeta2 integrin and its role in neutrophil function. Cell research. 9(3):171-178.

Libby P. 2002. Inflammation in atherosclerosis. Nature. 420(6917):868-874.

Lim J, Hotchin NA. 2012. Signalling mechanisms of the leukocyte integrin alphambeta2: Current and future perspectives. Biol Cell. 104(11):631-640.

Lishko VK, Podolnikova NP, Yakubenko VP, Yakovlev S, Medved L, Yadav SP, Ugarova TP. 2004. Multiple binding sites in fibrinogen for integrin alphambeta2 (mac-1). The Journal of biological chemistry. 279(43):44897-44906.

Liu YJ, Le Berre M, Lautenschlaeger F, Maiuri P, Callan-Jones A, Heuze M, Takaki T, Voituriez R, Piel M. 2015. Confinement and low adhesion induce fast amoeboid migration of slow mesenchymal cells. Cell. 160(4):659-672.

Locatelli G, Theodorou D, Kendirli A, Jordao MJC, Staszewski O, Phulphagar K, Cantuti-Castelvetri L, Dagkalis A, Bessis A, Simons M et al. 2018. Mononuclear phagocytes locally specify and adapt their phenotype in a multiple sclerosis model. Nature neuroscience. 21(9):1196-1208.

Lontchi-Yimagou E, Sobngwi E, Matsha TE, Kengne AP. 2013. Diabetes mellitus and inflammation. Current diabetes reports. 13(3):435-444.

Lowe DB, Storkus WJ. 2011. Chronic inflammation and immunologic-based constraints in malignant disease. Immunotherapy. 3(10):1265-1274.

Lumeng CN, Saltiel AR. 2011. Inflammatory links between obesity and metabolic disease. The Journal of clinical investigation. 121(6):2111-2117.

Luo BH, Carman CV, Springer TA. 2007. Structural basis of integrin regulation and signaling. Annual review of immunology. 25:619-647.

Luo D, McGettrick HM, Stone PC, Rainger GE, Nash GB. 2015. The roles of integrins in function of human neutrophils after their migration through endothelium into interstitial matrix. PloS one. 10(2):e0118593.

Lusis AJ. 2000. Atherosclerosis. Nature. 407(6801):233-241.

Luster AD, Alon R, von Andrian UH. 2005. Immune cell migration in inflammation: Present and future therapeutic targets. Nature immunology. 6(12):1182-1190.

Mabon PJ, Weaver LC, Dekaban GA. 2000. Inhibition of monocyte/macrophage migration to a spinal cord injury site by an antibody to the integrin alphad: A potential new anti-inflammatory treatment. Experimental neurology. 166(1):52-64.

Mallat Z. 2014. Macrophages. Arterioscler Thromb Vasc Biol. 34(12):2509-2519.

McNelis JC, Olefsky JM. 2014. Macrophages, immunity, and metabolic disease. Immunity. 41(1):36-48.

Mendes PM. 2013. Cellular nanotechnology: Making biological interfaces smarter. Chemical Society reviews. 42(24):9207-9218.

Meyer AS, Hughes-Alford SK, Kay JE, Castillo A, Wells A, Gertler FB, Lauffenburger DA. 2012. 2d protrusion but not motility predicts growth factor-induced cancer cell migration in 3d collagen. The Journal of cell biology. 197(6):721-729.

Mitroulis I, Alexaki VI, Kourtzelis I, Ziogas A, Hajishengallis G, Chavakis T. 2015. Leukocyte integrins: Role in leukocyte recruitment and as therapeutic targets in inflammatory disease. Pharmacology & therapeutics. 147:123-135.

Moore KJ, Sheedy FJ, Fisher EA. 2013. Macrophages in atherosclerosis: A dynamic balance. Nature reviews Immunology. 13(10):709-721.

Moore KJ, Tabas I. 2011. Macrophages in the pathogenesis of atherosclerosis. Cell. 145(3):341-355.

Moutasim KA, Nystrom ML, Thomas GJ. 2011. Cell migration and invasion assays. Methods Mol Biol. 731:333-343.

Niu G, Chen X. 2011. Why integrin as a primary target for imaging and therapy. Theranostics. 1:30-47.

Noti JD. 2002. Expression of the myeloid-specific leukocyte integrin gene cd11d during macrophage foam cell differentiation and exposure to lipoproteins. Int J Mol Med. 10(6):721-727.

Noti JD, Johnson AK, Dillon JD. 2000. Structural and functional characterization of the leukocyte integrin gene cd11d. Essential role of sp1 and sp3. The Journal of biological chemistry. 275(12):8959-8969.

Nourshargh S, Alon R. 2014. Leukocyte migration into inflamed tissues. Immunity. 41(5):694-707.

Palecek SP, Loftus JC, Ginsberg MH, Lauffenburger DA, Horwitz AF. 1997. Integrin-ligand binding properties govern cell migration speed through cell-substratum adhesiveness. Nature. 385(6616):537-540.

Pals ST, de Gorter DJ, Spaargaren M. 2007. Lymphoma dissemination: The other face of lymphocyte homing. Blood. 110(9):3102-3111.

Panigrahi S, Ma Y, Hong L, Gao D, West XZ, Salomon RG, Byzova TV, Podrez EA. 2013. Engagement of platelet toll-like receptor 9 by novel endogenous ligands promotes platelet hyperreactivity and thrombosis. CircRes. 112(1):103-112.

Parisi L, Gini E, Baci D, Tremolati M, Fanuli M, Bassani B, Farronato G, Bruno A, Mortara L. 2018. Macrophage polarization in chronic inflammatory diseases: Killers or builders? Journal of immunology research. 2018:8917804.

Petrie RJ, Doyle AD, Yamada KM. 2009. Random versus directionally persistent cell migration. Nature reviews Molecular cell biology. 10(8):538-549.

Pluskota E, Woody NM, Szpak D, Ballantyne CM, Soloviev DA, Simon DI, Plow EF. 2008. Expression, activation, and function of integrin alphambeta2 (mac-1) on neutrophil-derived microparticles. Blood. 112(6):2327-2335.

Qin S, Zheng JH, Xia ZH, Qian J, Deng CL, Yang SL. 2019. Cthrc1 promotes wound repair by increasing m2 macrophages via regulating the tgf-beta and notch pathways. Biomedicine & pharmacotherapy = Biomedecine & pharmacotherapie. 113:108594.

Qu A, Leahy DJ. 1995. Crystal structure of the i-domain from the cd11a/cd18 (lfa-1, alpha l beta 2) integrin. Proc Natl Acad Sci U S A. 92(22):10277-10281.

Reig G, Pulgar E, Concha ML. 2014. Cell migration: From tissue culture to embryos. Development. 141(10):1999-2013.

Roszer T. 2015. Understanding the mysterious m2 macrophage through activation markers and effector mechanisms. Mediators of inflammation. 2015:816460.

Schneider T, Issekutz AC. 1996. Quantitation of eosinophil and neutrophil infiltration into rat lung by specific assays for eosinophil peroxidase and myeloperoxidase. Application in a brown norway rat model of allergic pulmonary inflammation. Journal of immunological methods. 198(1):1-14.

Shapiro MD, Fazio S. 2017. Apolipoprotein b-containing lipoproteins and atherosclerotic cardiovascular disease. F1000Research. 6:134.

Sheikh S, Rahman M, Gale Z, Luu NT, Stone PC, Matharu NM, Rainger GE, Nash GB. 2005. Differing mechanisms of leukocyte recruitment and sensitivity to conditioning by shear stress for endothelial cells treated with tumour necrosis factor-alpha or interleukin-1beta. Br J Pharmacol. 145(8):1052-1061.

Shi C, Pamer EG. 2011. Monocyte recruitment during infection and inflammation. Nature reviews Immunology. 11(11):762-774.

Shirin A, Della Rossa F, Klickstein I, Russell J, Sorrentino F. 2019. Optimal regulation of blood glucose level in type i diabetes using insulin and glucagon. PloS one. 14(3):e0213665.

Shoelson SE, Lee J, Goldfine AB. 2006. Inflammation and insulin resistance. The Journal of clinical investigation. 116(7):1793-1801.

Smith A, Stanley P, Jones K, Svensson L, McDowall A, Hogg N. 2007. The role of the integrin lfa-1 in t-lymphocyte migration. Immunological reviews. 218:135-146.

Soman P, Kelber JA, Lee JW, Wright TN, Vecchio KS, Klemke RL, Chen S. 2012. Cancer cell migration within 3d layer-by-layer microfabricated photocrosslinked peg scaffolds with tunable stiffness. Biomaterials. 33(29):7064-7070.

Sridharan R, Cavanagh B, Cameron AR, Kelly DJ, O'Brien FJ. 2019. Material stiffness influences the polarization state, function and migration mode of macrophages. Acta biomaterialia.

Stelmaszynska T, Kukovetz E, Egger G, Schaur RJ. 1992. Possible involvement of myeloperoxidase in lipid peroxidation. The International journal of biochemistry. 24(1):121-128.

Sun T, Jackson S, Haycock JW, MacNeil S. 2006. Culture of skin cells in 3d rather than 2d improves their ability to survive exposure to cytotoxic agents. Journal of biotechnology. 122(3):372-381.

Swirski FK, Nahrendorf M. 2013. Leukocyte behavior in atherosclerosis, myocardial infarction, and heart failure. Science. 339(6116):161-166.

Tabas I, Bornfeldt KE. 2016. Macrophage phenotype and function in different stages of atherosclerosis. Circ Res. 118(4):653-667.

Takada Y, Ye X, Simon S. 2007. The integrins. Genome biology. 8(5):215.

Tellechea A, Leal EC, Kafanas A, Auster ME, Kuchibhotla S, Ostrovsky Y, Tecilazich F, Baltzis D, Zheng Y, Carvalho E et al. 2016. Mast cells regulate wound healing in diabetes. Diabetes. 65(7):2006-2019.

Thomas D, Apovian C. 2017. Macrophage functions in lean and obese adipose tissue. Metabolism. 72:120-143.

Van der Vieren M, Crowe DT, Hoekstra D, Vazeux R, Hoffman PA, Grayson MH, Bochner BS, Gallatin WM, Staunton DE. 1999. The leukocyte integrin alpha d beta 2 binds vcam-1: Evidence for a binding interface between i domain and vcam-1. J Immunol. 163(4):1984-1990.

Van der Vieren M, Le Trong H, Wood CL, Moore PF, St John T, Staunton DE, Gallatin WM. 1995. A novel leukointegrin, alpha d beta 2, binds preferentially to icam-3. Immunity. 3(6):683-690.

Van Goethem E, Guiet R, Balor S, Charriere GM, Poincloux R, Labrousse A, Maridonneau-Parini I, Le Cabec V. 2011. Macrophage podosomes go 3d. European journal of cell biology. 90(2-3):224-236.

van Spriel AB, Leusen JH, van Egmond M, Dijkman HB, Assmann KJ, Mayadas TN, van de Winkel JG. 2001. Mac-1 (cd11b/cd18) is essential for fc receptor-mediated neutrophil cytotoxicity and immunologic synapse formation. Blood. 97(8):2478-2486.

Vats D, Mukundan L, Odegaard JI, Zhang L, Smith KL, Morel CR, Wagner RA, Greaves DR, Murray PJ, Chawla A. 2006. Oxidative metabolism and pgc-1beta attenuate macrophage-mediated inflammation. Cell Metab. 4(1):13-24.

Verollet C, Charriere GM, Labrousse A, Cougoule C, Le Cabec V, Maridonneau-Parini I. 2011. Extracellular proteolysis in macrophage migration: Losing grip for a breakthrough. Eur J Immunol. 41(10):2805-2813.

Verreck FA, de Boer T, Langenberg DM, Hoeve MA, Kramer M, Vaisberg E, Kastelein R, Kolk A, de Waal-Malefyt R, Ottenhoff TH. 2004. Human il-23-producing type 1 macrophages promote but il-10-producing type 2 macrophages subvert immunity to (myco)bacteria. Proc Natl Acad Sci U S A. 101(13):4560-4565.

Wang F, Zhang Z, Fang A, Jin Q, Fang D, Liu Y, Wu J, Tan X, Wei Y, Jiang C et al. 2018. Macrophage foam cell-targeting immunization attenuates atherosclerosis. Frontiers in immunology. 9:3127.

Watson GS, Craft S. 2006. Insulin resistance, inflammation, and cognition in alzheimer's disease: Lessons for multiple sclerosis. Journal of the neurological sciences. 245(1-2):21-33.

Weber C, Zernecke A, Libby P. 2008. The multifaceted contributions of leukocyte subsets to atherosclerosis: Lessons from mouse models. Nature reviews Immunology. 8(10):802-815.

Weber KS, Klickstein LB, Weber C. 1999. Specific activation of leukocyte beta2 integrins lymphocyte function-associated antigen-1 and mac-1 by chemokines mediated by distinct pathways via the alpha subunit cytoplasmic domains. Mol Biol Cell. 10(4):861-873.

Wiesner C, Le-Cabec V, El Azzouzi K, Maridonneau-Parini I, Linder S. 2014. Podosomes in space: Macrophage migration and matrix degradation in 2d and 3d settings. Cell adhesion & migration. 8(3):179-191.

Wolf K, Muller R, Borgmann S, Brocker EB, Friedl P. 2003. Amoeboid shape change and contact guidance: T-lymphocyte crawling through fibrillar collagen is independent of matrix remodeling by mmps and other proteases. Blood. 102(9):3262-3269.

Woollard KJ, Geissmann F. 2010. Monocytes in atherosclerosis: Subsets and functions. Nature reviews Cardiology. 7(2):77-86.

Wynn TA, Vannella KM. 2016. Macrophages in tissue repair, regeneration, and fibrosis. Immunity. 44(3):450-462.

Yakubenko VP, Belevych N, Mishchuk D, Schurin A, Lam SC, Ugarova TP. 2008. The role of integrin alpha d beta2 (cd11d/cd18) in monocyte/macrophage migration. Exp Cell Res. 314(14):2569-2578.

Yakubenko VP, Cui K, Ardell CL, Brown KE, West XZ, Gao D, Stefl S, Salomon RG, Podrez EA, Byzova TV. 2018. Oxidative modifications of extracellular matrix promote the second wave of inflammation via beta2 integrins. Blood.

Yakubenko VP, Lishko VK, Lam SC, Ugarova TP. 2002. A molecular basis for integrin alphambeta 2 ligand binding promiscuity. The Journal of biological chemistry. 277(50):48635-48642.

Yakubenko VP, Yadav SP, Ugarova TP. 2006. Integrin alphadbeta2, an adhesion receptor up-regulated on macrophage foam cells, exhibits multiligand-binding properties. Blood. 107(4):1643-1650.

Yamaguchi H, Wyckoff J, Condeelis J. 2005. Cell migration in tumors. Curr Opin Cell Biol. 17(5):559-564.

Ye Q, Zund G, Benedikt P, Jockenhoevel S, Hoerstrup SP, Sakyama S, Hubbell JA, Turina M. 2000. Fibrin gel as a three dimensional matrix in cardiovascular tissue engineering. European journal of cardio-thoracic surgery : official journal of the European Association for Cardio-thoracic Surgery. 17(5):587-591.

Young SP, Kapoor SR, Viant MR, Byrne JJ, Filer A, Buckley CD, Kitas GD, Raza K. 2013. The impact of inflammation on metabolomic profiles in patients with arthritis. Arthritis Rheum. 65(8):2015-2023.

Yu X, Machesky LM. 2012. Cells assemble invadopodia-like structures and invade into matrigel in a matrix metalloprotease dependent manner in the circular invasion assay. PloS one. 7(2):e30605.

Yu XH, Fu YC, Zhang DW, Yin K, Tang CK. 2013. Foam cells in atherosclerosis. Clinica chimica acta; international journal of clinical chemistry. 424:245-252.

Zaman MH, Kamm RD, Matsudaira P, Lauffenburger DA. 2005. Computational model for cell migration in three-dimensional matrices. Biophysical journal. 89(2):1389-1397.

Zengel P, Nguyen-Hoang A, Schildhammer C, Zantl R, Kahl V, Horn E. 2011. Mu-slide chemotaxis: A new chamber for long-term chemotaxis studies. BMC cell biology. 12:21.

Zernecke A, Bernhagen J, Weber C. 2008. Macrophage migration inhibitory factor in cardiovascular disease. Circulation. 117(12):1594-1602.

Zerouga M, Stillwell W, Stone J, Powner A, Jenski LJ. 1996. Phospholipid class as a determinant in docosahexaenoic acid's effect on tumor cell viability. Anticancer research. 16(5A):2863-2868.

Zhong J, Baquiran JB, Bonakdar N, Lees J, Ching YW, Pugacheva E, Fabry B, O'Neill GM. 2012. Nedd9 stabilizes focal adhesions, increases binding to the extra-cellular matrix and differentially effects 2d versus 3d cell migration. PloS one. 7(4):e35058.

VITA

KUI CUI

Education: East Tennessee State University, Johnson City, TN, USA, Ph.D.

Biochemistry, 2019

Soochow University, Suzhou, CHINA, M.Sc., Pharmacology, 2013

Xuzhou Medical University, Xuzhou, CHINA, B.S. Pharmacy, 2010

Professional

Experience: Research Associate, East Tennessee State University, Johnson City, TN,

Publications: 1. Kui Cui, Christopher Ardell, Nataly Podolnikova, Tatiana Ugarova,

Eugene Podrez, Tatiana Byzova, Valentin Yakubenko. Inhibition of

macrophage adhesion mediated by integrin $\alpha_D\beta_2$ prevents macrophage

accumulation during inflammation. (*under review in JBC*)

2. Kui Cui, Christopher L. Ardell, Nataly P. Podolnikova Ph.D., Valentin

P. Yakubenko Ph.D. Distinctmigratory properties of resident, classically

and alternatively-activated macrophages are regulated by $\alpha_D\beta_2$ and $\alpha_M\beta_2$

integrin-mediated adhesion. *Frontiers in immunology*, 2018. 9: 2650

3.Valentin P. Yakubenko, Kui Cui, Christopher L. Ardell, Moammir H.

Aziz, Kathleen E. Brown, XiaoxiaZ.West, Robert G. Salomon, Eugene A.

Podrez, Tatiana V. Byzova. Oxidative modifications ofextracellular matrix

promote the second wave of inflammation via β2 Integrins. *Blood,*

2018,132(1):78-88.

4. Aziz MH*, Cui K*, Das M, Brown KE, Ardell CL, Febbraio M,

Pluskota E, Han J, Wu H, Ballantyne CM, Smith JD, Cathcart MK,

Yakubenko VP.The Upregulation of Integrin alphaDbeta2 (CD11d/CD18)

on Inflammatory Macrophages Promotes Macrophage Retention in

Vascular Lesions and Development of Atherosclerosis. *J Immunol*. 2017;

198 (12):4855-4867. (*First author)

5.Wang Y, Musich PR, Cui K, Zou Y, Zhu MY. Neurotoxin-induced DNA

damage is persistent in SH- SY5Y cells and LC neurons. *Neurotoxicity Research* 2015; 27:368-383.

6.Wang Y, Hilton BA, Cui K, Zhu MY. Effects of antidepressants on DSP4/CPT-induced DNA damageResponse in neuroblastoma SH-SY5Y cells. *Neurotoxicity Research* 2015, 28:154-170

7.Kui Cui, Jian-Qun Kou, Jin-Hua Gu, Rong Han, Guanghui Wang, Xuechu Zhen and Zheng-HongQin. Naja naja atra venom ameliorates pulmonary fibrosis by inhibiting inflammatory response andoxidativestress. *BMC Complementary and Alternative Medicine* 2014,14:461

8.Zhu J*, Cui K*, Kou J,Wang S, Xu Y, Ding Z, Han R, Qin Z: Naja naja atra venom protects againstmanifestations of systemic lupus erythematosus in MRL/lpr mice. *Evidence-basedComplementary and Alternative Medicine*: eCAM 2014, 2014:969482. (*First author)

9.Fan Y, Chen P, Li Y, Cui K, Noel DM, Cummins ED, Peterson DJ, Brown RW, Zhu MY. Corticosterone administration up-regulated expression of norepinephrine transporter and dopamine. *J Neurochem*. 2014,128(3):445-58.

10. Kui Cui, Tan Zhang, Lingshu Gu, et al. Effect of oxymatrine on learning and memory abilityon elderly mice. *World Clinical Drugs* 2011, 32(2):102-106.

Honors and Awards:

Travel grant for Experimental Biology, San Diego, CA, 2018

Awarded First Place Presentation by The Tennessee Physiological Society 2017

Co-author of abstract for the American Heart Association Scientific Sessions meeting, that received the ATVB Council award for Outstanding Research by Early Career Investigator, New Orleans, USA, 2016